Land Cover Classification and Assessment of Carrying Capacities and Stocking Rates of Crown Lands in Manitoba

by

Jan Bryan Meneses Encabo

A thesis submitted to the Faculty of Graduate Studies of

The University of Manitoba

In partial fulfillment of the requirements for the degree of

MASTER OF SCIENCE

Department of Animal Science

University of Manitoba

Winnipeg, Manitoba, Canada

ABSTRACT

Understanding the carrying capacity and the stocking rates of crown lands is critical for the beef industry in the Prairies that relies heavily on these lands for grazing. The overall goal of this study was to examine the current carrying capacities and stocking rates of the crown lands in Manitoba. The main objectives of this study were to i) classify each crown land parcel in the province by land cover type or vegetation type and ii) estimate the carrying capacities and stocking rates of each parcel and compare these to the current stocking rates allowed by the provincial crown land leases. This study used remote sensing and geographic information system (GIS) technologies for land cover monitoring and estimation of carrying capacities and stocking rates. Based on the assessment of remotely sensed land cover inventories, forest and shrubland were found to be the dominant land cover types in the crown lands compared to native and tame grasslands, which are more desirable for grazing due to higher forage quality and palatability. Then, the carrying capacities were estimated from past field surveys that measured forage productivity in different ecoregions of Manitoba. The carrying capacities were used to calculate the stocking rates based on the delineated land cover types within each crown land parcel. Results show that the current stocking rates of the majority of the crown lands were lower than the estimated stocking rates. This suggests that these parcels were being undergrazed compared to the current grazing intensities permitted by the lease contracts. Overall, the forage resources of the crown lands in Manitoba were being undergrazed by -44.64%. This study can contribute to the existing management of crown lands and it also demonstrated the potential of remote sensing technology to improve and expedite land cover monitoring and stocking rate estimation for crown land managers in the future.

ACKNOWLEDGMENTS

First and foremost, I would like to extend my deepest gratitude to my advisor, Dr. Marcos Cordeiro for his continuous patience, encouragement and graciousness throughout my study. I will always be grateful for his trust and confidence in me that I can finish this project. I would also like to thank my committee members, Dr. David Walker and Dr. Emma McGeough, for their time spent on providing constructive comments and advice on my project.

I would also like to thank a few people who have assisted me by providing information and expertise in their respective fields. I want to thank Dr. Nasem Badreldin for helping me with the remote sensing analysis and for providing the Manitoba Grassland Inventory (MGI), which was very pivotal to the success of my project. I want to thank Melanie Bell, Glenn Friesen and Tyson Gillis of the Agriculture and Resource Development (ARD) for their expertise on the crown lands, as well as for providing me with the critical crown land data I needed for this research. I also want to thank Mae Elsinger of the Agriculture and Agri-Food Canada (AAFC) for providing me with the forage benchmarking data necessary for estimating carrying capacities.

I would like to express my sincere love and thanks to my family, my parents, Nette and Jhun, and my brothers, Tristan and Janzen. To my closest friends, Jaypee, Patricia and Netanya, for their unwavering encouragement throughout my program, even when I considered quitting numerous times in my final year. To Kassell for being such a significant part of my support system during my first year of graduate school. I want to also express my appreciation to Jacqueline of the Student Counselling Centre for facilitating my therapy through the lowest points in my life when I was experiencing a whirlwind of emotions due to the uncertainty of my future. And, finally, I want to thank Ash for bringing me joy and happiness every day, even if you can be bothersome at times.

DEDICATION

This thesis is dedicated to my late Lola Loring, who was instrumental in moulding me into the person I am today. I know she is up there, guiding me every step of the way. May her gentle soul rest in peace.

FOREWORD

This thesis follows a manuscript-style format based on the Canadian Journal of Animal Science standards and consists of two manuscripts. Each manuscript is comprised of an abstract, introduction, materials and methods, results, discussion and conclusion. Both manuscripts have not been submitted for publication at this time.

Contributions of Authors:

This study was conceived and designed by Bryan Encabo and Dr. Marcos Cordeiro. The data were collected and analyzed by Bryan Encabo. The two manuscripts were prepared by Bryan Encabo and Dr. Marcos Cordeiro. The first manuscript (**Chapter 4**) was revised by Dr. Nasem Badreldin, Dr. Emma McGeough and Dr. David Walker. The last manuscript (**Chapter 5**) was revised by Dr. Emma McGeough and Dr. David Walker.

TABLE OF CONTENTS

LIST OF TABLES

LIST OF FIGURES

LIST OF ABBREVIATIONS

AAFC	Agriculture and Agri-Food Canada
ACI	Annual Crop Inventory
ACL	agricultural crown lands
AD	Assiniboine Delta
AGB	aboveground biomass
AIC	Akaike information criterion
AOP	Aspen/Oak Parkland
AP	Aspen Parkland
ARD	Agriculture and Resource Development
ATSAVI	adjusted transformed soil-adjusted vegetation index
AUM	animal unit month
AVHRR	Advanced Very High Resolution Radiometer
BMP	beneficial management practice
CC	carrying capacity
CMI	Hogg's climate moisture index
CP	crude protein
DM	dry matter
DT	decision trees
EVI	enhanced vegetation index
GAM	generalized additive model
GDD	growing degree-days
GHG	greenhouse gas
GIS	geographic information system
GR	grazing rate
GVI	Grassland Vegetation Inventory
IP	Interlake Plain
ISODATA	Iterative Self-Organizing Data Analysis Technique
LiDAR	light detection and ranging

LDA	linear discriminant analysis
LOESS	locally estimated scatterplot smoothing
LW	Lake of the Woods
MAP	mean annual precipitation
MASC	Manitoba Agricultural Services Corporation
MAT	mean annual temperature
MBUT	Mid-Boreal Upland and Transition
MERIS	Medium Resolution Imaging Spectrometer
MGI	Manitoba Grassland Inventory
MLC	maximum likelihood classification
MLR	multiple linear regression
MODIS	Moderate Resolution Imaging Spectroradiometer
MSAVI	modified soil-adjusted vegetation index
MSP	mean May-to-September precipitation
NAD 83	North American Datum of 1983
NDVI	normalized difference vegetation index
NIR	near-infrared
NPP	net primary production
OSAVI	optimized soil-adjusted vegetation index
PAS	The Pas
PLI	Prairie Landscape Inventory
PFRA	Prairie Farm Rehabilitation Administration
PR	polynomial regression
PRISM	Parameter Regression of Independent Slopes Model
R^2	coefficient of determination
R^2_{adj}	adjusted coefficient of determination
RF	random forests
RMSE	root-mean-square error
SAR	synthetic aperture radar
SAVI	soil-adjusted vegetation index

SMU	Southwest Manitoba Uplands
SOC	soil organic carbon
SPLSR	sparse partial least square regression
SPOT	*Satellite Pour l'Observation de la Terre*
SR	stocking rate
SU	sheep unit
TGP	Tall Grass Prairie
TSAVI	transformed soil-adjusted vegetation index
UTM	Universal Transverse Mercator
VI	vegetation index
WGS 84	World Geodetic System of 1984

CHAPTER 1: GENERAL INTRODUCTION

Similar to other Prairie Provinces, the Manitoba Government operates a provincial land leasing program for agricultural crown lands administered by Agriculture and Resource Development (ARD). During the growing season from May to September, agricultural crown lands are used by leaseholders for grazing, haying and annual cropping. The provincial government estimates that approximately 1,750 leaseholders use the parcels for grazing, which can feed almost 90,000 cattle throughout the grazing season, while only 60 leaseholders use them for cropping (Manitoba Agriculture and Resource Development 2019a).

Over most of the crown lands, native grasses and forbs are the primary sources of forages for beef cattle, particularly weaned calves in cow-calf operations. In 2021, cow-calf operations accounted for 64% of all beef cattle operations in Canada, with the Prairie Provinces responsible for 81% of these operations. Of the Prairie Provinces, Manitoba was home to 787,800 head of cattle or 12% of the national herd used for cow-calf operations (Statistics Canada 2022a). Furthermore, the province generated $629 million in gross revenue from the sale of cattle or mature cows and calves in the same year (Statistics Canada 2022b). This highlights the importance of the cow-calf sector in the agriculture industry of Manitoba. With this, crown lands, especially the grasslands that comprise them, continue to be an essential component of the cow-calf sector, which utilizes these rangelands for grazing.

Due to the environmental sensitivity of grassland landscapes, critical and stringent management practices must be adopted to improve the environmental sustainability of the crown lands while increasing beef production (Qin et al. 2021). At the same time, these crown lands can play a significant role in multiple ecosystem services, such as forage production and soil regulation (Pogue et al. 2018). Among these services is carbon sequestration as grasslands,

which cover about one-third of the Earth's land surface, are estimated to store 50% more carbon than forests (Conant 2010; Reinermann et al. 2020).

Part of creating sustainable grazing management plans is setting appropriate stocking rates. Stocking rates are determined by the carrying capacity of the land as influenced by forage production and quality (Meshesha et al. 2019; Qin et al. 2021). As carrying capacity depends on productivity, it is essential to have timely data on vegetation productivity and distribution, which fluctuates depending on the variable precipitation (Willms and Jefferson 1993; Thorpe et al. 2008; Li and Guo 2012). Traditional methods of assessing grassland vegetation, such as field surveys (e.g., manual clippings), can be expensive when done annually (Ali et al. 2016; Murphy et al. 2021), especially in a large-scale program that handles thousands of crown land parcels. For these large-scale assessments, cost-effective and time-efficient methods for gathering vegetation data must be used, such as remote sensing technology (Reinermann et al. 2020). Remote sensing allows data to be collected in various spatial scales and different temporal resolutions, allowing for consistent and complete spatiotemporal coverage.

The ability to assess forage production and carrying capacity through remote sensing enables range managers to efficiently amend their management plans to ensure the sustained health of forage resources while optimizing animal performance, especially with the rapidly changing climate. Crown land managers in Manitoba now have access to one of these remote sensing datasets recently derived for grassland assessments, namely, the Manitoba Grassland Inventory (MGI), with 10-m resolution imagery captured from the Sentinel-1 and Sentinel-2 sensors (Grassland Analytica 2021).

Despite their usefulness, remotely sensed datasets, such as the MGI, have to be validated against official government records in order to assess their usefulness for crown land

management. The main purpose of this study was to estimate the stocking rates of the crown lands in Manitoba using the MGI dataset. To accomplish this, specific objectives of land cover classification of the parcels and subsequent estimation of the carrying capacity of each parcel based on the identified land cover or vegetation were achieved using remote sensing and geographic information system (GIS) techniques. The workflow of the methodology used in this thesis is shown in Figure 1.

The content of this thesis is divided into six chapters. The first chapter presents a brief overview of the beef industry in Manitoba, the importance of crown lands for cow-calf grazing and the methodological workflow of this study. The second chapter provides a literature review of the grassland distribution in Canada and the remote sensing approaches of grasslands, such as vegetation monitoring, land cover classification and carrying capacity estimation. The third chapter outlines the hypothesis and the objectives of this study. The next two chapters, follow a manuscript-style format, with chapter four describing the land cover classification of crown lands using remotely sensed datasets and chapter five covering the estimation of carrying capacities and stocking rates of these crown lands. The last chapter summarizes the general discussion and the main findings of this study, and recommendations for future research.

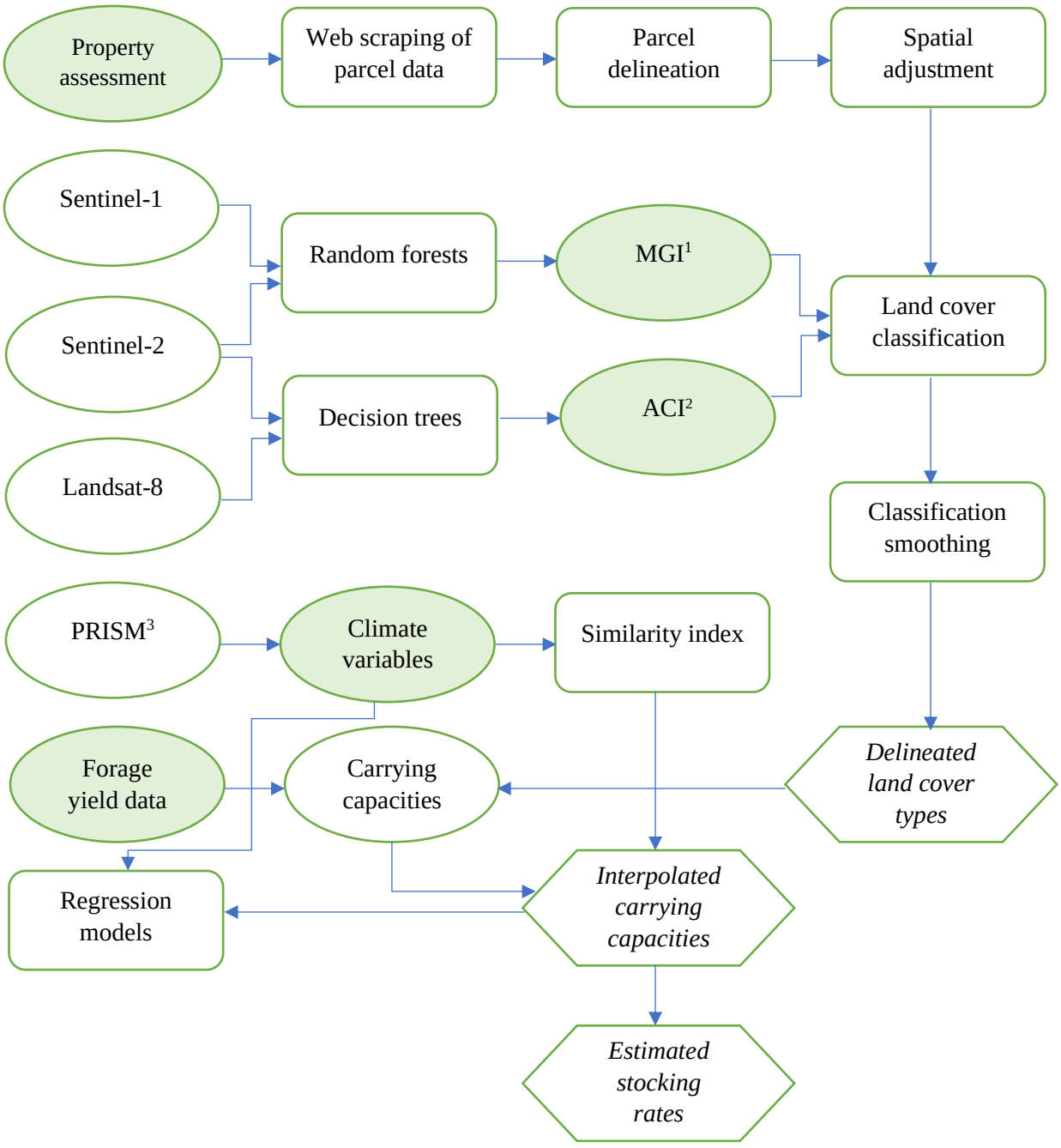

Figure 1: Flowchart of the methodology of this study. Circles represent data sources. Rectangles represent methods. Hexagons represent the resulting outputs. Shaded datasets were acquired from external sources for use in this study.
[1]Manitoba Grassland Inventory
[2]Annual Crop Inventory
[3]Parameter Regression of Independent Slopes Model

CHAPTER 2: LITERATURE REVIEW

2.1. Grassland distribution in Canada

Grasslands are one of the most important ecosystems on the Earth, accounting for approximately 26% of its terrestrial surface and about 70% of total global agricultural land (Conant 2010; Reinermann et al. 2020; Qin et al. 2021). The North American Great Plains is a large expanse of flatlands that contains one of the largest grassland distributions in the world. Canada accounts for 16% of the Great Plains, constituting about 5% of Canada's land area (Gauthier and Wiken 2003). This region, known as the Canadian Prairies, encompasses the provinces of Alberta, Saskatchewan and Manitoba.

Based on the 2021 federal census, Canada has 18.6 million hectares of grasslands, with 13.7 million hectares of native rangelands and 4.8 million hectares of tame pastures (Statistics Canada 2022c). The Prairie Provinces constitute 89% of all these grasslands. Of this, Manitoba accounts for 9% or 1.6 million hectares of grasslands while Saskatchewan and Alberta account for 36% and 44%, respectively. In terms of forage origin, 71-81% of these grasslands in each province are native while only 19-29% are tame (Table 1). Native forages are indigenous to an area as opposed to tame forages which were introduced, mostly originating from Europe and Asia (Aasen and Bjorge 2009).

Table 1: Grassland distribution by province in Canada, divided by forage origin.[1]

	Tame grasslands		Native grasslands		Total	
Province	Area (ha)	%	Area (ha)	%	Area (ha)	%
Newfoundland and Labrador	TU[2]	N/A	TU[2]	N/A	N/A	N/A
Prince Edward Island	6,172	0.13	TU[2]	N/A	N/A	N/A
Nova Scotia	11,164	0.23	TU[2]	N/A	N/A	N/A
New Brunswick	9,557	0.20	TU[2]	N/A	N/A	N/A
Quebec	86,644	1.79	80,617	0.59	167,261	0.90
Ontario	162,068	3.36	253,481	1.85	415,549	2.24
Manitoba	315,845	6.54	1,321,851	9.63	1,637,696	8.82
Saskatchewan	1,934,070	40.05	4,672,235	34.03	6,606,305	35.59
Alberta	2,124,583	44.00	6,121,309	44.58	8,245,892	44.43
British Columbia	177,696	3.68	1,246,042	9.07	1,423,738	7.67
Canada	4,828,538	100	13,731,114	100	18,559,652	100

[1](Statistics Canada 2022c)
[2]TU = too unreliable to be published

Aside from their origin, grasslands can also be classified according to their plant communities. The main types in the Canadian Prairies are fescue, tallgrass and mixed-grass prairies as seen in Figure 2. These are commonly associated with underlying Chernozemic soil zones across the Prairie Provinces (Coupland 1961).

Fescue prairies, which are associated with Black Chernozemic soils, can be found in the foothills of Alberta and the Cypress Upland ecoregion. Mountain rough fescue (*Festuca campestris*), bluebunch fescue (*Festuca idahoensis*) and Parry's oatgrass (*Danthonia parryi*) are the major grasses in the Foothills Fescue region (Downing and Pettapiece 2006). The Cypress Upland is unique in that fescue grasslands occur mainly at higher elevations, particularly above 1,000 metres. Below these elevations, it transitions to a mixed-grass prairie which is associated with Dark Brown and Brown soils (Thorpe 2014a).

Mixed-grass prairies are dominated by both short and mid-height grasses located in southeastern Alberta and the majority of southern Saskatchewan (Ecological Stratification Working Group et al. 1995; Downing and Pettapiece 2006). It is also the largest grassland

distribution in the Prairies and is usually divided between Dry and Moist Mixed Grasslands based on precipitation patterns. The Dry Mixed Grassland is identified with Brown soils and dominated by shortgrass blue grama (*Bouteloua gracilis*) and mid-grasses needle-and-thread (*Hesperostipa comata*) and western wheatgrass (*Pascopyrum smithii*). The Moist Mixed Grassland is associated with Dark Brown soils and is the northernmost extension of open grasslands in the Prairies. This ecoregion supports similar grass communities as the Dry Mixed Grassland but offers higher productivity due to increased growing season precipitation and cooler temperatures in the summer (Ecological Stratification Working Group et al. 1995; Downing and Pettapiece 2006).

Small remnants of the tallgrass prairie remain along the Red River in southern Manitoba, which is considered one of the rarest grassland systems in the world (Samson and Knopf 1994). The remaining tallgrass prairie in Manitoba has been reduced to less than 1% of its historic native range. It is dominated by big bluestem (*Andropogon gerardii*), switchgrass (*Panicum virgatum*) and Indiangrass (*Sorghastrum nutans*) (Simms and Risser 2000, cited in Sveinson 2003).

The Aspen Parkland ecoregion is the transition zone or ecotone between the open grasslands to the south and boreal forests to the north. As a result, its landscape is characterized as a mosaic of fescue prairies in drier areas and trembling aspen (*Populus tremuloides*) forests in moister areas. Like the tallgrass prairie, the Aspen Parkland occupies the Black soil zone (Ecological Stratification Working Group et al. 1995; Downing and Pettapiece 2006).

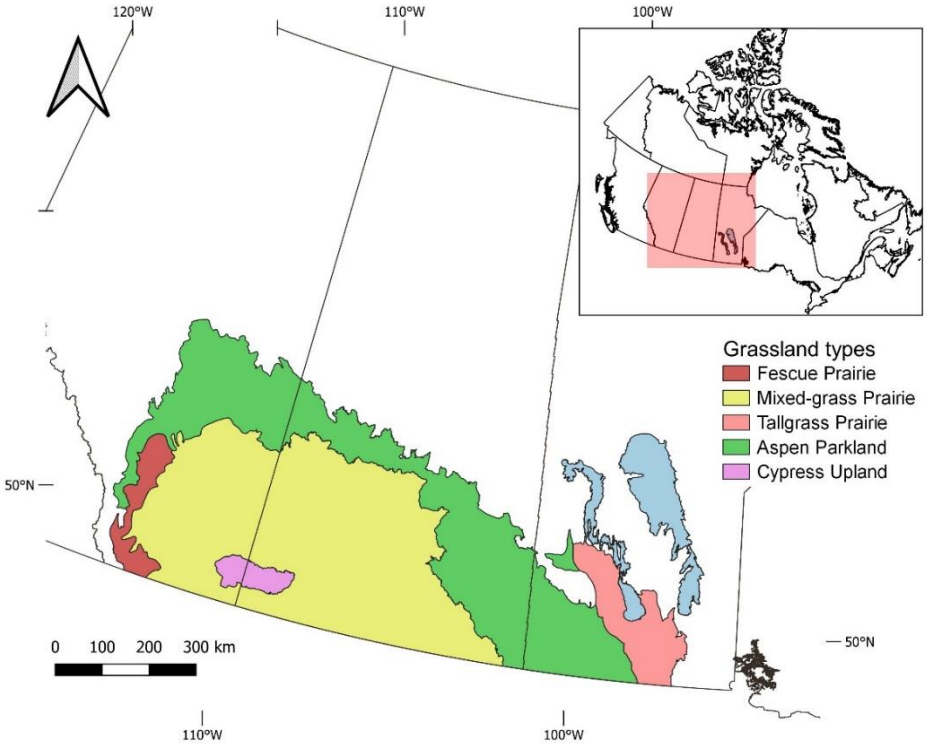

Figure 2: Main grassland types in the Canadian Prairies (fescue, tallgrass and mixed-grass). The Aspen Parkland serves as a transition zone between the prairies and the boreal forests. The Cypress Upland is a predominantly fescue prairie at higher elevations and a mixed-grass prairie at decreasing elevations (Ecological Stratification Working Group et al. 1995; Gauthier and Wiken 2003; Manitoba Museum 2014).

Current estimates reveal that only 25-30% of the original Canadian grassland distribution remains in the Prairies (Gauthier and Wiken 2003). Native grasslands have degraded as a result of different disturbances, such as conversion to cropland, overgrazing, drought and fire (Conant 2010). Recent studies have reported 1-5% annual conversion rates from grasslands to cropland (Gage et al. 2016; World Wildlife Fund 2016). Large undisturbed native grasslands that have not been impacted by European settlement are becoming increasingly rare in the Prairies (Gauthier and Wiken 2003). The loss of historic ranges of native prairies in the Prairies has been attributed to agricultural expansion or conversion to cropland. In Manitoba, estimated reductions of native tallgrass and mixed-grass prairies were as high as 99.9% (Samson and Knopf 1994). Declines of

native mixed-grass prairie in Alberta and Saskatchewan were 61% and 81%, respectively. The native shortgrass prairie in Saskatchewan has decreased by 86%. Given these estimates are several decades old, the reductions in grassland coverage could be even larger due to the recent pressure of land conversion. Recent census analysis showed a continuing downward trend in the land cover of grasslands used for grazing (Statistics Canada 2017, 2022c). Between the 2011 and the 2021 agricultural censuses, a decline of 1.7 million hectares or -8% was seen across Canada. The Prairie Provinces experienced losses ranging from 4% to 13%, with Manitoba suffering the worst decline. In terms of forage origin, native grasslands decreased by -7% while tame grasslands saw a decline of -13% (Table 2).

Table 2: Changes in grassland distribution by province in Canada, divided by forage origin.[1]

Province	Tame grasslands			Native grasslands			Total		
	2011 (ha)	2021 (ha)	% Change	2011 (ha)	2021 (ha)	% Change	2011 (ha)	2021 (ha)	% Change
Newfoundland and Labrador	1,612	TU	N/A	8,602	TU	N/A	10,214	N/A	N/A
Prince Edward Island	8,501	6,172	-27.40	9,230	TU	N/A	17,731	N/A	N/A
Nova Scotia	21,153	11,164	-47.22	25,148	TU	N/A	46,301	N/A	N/A
New Brunswick	16,987	9,557	-43.74	22,731	TU	N/A	39,718	N/A	N/A
Quebec	126,334	86,644	-31.42	134,147	80,617	-39.90	260,481	167,261	-35.79
Ontario	262,543	162,068	-38.27	398,538	253,481	-36.40	661,081	415,549	-37.14
Manitoba	415,322	315,845	-23.95	1,466,968	1,321,851	-9.89	1,882,290	1,637,696	-12.99
Saskatchewan	2,057,957	1,934,070	-6.02	4,816,782	4,672,235	-3.00	6,874,739	6,606,305	-3.90
Alberta	2,395,944	2,124,583	-11.33	6,435,825	6,121,309	-4.89	8,831,769	8,245,892	-6.63
British Columbia	226,298	177,696	-21.48	1,385,359	1,246,042	-10.06	1,611,657	1,423,738	-11.66
Canada	5,532,652	4,828,538	-12.73	14,703,330	13,731,114	-6.61	20,235,982	18,559,652	-8.28

[1]Statistics Canada (2017, 2022c)
[2]TU = too unreliable to be published

2.2. Classification of grasslands

The use of remote sensing has been pivotal in the identification of land use/land cover types due to its practicality compared to the traditional methods of field surveys and manual interpretation of aerial photographs which are time-consuming and expensive (Ali et al. 2016; Murphy et al. 2021). The reflectances or spectral signatures of different objects, such as vegetation, built-up areas, bare soils and water bodies on Earth allow their separability in remotely sensed images. There are different ways of grouping different classification techniques of remotely sensed images. The most common way is dividing them between unsupervised and supervised classification (Lu and Weng 2007).

Unsupervised classification puts pixels into different clusters based on their natural groupings present in their spectral values. Clustering is purely based on pixel-based statistics and does not require a priori knowledge of the characteristics of the study area or class definitions to be used. Some examples of unsupervised algorithms are K-means and ISODATA clustering (Xie et al. 2008; Ali et al. 2016). On the other hand, in supervised classification, the analyst selects training areas corresponding to each class they defined. The classifier would use the training areas to identify the classes of interest (Lu and Weng 2007). The most popular classifier in this category is maximum likelihood classification (MLC) in which pixels are assigned to the class with the highest probability of belonging to it. Its results are only accurate if the data follows a normal distribution (Xie et al. 2008; Ali et al. 2016).

The traditional supervised classifier, MLC, has been used in different studies to identify broad land cover classes, such as grasslands. A study carried out in the rangelands of Utah using the MLC included a broad herbaceous class, containing both perennial and annual grasses and forbs (Boswell et al. 2017). The resulting classification had class accuracies between 82% and

93% with an overall accuracy of 91% and kappa statistic (i.e., coefficient of agreement between the observed true accuracy and the accuracy of values assigned by chance) of 0.88. In this study, the herbaceous class recorded 91 – 93% class accuracies. Another study conducted in Texas rangelands using MLC on images stacked with NDVI (normalized difference vegetation index) and OSAVI (optimized soil-adjusted vegetation index) found overall accuracies between 90% and 96% and kappa statistics of 0.85 – 0.94, with its herbaceous class having good accuracies of 87 – 96% (Fern et al. 2018). Classification accuracy was slightly lower during the pre-grazing year compared to the post-grazing due to the presence of higher amounts of non-photosynthetic vegetation, such as dead litter and senesced plants, that produce similar reflectances of NIR and red bands, lowering the contrast between these bands. Because the OSAVI stacked pictures performed marginally better, the study suggests that they may be used on semi-arid rangelands to compensate for the high soil background effect.

There is a hybrid classification technique that incorporates the aspects of both supervised and unsupervised classification, improving the accuracy and efficiency of both methods. One possible approach is to run an unsupervised classification to help identify all unique classes that need to be defined, then create training areas based on these defined classes and follow through with a supervised classification of the image (Lillesand et al. 2015). A hybrid classification of linear discriminant analysis (LDA), a supervised classifier, and ISODATA, an unsupervised classifier, was conducted in Missouri Couteau wetlands in southern Saskatchewan, which had grassland classes of low prairie, wet meadow, native prairie and tame grass (Dechka et al. 2002). The LDA was performed using the original wetland classification scheme, which resulted in a low overall accuracy of 47%. Of all the grassland classes, only the wet meadow and native prairie classes had class accuracies of 50% or greater. Low accuracies were attributed to the

original classification scheme not being suitable for remote sensing classifiers due to the unique spectral signatures of specific vegetation communities, which necessitated further subdividing of the broad classes. The subsequent ISODATA clustering algorithm resulted in 25 unique clusters or classes, improving the overall accuracy to 84%.

Aside from the identification of broad grassland classes, remotely sensed images have been used to identify specific grass species or types that can be separated by their unique spectral signatures or phenological profiles. Native and tame grasses can be separated by the timing of their seasonal growth as studies have found that tame grasses green up earlier than native grasses. For example, in the Dry Mixedgrass Prairie region of Alberta, McInnes et al. (2015). used LDA and MLC to discriminate between native and tame grasses based on temporal images captured on specific dates during the growing season to represent the distinct green-up dates of each grass type. The LDA was first used to determine the best dates that would make up its classification model, while MLC was performed separately for images taken from each date used in LDA. The multitemporal LDA classification performed marginally better than the single-date MLC, resulting in 73% overall accuracy compared to the single-date overall accuracies of 65 – 71%. Nevertheless, the class accuracies of native and tame grasses were also not statistically different between LDA and MLC results. Both methodologies showed an overrepresentation of native grasses and an underrepresentation of tame grasses in the classified images.

Relatively newer multispectral sensors, such as Landsat-8, Sentinel-2 and WorldView-2, can detect subtle variations in seasonal spectral signatures between C_3 and C_4 grasses. A South African study that used these sensors to classify *Festuca*, a C_3 species, and *Themeda*, a C_4 species, using LDA found overall accuracies of 90% or higher for all species (Shoko and Mutanga 2017b). WorldView-2 and Sentinel-2 had marginally higher accuracies than Landsat-8

due to the presence of red-edge bands in these sensors which are very influential in species discrimination.

Advanced classification methods built upon the traditional unsupervised and supervised classifications have also been developed to further improve their accuracies. The MLC, a traditional supervised classifier, assumes that the data being analyzed is normally distributed (Xie et al. 2008; Ali et al. 2016). In areas where there is a complex variability in vegetation communities, the use of MLC can lead to misclassification, as many ecological variables do not conform to the normality assumption. Advanced methods, such as decision trees (DT) and random forest (RF) classifiers, have been introduced that can be applied to non-parametric distributions and are independent of the type of data distribution (Xie et al. 2008; Ali et al. 2016). For example, DT had been used in classifying grasslands in southern Alberta using Radarsat-2 and Landsat-5 images (Smith and Buckley 2011). The authors found that native grasslands were difficult to separate from tame grasslands, particularly in Radarsat-2 images, due to similar surface backscatter values, although both grass types were discriminated from crops. Moreover, Landsat-5 images had higher overall accuracy and class accuracies than Radarsat-2, with overall accuracies of 88% and 78%, respectively. The RF classifier consists of multiple decision trees, which make them more robust and increase classification accuracies (Ali et al. 2016). The predictions of each decision tree are combined to produce the final classification. A study conducted in China for land cover mapping of broad classes using RF found that the inclusion of the greatest number of variables had greatly improved the overall accuracy of the final classification model from 74% to 89% (Jin et al. 2018). The variables used were Landsat-5 spectral variables, topographic variables, textural variables and NDVI values. Most of the class accuracies ranged between 81% and 94%, except for the grassland class which had 73 – 81%

accuracies with some of its pixels being misclassified as forest less than 8% of the time. In Canada, RF has been used recently to classify grasslands in Saskatchewan (Badreldin et al. 2021) and in Manitoba (Grassland Analytica 2021), which reported high accuracies of 90% and 97%, respectively.

2.3. Estimation of grassland vegetation biomass

Understanding the responses of vegetation biomass to climate change is critical for the current and future state of our ecosystems and agricultural sustainability. The first step in understanding this process is to accurately estimate vegetation distribution and productivity at all scales, from local and regional to global scale (Lu 2006). There are four main types of vegetation biomass, i) aboveground biomass (AGB), ii) belowground biomass, which consists of live roots, iii) non-living dead mass and iv) litter (Eisfelder et al. 2012). The majority of studies on evaluating biomass, whether they are direct field measurements or remote sensing methods, are focused on quantifying aboveground biomass (Lu 2006). Simultaneously, most of these studies were conducted in forested areas compared to non-forested areas such as the semi-arid Canadian Prairies (Eisfelder et al. 2012).

Field measurements are considered more accurate than remote sensing methods but require more time and money to implement and can be only completed at a local scale (Ali et al. 2016). They can be performed either in a destructive or non-destructive manner. Destructive field measurements involve clipping or cutting the grass which is subsequently dried and weighed to determine the dry matter (DM) yield (Ali et al. 2016). These forage clippings are commonly employed as the reference parameters in yield and nutritive quality estimation models (Murphy et al. 2021). Non-destructive measurements can be classified into three types: visual assessment, rising plate meter and field spectroscopy (Ali et al. 2016; Murphy et al. 2021).

Visual assessment involves a farmer or an expert analyzing and estimating herbage mass based on their subjective observation. The most accurate and established non-destructive field procedure, the rising plate meter, uses a weighted disc that is dropped onto the grass canopy and a plate rises as it measures the compressed sward height of the pasture. Field spectroscopy uses spectrometers or ground sensors to measure the vegetation reflectance at different wavelengths which can be used to identify grassland distribution and biophysical parameters, and discriminate grass species (Ali et al. 2016; Murphy et al. 2021). Field spectroscopy adheres to the core principle of remote sensing in that it identifies the reflectance of vegetation, soils and other environmental features but they tend to be costly for personal use compared to spaceborne remote sensors, with some having their products available for public use. Data obtained from different types of field measurements are important for validating estimated biophysical variables and training derived models or algorithms from remotely sensed products (Ali et al. 2016). Remote sensing methods allow the estimation of biomass yields and biophysical parameters without the need for direct contact with vegetation.

Both remote sensing and field spectroscopy calculate vegetation indices (VIs), which are considered measures of the photosynthetic capacity or primary production of a vegetation canopy and are also regarded as vegetation "greenness" indices (Tucker and Sellers 1986). These indices are composed of different bands or wavelengths which depend on the biophysical properties of the vegetation being measured. They are more sensitive to biomass discrimination than individual spectral bands. Remote sensing is used to estimate AGB by establishing an empirical relationship between the measured biomass from field surveys and the transformations of two or more spectral bands into VIs both obtained over the same time period (Virk and Mitchell 2014).

The normalized difference vegetation index (NDVI) is the most popular vegetation index used in the literature (Reinermann et al. 2020) which is a ratio of vegetation reflectances of near-infrared and red bands (Silleos et al. 2006). The rationale for NDVI is based on the fact that healthy, green vegetation strongly absorbs photosynthetically active radiation or PAR (0.4 – 0.7 μm) due to its plant pigments, chlorophylls a and b, and carotenoids. The PAR spectral region roughly corresponds to the visible spectrum. On the other hand, light scattering within the leaf structure results in high levels of reflectance of near-infrared light (0.75 – 1.1 μm) (Tucker and Sellers 1986). Thus, dense vegetation canopies strongly reflect near-infrared light while strongly absorbing visible light, specifically red light. In the case of NDVI, the ratio is normalized so the closer it is to 1, the higher amount of green vegetation present.

In eastern Ethiopia, where grazing is the major mode of feed intake for livestock in a pastoralist society, a study was conducted to develop a VI model for grass biomass estimation (Meshesha et al. 2020). The NDVI values were calculated from Sentinel-2 images with a high spatial resolution of 10 m. A regression model calibrated using a polynomial function indicated that biomass and NDVI were significantly correlated (R^2= 0.81) and explained 87% of the variation in forage biomass in the district based on validation data. The average field-measured biomass (0.74 t/ha) was also comparable with the average biomass estimate of the NDVI model (0.76 t/ha). Other studies that used images from sensors with lower spatial resolutions have also shown significant correlations between field-measured biomass production and NDVI values. A study carried out in a northern mixed-grass prairie in western South Dakota using the 250-m resolution MODIS sensor found a strong relationship between annual field-measured biomass production and time-integrated NDVI (R^2= 0.69) (Rigge et al. 2013). As the sampled mixed-grass prairie both contained cool-season (C_3) and warm-season (C_4) grasses, cool-season grass

percentages for both field biomass measurements and NDVI values were also calculated. The results indicated that field measurements varied between 55.4% and 69% while NDVI varied between 78.9% and 84.4% (R^2= 0.58). According to the authors, the overestimation of the C_3 grass percentage by NDVI was caused by the temporal overlap of the production of both C_3 and C_4 grasses around the start of summer, especially in June. Bédard et al. (2006) also used the 250-m resolution MODIS and an even lower spatial resolution sensor, 1-km resolution AVHRR, in Alberta rangelands and found a significant but weak relationship between field-measured biomass and NDVI values (R^2= 0.55 for MODIS and R^2= 0.50 for AVHRR). The increased spatial resolution of MODIS did not significantly increase the correlation with the field data. The authors hypothesized that the weaker relationship between field data and remotely sensed NDVI could be a result of different grassland types within Alberta, such as mixed-grass prairie, fescue grassland and cypress uplands. They also suggested that NDVI models focused on regional differences could yield better correlation.

The use of images with higher spatial resolution does not always result in a stronger relationship between field-measured biomass and NDVI biomass estimates. In a French study using 20-m resolution SPOT-4 images, Dusseux et al. (2015) found that only 30% of the variation in the field biomass measurements was explained by the NDVI linear regression model. It should be noted that this study employed linear regression as opposed to the Ethiopian study described in the previous paragraph, which used a polynomial function model to account for the nonlinearity of NDVI values in areas with denser grass canopies.

The major problem of using NDVI is its tendency to approach saturation asymptotically, causing its values to plateau at high biomass yield levels. As a result, NDVI becomes insensitive to small changes in biomass production of dense vegetation canopies, making it difficult to

estimate their biomass accurately at these levels (Mutanga and Skidmore 2004). The sill in the NDVI-biomass relationship can be explained by how the absorption of red light by vegetation peaks at maximum plant productivity while near-infrared reflectance continues to increase due to the addition of new leaves, resulting in multiple light scattering. The small decrease in red reflectance but a much larger increase in near-infrared reflectance results in a slight change in the NDVI value, rather than an increase of the NDVI value due to the thicker canopy, causing a poor relationship with biomass.

There are many solutions proposed to counter the NDVI saturation effect. One of them is to employ time-integrated NDVI which uses NDVI values above a particular baseline for the entire duration of the growing season (Tieszen et al. 1997). Certain phenological metrics, such as the onset and the end of the growing season and the maximum NDVI during peak growth are determined to identify the baseline where NDVI values would be considered for biomass estimation. Rigge et al. (2013) used NDVI values above the baseline of 20% of the total amplitude of the growing season profile and found it to be sufficient to reduce the NDVI saturation effect.

In addition to NDVI, there are other existing indices that use the red and NIR bands for biomass estimation, which are listed in Table 3. One of these is the enhanced vegetation index (EVI) which has a soil adjustment factor L and atmospheric resistant coefficients C_1 and C_2 which weigh the use of the blue band in the aerosol correction of the red band (Silleos et al. 2006). As a result, EVI reduces the influence of soil background and atmospheric effects on vegetation reflectance and does not saturate as rapidly as NDVI in dense vegetation. The performance of EVI in estimating grass biomass has been similar to that of NDVI in different studies. For example, Meshesha et al. (2020) reported that the EVI model performed slightly

better than NDVI in correlation with the field data when estimating grass biomass (R^2= 0.87 for EVI and R^2= 0.81 for NDVI). Using the validation data, EVI explained 92% of the variation in forage biomass while NDVI explained 87%. On the other hand, a study conducted in the Pampas grassland in Brazil using 20-m resolution Sentinel-2 images found that NDVI was slightly better than EVI in estimating total biomass (R^2= 0.171 for EVI and R^2= 0.283 for NDVI) and total green biomass (R^2= 0.178 for EVI and R^2= 0.238 for NDVI) (Filho et al. 2020). Shoko et al. (2018) and Munyati (2022) both reported similar observations in studies conducted in South Africa.

Table 3: Vegetation indices (VIs) mentioned in this literature review.

Formula
$NDVI = \frac{NIR - R}{NIR + R}$
$simple\ ratio = \frac{NIR}{R}$
$EVI = 2.5\frac{NIR - R}{NIR + C_1 * R - C_2 * B + L}$
$SAVI = \frac{NIR - R}{NIR + R + L}(1 + L)$
$MSAVI = 0.5\ [(2 * NIR + 1) - \sqrt{(2 * NIR + 1)^2 - 8(NIR - R)}]$
$OSAVI = 1.16\frac{NIR - R}{NIR + R + 0.16}$
$TSAVI = \frac{a(NIR - a * R - b)}{a * NIR + R + a * b}$
$ATSAVI = \frac{a(NIR - a * R - b)}{a * NIR + R + a * b + 0.08(1 + a^2)}$

NDVI = normalized difference vegetation index; *EVI* = enhanced vegetation index; *SAVI* = soil-adjusted vegetation index; *MSAVI* = modified soil-adjusted vegetation index; *OSAVI* = optimized soil-adjusted vegetation index; *TSAVI* = transformed soil-adjusted vegetation index; *ATSAVI* = adjusted transformed soil-adjusted vegetation index
NIR = near-infrared reflectance; *R* = red reflectance; *C* = atmospheric resistant coefficient; *B* = blue reflectance; *L* = soil adjustment factor; *a* = slope of the soil line; *b* = intercept of the soil line

The vegetation sparseness and soil aridity of grasslands increase the background effect of bare soil, which compromises the accurate estimation of grass biomass by remote sensors

(Silleos et al. 2006). The soil-adjusted vegetation index (SAVI) was introduced to limit the soil backscatter by including a soil adjustment factor *L* that varies according to vegetation density, with 1 being used for very sparse canopies and 0.25 for very dense canopies (Silleos et al. 2006). In contrast to the purpose of SAVI, Ren and Feng (2015) found that SAVI and its derivations (modified soil-adjusted vegetation index, MSAVI; optimized soil-adjusted vegetation index, OSAVI; transformed soil-adjusted vegetation index, TSAVI and adjusted transformed soil-adjusted vegetation index, ATSAVI) did not improve the biomass estimation accuracy in arid and semi-arid grasslands compared with NDVI and simple ratio. The NDVI and simple ratio, which do not have soil adjustment factors, accounted for 71% and 72% of the variation in measured biomass, respectively, while the soil-adjusted indices only accounted for 56% to 67%. Ren and Feng (2015) conducted this study in the desert steppe region of Xilingol grasslands in China characterized by low grass biomass yields. On the other hand, Jin et al. (2014) found that SAVI and MSAVI performed slightly better than NDVI in the same region (R^2= 0.493 for SAVI, R^2= 0.490 for MSAVI, and R^2= 0.484 for NDVI). These authors also found that NDVI was a better estimator of grass biomass than SAVI and MSAVI in meadow steppe and typical steppe regions which have higher grass biomass.

In a Canadian context, a study carried out in the Grasslands National Park in Saskatchewan, characterized by its semi-arid mixed prairie composed of native grasses, found that ATSAVI had the same performance as NDVI (R^2= 0.45) in accounting for the variability in grass biomass despite its soil adjustment factor which is supposed to improve its biomass estimation in sparse vegetation canopies (Zhang and Guo 2008). The authors hypothesized that the accumulation of dead litter in the mixed prairie affected the performance of ATSAVI due to

the similar spectral profiles of the mixed prairie and bare soil based on SPOT-4 and Landsat-5 bands. This means that there was difficulty in distinguishing grass canopies from bare soil.

Some researchers have developed new indices and methods that use different bands from those used by NDVI. Narrow bands located in the red edge point (0.68 – 0.75 μm) between the boundary of red and near-infrared bands have shown better performance compared to NDVI and other indices that only uses the red and near-infrared bands (Mutanga and Skidmore 2004). The shorter wavelengths of the red edge are sensitive to chlorophyll content which produces lower reflectance while multiple scattering from the leaves at its longer wavelengths produces higher reflectance, confirming the strong relationship between the red edge and biomass or leaf area index. In South Africa, Ramoelo et al. (2015) used RF modelling on 2-m resolution WorldView-2 images and reported that red-edge indices, such as red-edge based simple ratio and MERIS terrestrial chlorophyll index (MTCI), were the most important variables for predicting grass biomass, as well as its leaf nitrogen. The NDVI was only moderately important during the wet season when the productivity is at its optimum. Red-edge bands and indices have also shown good performance in estimating grass biomass based on species phenology. Another study conducted in South Africa dealt with predicting the AGB of two different grass species with variations in their photosynthetic systems: *Festuca*, a C_3 species, and *Themeda*, a C_4 species (Shoko et al. 2018). The red-edge NDVI at 0.705 μm was found to have the highest frequency of importance in the sparse partial least square regression (SPLSR) model for predicting biomass based on species, whereas the standard NDVI came in second. When single spectral bands and indices were all incorporated in one SPLSR model, two red-edge NDVI indices at 0.705 and 0.74 μm performed better than the standard NDVI, and three single red-edge bands and the NIR band outperformed these NDVI indices significantly. In the same combined SPLSR model, most VIs

that used the red and NIR bands have similar moderate frequencies of importance within the model. In a study in Pampas, Brazil, Guerini Filho et al. (2020) also used the red-edge counterparts of NDVI and EVI and found that they performed better than the standard indices in estimating total green biomass (R^2= 0.238 for NDVI and R^2= 0.291 for red-edge NDVI; R^2= 0.178 for EVI and R^2= 0.328 for red-edge EVI). On the other hand, Munyati (2022) found that red-edge indices have lower estimation accuracies than standard indices, such as EVI, SAVI and NDVI, in estimating grass biomass in South African savannahs.

The lack of studies using red-edge indices in biomass estimation is typically caused by the absence of narrow red-edge bands in older remote multispectral sensors (Ramoelo et al. 2015). The majority of research conducted up to the early 2000s used field hyperspectral spectroradiometers that contain narrow bands to estimate vegetation productivity. More recently, new remote multispectral sensors with red-edge bands, such as Sentinel-2 and WorldView-2, have been introduced, which may improve the estimation accuracy of vegetation biophysical properties when compared to older multispectral sensors like Landsat and MODIS. These sensors have the advantage of covering larger geographic areas than field hyperspectral spectroradiometers.

The empirical modelling of VIs with field biomass data has been the most used approach in estimating grass AGB. This approach can be classified into two broad groups: traditional regression models and machine-learning algorithms. Traditional regression models are either linear or nonlinear in structure (Shoko et al. 2016; Ali et al. 2016). Due to the NDVI saturation, the relationship between NDVI and biophysical parameters like biomass is non-linear. Linearity between NDVI and biomass only exists in low vegetation cover as proven by Ren and Feng (2015) in a desert steppe region that has sparse grasslands. On the other hand, Dusseux et al.

(2015) observed the NDVI saturation effect in grasslands specifically used for grazing due to their high biomass. Linear regression models can still be used with other VIs such as SAVI which do not suffer from saturation (Jin et al. 2014). Nonlinear regression models, such as power (Jin et al. 2014), exponential (Grant et al. 2013) and logarithmic regression models (Wang et al. 2019a), are usually favoured for estimating grass biomass using NDVI.

Machine-learning algorithms are regarded as more advanced tools for addressing the complex relationship between VIs and field data. Some of these algorithms are the SPLSR (Shoko et al. 2018) and RF models (Ramoelo et al. 2015), which incorporate all spectral bands and VIs into one model to identify the most important remote sensing variables in estimating the grass biomass, as opposed to individual modelling for each VI done by traditional regression models. Machine learning algorithms reduce dimensionality, can handle large volumes of data, and are independent of the distribution of the data, whether it is normally distributed or not (Shoko et al. 2016). Other than empirical modelling, the physical-based approach using radiative transfer models is another approach for estimating grass AGB through remote sensing (Shoko et al. 2016). They are less commonly used than empirical modelling in the literature. They estimate biophysical parameters using physical laws and model inversion of remote sensing data. The computational processing capacity of model inversion and the requirement of additional input variables in the model have hindered its use in the literature. Some examples of radiative transfer models are the PROSAIL and CASA models (Reinermann et al. 2020).

2.4. Estimation of grassland carrying capacity

Carrying capacity is the maximum number of animals that can be sustained indefinitely by a habitat without permanently destroying its productivity (Rees 1996). The calculation of the carrying capacity of a pasture consists of measuring the forage biomass yield available for

grazing and applying proper use factors or utilization rates that take into account how much forage has been lost due to various factors such as trampling or soil erosion, as well as using livestock feed nutritive requirements based on the length of time the pasture can be grazed (Qin et al. 2021). On the other hand, the stocking rate is the number of animals on the pasture for a specified length of grazing season (Meshesha et al. 2019). While the carrying capacity of grazing land cannot be changed as it is determined by its overall productivity, the stocking rate can be changed as it depends on the number of animals allocated to a specific area of land by range managers and the available forage for that particular grazing season which can vary depending on precipitation and drought conditions. If the carrying capacity is calculated as a number of livestock per unit area, this can be multiplied by the total grazed area to get the stocking rate as the number of animal units, which would be the maximum stocking rate or the "ecologically sustainable stocking rate" for that area (Alberta Sustainable Resource Development 2004). In some instances in the literature, carrying capacity and stocking rate are both measured in terms of the number of livestock or animal units. In this case, it is usually recommended that the stocking rate of a pasture should not exceed its carrying capacity (Yu et al. 2010; Qin et al. 2021). There are also situations where carrying capacity and stocking rate are used interchangeably and have the same definition. In the beef cattle industry, an animal unit month (AUM) is defined as the amount of forage consumed in a month by a 454-kg mature cow with or without a calf which totals to 355 kg; therefore, one AUM equals 355 kg of forage (Society for Range Management 1998).

As discussed in section 2.3, remote sensing technology can be used to estimate grass biomass yields which can subsequently be validated with DM samples measured on the ground. Once grass biomass has been estimated, this can be used to calculate the possible carrying

capacity of that area. Aside from biomass estimation, vegetation classification derived from remotely sensed images can be used to identify the coverage of grasslands and their total grazable area, from which carrying capacity and stocking rate are calculated. In the alpine meadows of Golog Prefecture, China, Yu et al. (2010) classified MODIS images using the maximum likelihood classification. The NDVI values were calculated from these images and were used to estimate grass biomass by creating a logarithmic regression with field biomass samples. Then, the carrying capacity of each county was calculated using the biomass estimates, the utilization rate of 55% with additional reduction rates to account for distance to water, slope angle and soil erosion gradient, and the daily forage requirement for one sheep unit (SU) to be accounted for a year's grazing. The estimated carrying capacities were compared to the actual stocking rates from the official statistics. Using only the 55% utilization rate, only two of the six counties were undergrazed, with Madoi County undergrazing by 56% and the whole prefecture overgrazing by 3%. When the reduction rates were factored into the carrying capacity calculations, only Madoi County was undergrazed, while the entire prefecture was overgrazing by 72%. With the inclusion of reduction rates, the overgrazing rates in the two counties increased to more than 100%, with Gadê County being overgrazed by 173% and Baima County being overgrazed by 294%.

Aside from NDVI, remote sensing products containing net primary production (NPP) have also been used to estimate grass biomass before conversion into carrying capacities. The MODIS MOD17 product calculates the gross primary production (GPP), or the rate of photosynthesis based on a light use efficiency model. Then, NPP is calculated from GPP by subtracting the growth respiration of the vegetation and it can subsequently be converted to biomass estimates due to their direct correlation (de Leeuw et al. 2019). A study done in the

alpine meadows of the Three-River Headwaters region, a region also covering the Golog Prefecture, used the MODIS NPP dataset and calculated carrying capacities based on its biomass conversions, utilization rates according to the grassland type and annual forage requirement for one SU (Zhang et al. 2014). The actual stocking rate of the entire region was 18.72 million SU, exceeding the estimated carrying capacity of 12.19 million SU, which represents overgrazing by a rate of 68%. In this study, only five out of 17 counties were undergrazed and of all the 12 overgrazed counties, six counties had overgrazing rates of over 100%, with Tongde County reaching 324%.

Another study using the MODIS NPP images assessed the carrying capacity of mountain pastures in Azerbaijan using a model with only a 65% utilization rate based on forage availability and another model with additional reduction rates dependent on slope steepness (de Leeuw et al. 2019). A carrying capacity of 12.7 SU/ha was estimated using only the 65% utilization rate which is equivalent to 8.05 million SU when multiplied by the total area of the mountain pastures. These values decreased to 6.2 SU/ha and 3.93 million SU when slope reduction rates were added to the model. Both estimates were lower than the prevailing total stocking rate of at least 8 million sheep and 0.5 million goats and additional cows, which suggests that the entire area was overgrazed as evidenced by signs of complete denudation of the pastures at the end of the grazing season.

Radiative transfer models can also be used for predicting NPP for biomass conversions. Qin et al. (2021) used the CASA model to estimate monthly NPP in sandy and steppe grasslands in Inner Mongolia, China. Carrying capacity calculations used utilization rates based on the degree of sand mobility and steppe degradation according to grazing management strategies. The total estimated carrying capacity in the region was 237.46 thousand cattle units compared to the

actual stocking rate of 283.32 thousand cattle units, resulting in an overgrazing rate of 19.32%. At the Gacha or village level, the model determined that 71 out of 109 Gachas exhibited overgrazing. Upon close inspection by the authors, livestock in some of the overgrazed Gachas did not rely on forage grazing but instead, were fed grain concentrates and straw fodder. The exclusion of these non-grazing dominated Gachas left 51 overgrazed Gachas. The model also found that 20 Gachas had underutilized grazing potential due to undergrazing.

Currently, there are gaps in the scientific literature regarding the use of remote sensing technology in estimating carrying capacity and stocking rates of grasslands in the Canadian Prairies. No research has been conducted on the inventory and monitoring of the agricultural crown lands in Manitoba using remote sensing technology, despite the provincial government's exploration of this technology as early as 1976 (Thompson 1977). This thesis addresses these gaps by using the Manitoba Grassland Inventory, a recently developed remote sensing product, to analyze the land cover on these crown lands and determine their carrying capacity and stocking rates for grazing.

CHAPTER 3: HYPOTHESIS AND OBJECTIVES

3.1. Hypothesis

Chapter 4: Remote sensing technology will detect lower proportions of tame grasslands than native grasslands, which may constitute the largest vegetation type in agricultural crown lands in Manitoba.

Chapter 5: Remote sensing technology will improve the estimation of stocking rates of agricultural crown lands in Manitoba, which will indicate a grazing potential for improved cattle production.

3.2. Objectives

The specific objectives of this study were to:

Chapter 4:

1. Delineate each agricultural crown land parcel in Manitoba.
2. Classify each parcel by land cover type using remotely sensed inventories.
3. Assess agreements and discrepancies in grassland classifications between remotely sensed inventories and official government records.

Chapter 5:

1. Estimate the carrying capacities and stocking rates of each agricultural crown land parcel in Manitoba using remotely sensed inventories.
2. Evaluate the relationship between climate variables and carrying capacity of crown lands through regression models.
3. Compare the estimated stocking rates to the actual stocking rates of the crown land parcels currently allowed by the provincial crown land leases.

CHAPTER 4: LAND COVER CLASSIFICATION OF CROWN LANDS IN MANITOBA, CANADA USING REMOTELY SENSED INVENTORIES

4.1. Abstract

Land cover classification is one of the most common applications of remote sensing and is used for developing and modifying land management policies on agricultural landscapes to achieve conservation and economic goals, such as reducing grassland degradation and improving livestock and crop production. In this study, the grassland classification of the crown lands (public grasslands in Canada) from a newly developed remotely sensed dataset in the Prairie Province of Manitoba (i.e., the Manitoba Grassland Inventory, MGI) was assessed in terms of accuracy by comparison to non-spatial government records. The analysis consisted of i) converting non-spatial records from the provincial crown land database to spatially-defined parcels by performing parcel delineations using geographic information system (GIS) and R programming tools, ii) summarizing the MGI classification at the same spatial scale, and iii) comparing the agreement between MGI and the crown land database. The most common land cover types identified were: forest (30%) and shrubland (25%), followed by native (10%) and tame (9%) grasslands. However, the class agreement between woody (i.e., forests and shrublands) and grassy (i.e., native and tame grasslands) vegetation classes were low between these datasets because of their spectral similarities. Based on these results, we suggest additional refinements on both sensor and ground data to improve the classification agreement between these datasets. This study is one of the first attempts to compare ground-collected government records against a remotely sensed product in Manitoba.

4.2. Introduction

Grasslands are one of the most important ecosystems on the Earth because of their several ecosystem services, such as forage production and carbon sequestration. They account

for roughly 26% of the terrestrial surface and about 70% of total global agricultural land (Conant 2010; Reinermann et al. 2020; Qin et al. 2021). The North American Great Plains contains one of the largest grassland areas in the world with Canada accounting for 16% of the total land area (Gauthier and Wiken 2003). This region, commonly referred to as the Canadian Prairies, encompasses the provinces of Alberta, Saskatchewan and Manitoba, and is home to 89% of the country's native and tame grasslands (Statistics Canada 2022c). It is currently estimated that only 25-30% of the pre-European distribution of native grasslands remains in the Canadian Prairies (Gauthier and Wiken 2003).

Grasslands provide various ecosystem services, including forage production, soil regulation (e.g., providing high soil organic matter), water regulation (e.g., sediment filtration), carbon sequestration and habitat maintenance for various species of flora and fauna (Bailey et al. 2010; Conant 2010; Pogue et al. 2018). However, disturbances, such as overgrazing, drought and conversion to cropland, have led to substantial carbon losses from grassland systems and the degradation of native grasslands (Conant 2010). The historic loss of native grasslands in the Prairies has been attributed to agricultural expansion or conversion to cropland (Samson and Knopf 1994; Doherty et al. 2018). In previous studies, annual conversion rates have been reported to range between 1% to 5% per year (Gage et al. 2016). A study by the World Wildlife Fund estimated a 1.5% annual rate of grassland conversion to cropland in the Northern Great Plains between 2009 and 2013 (Gage et al. 2016; World Wildlife Fund 2016). In addition to agricultural conversion, woody encroachment has contributed to grassland loss, particularly in Aspen Parkland, a region extending across the Canadian Prairies and serves as an ecotone between open fescue prairies and mixedwood and boreal forests. Since European settlement, the Aspen Parkland has expanded southward, particularly in southern Manitoba, due to a lack of

frequent fires, which were a natural impediment to aspen encroachment into grasslands (Ecological Stratification Working Group et al. 1995; Schütz 2010).

To prevent any further losses or degradation of grasslands in the Canadian Prairies, it is critical to monitor and assess grassland dynamics to determine stewardship and conservation activities. Traditional methods of monitoring grassland cover, such as biomass clipping, visual expert assessment and rising plate meter, are cost- and time-prohibitive because field measurements can only be taken on a local scale and require a large number of field researchers to undertake a regional survey (Ali et al. 2016; Murphy et al. 2021). Remote sensing technology allows for estimating vegetation distribution and productivity without the need for physical contact, thus, addressing the shortcomings of traditional methods while being able to detect immediate changes over a large area (Reinermann et al. 2020). Monitoring land cover using satellite imagery from optical spaceborne sensors, such as Landsat and Sentinel-2, has accelerated the modelling time to identify and discriminate various land cover classes based on their distinct surface reflectance and spectral signatures (Lu 2006; Xie et al. 2008; Shoko et al. 2016). Advanced supervised classification methods using machine learning, such as decision trees (DT) and random forests (RF), have produced higher classification accuracies than traditional classifiers, such as maximum likelihood classifier, k-means clustering and ISODATA (Xie et al. 2008; Ali et al. 2016). Advances in remote sensing technology by increasing spatial, spectral and temporal resolutions have made it suitable and attractive for monitoring complex land cover characteristics and dynamics, which supports tracking multitemporal aboveground biomass assessment and management of grasslands.

Numerous researchers in Canada have developed satellite-based land cover datasets, such as the Canada Centre for Remote Sensing's quinquennial Land Cover datasets (Latifovic 2010,

2015, 2020) and the Annual Crop Inventory (Grekousis et al. 2015; Davidson et al. 2017; Agriculture and Agri-Food Canada 2021a) but these efforts have failed to develop a nationwide grassland inventory. The closest product that delineates grassland cover across the country is the Annual Crop Inventory (ACI) created by the Agriculture and Agri-Food Canada (AAFC), which divides grassland cover into native grasses and tame forages (Canadian Forage & Grassland Association 2022). Despite the existence of ACI, there is still a need for a standalone national grassland inventory that distinguishes between native, tame and mixed grasslands.

Each province in the Canadian Prairies has its grassland inventory. Among these provinces, Alberta spearheaded the earliest grassland inventory in 1991 with its Native Prairie Vegetation Inventory (NPVI) using black-and-white aerial photographs that were mapped in a quarter section level (Environment and Parks Alberta 2012). This was further updated with the Grassland Vegetation Inventory (GVI) in 2006 using near-infrared aerial photography that was mapped based on soil polygons (Yang et al. 2017; Environment and Parks Alberta 2019). On the other hand, Saskatchewan and Manitoba have spaceborne remote sensing-based inventories developed by Grassland Analytica. Saskatchewan's Prairie Landscape Inventory (PLI) was created in 2019 using images captured by MODIS, Sentinel-1 and Sentinel -2 sensors. It was classified using the RF algorithm with an overall accuracy of 90.2% (Saskatchewan GeoHub 2021; Badreldin et al. 2021). Likewise, the Manitoba Grassland Inventory (MGI) was developed in 2020 using Sentinel-1 and Sentinel-2 images classified using the RF algorithm.

While the recent release of these remote sensing products represents a valuable asset for monitoring grasslands for conservation and management, there are no published attempts made to compare these datasets with ground-based government records in Manitoba. The main objective of this study was to compare the MGI satellite-based classification data to the

provincial crown land field records in Manitoba. The methodological approach of this study included i) delineating each agricultural crown land parcel in Manitoba, ii) classifying each parcel by land cover type using remotely sensed inventories and iii) assessing agreements and discrepancies in grassland classifications between remotely sensed data and official records.

4.3. Materials and Methods

4.3.1. Parcel delineation

The Manitoba agricultural crown land (ACL) records were stored in a database compiled by the Real Estate Services Division of the Manitoba Agriculture and Resource Development (ARD). This database contained historical information about legal land descriptions (i.e., in quarter section–section–township–range format), forage productivity index, land use codes, land cover types and cattle stocking rates (Manitoba Agriculture and Resource Development 2020a). The analysis was conducted at the quarter section level, which is a spatial unit defined by the Dominion Land Survey (DLS) to map areas in Western Canada for agricultural purposes. Quarter sections are square land parcels of roughly half-mile or 0.8 km on each side and have an area of approximately 65 ha or 0.65 km^2 (McKercher and Wolfe 1986). In some instances, some ACL parcels covered smaller parts of a quarter section.

Most of the ACL parcels were already delineated in a GIS geodatabase provided by ARD; however, some parcels required boundary refinements for their total areas to correspond to those indicated in the ACL records. Moreover, some parcels were not mapped in the ACL geodatabase; thus, the property assessment online geodatabase developed by Manitoba Municipal Relations was used as a reference for mapping the rectified and missing parcels (Manitoba Municipal Relations 2020). A semi-automated workflow for parcel delineation was developed using the R programming language (R Core Team 2020; RStudio Team 2020) and

ArcGIS (ESRI 2020). This workflow was comprised of the following steps: 1) acquiring property assessment information from the online geodatabase through web scraping, 2) aligning parcels spatially, and 3) transferring them to the original ACL geodatabase.

An R code was written to web scrape the property assessment information from the online geodatabase (Manitoba Municipal Relations 2020) for parcels requiring boundary refinements (Appendix A). Roll numbers, legal land descriptions, and total acreage were among the information scraped, which were then used to match the information from the ACL database using the Make Query Table tool on ArcGIS. Once the matched parcel records between the property assessment and the ACL databases were identified, the coordinate system of the former was transformed from WGS 84/Pseudo-Mercator (ESPG: 3857) to NAD 83/UTM zone 14N (ESPG: 26914) to match the latter geodatabase. After the coordinate system transformation, the remaining boundary distortions of the scraped property assessment parcels were automatically spatially-adjusted using a model constructed in ArcGIS ModelBuilder (Figure 3) which contained three main tools: Rubbersheet, Densify and Snap. Rubbersheeting is a technique for aligning and stretching a distorted layer with a more accurate reference layer, which is a common practice in historical geography for digitizing old maps and satellite images (Doytsher and Gelbman 1995; Shimizu and Fuse 2003). In this analysis, the cadastral mapping developed by the Manitoba Land Initiative, which contained boundaries of quarter sections and parish lots, was used as the reference layer for the property assessment layer (Manitoba Land Initiative 2018). As the rubbersheeting alone could not correct all of the distortions, the Densify and Snap tools were also used to further align the vertices of the property assessment parcels to the cadastral layer. The Densify tool was used to create additional vertices along the boundaries in order to improve the alignment with the cadastral lines when using the Snap tool. The geometries of the property

assessment parcels were transferred to the ACL geodatabase after the spatial adjustment, replacing the initially misaligned parcels. Finally, an R code utilizing the sf and dplyr packages (Pebesma et al. 2021; Wickham et al. 2021) was used to replace misaligned parcels in the geodatabase with spatially-adjusted ones (Appendix B).

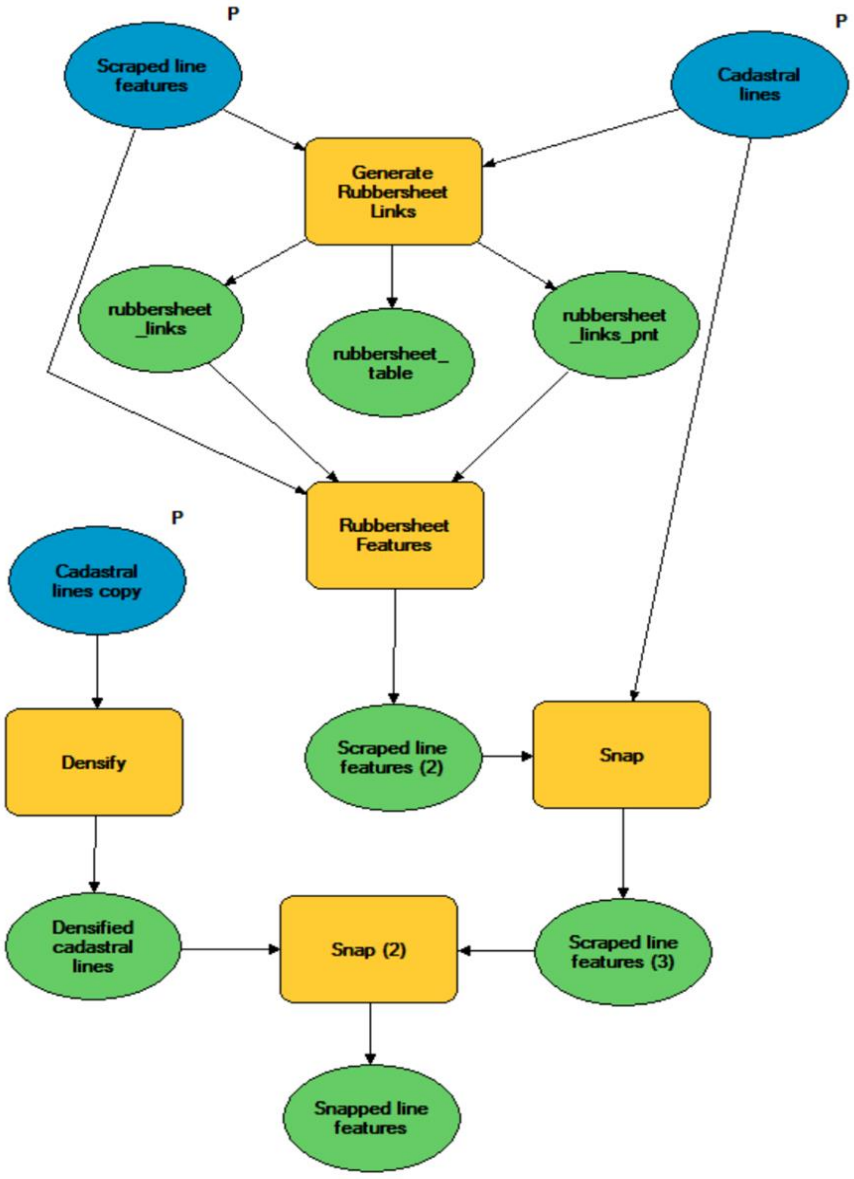

Figure 3: The spatial adjustment model created using ModelBuilder on ArcGIS.

After the spatial adjustment, there were still cases in which the areas of parcels mapped in the geodatabase differed from those recorded in the ACL database. For the purposes of this

study, any parcels with area differences greater than 2 ha (i.e., approximately 3% of the total quarter section area) were considered mapping or delineation errors and were not included in the analysis. Overall, these errors were found in 20% (3,265 parcels) of the total number of crown land parcels, which were excluded, and the study examined 13,098 parcels covering about 731,000 ha (Figure 4).

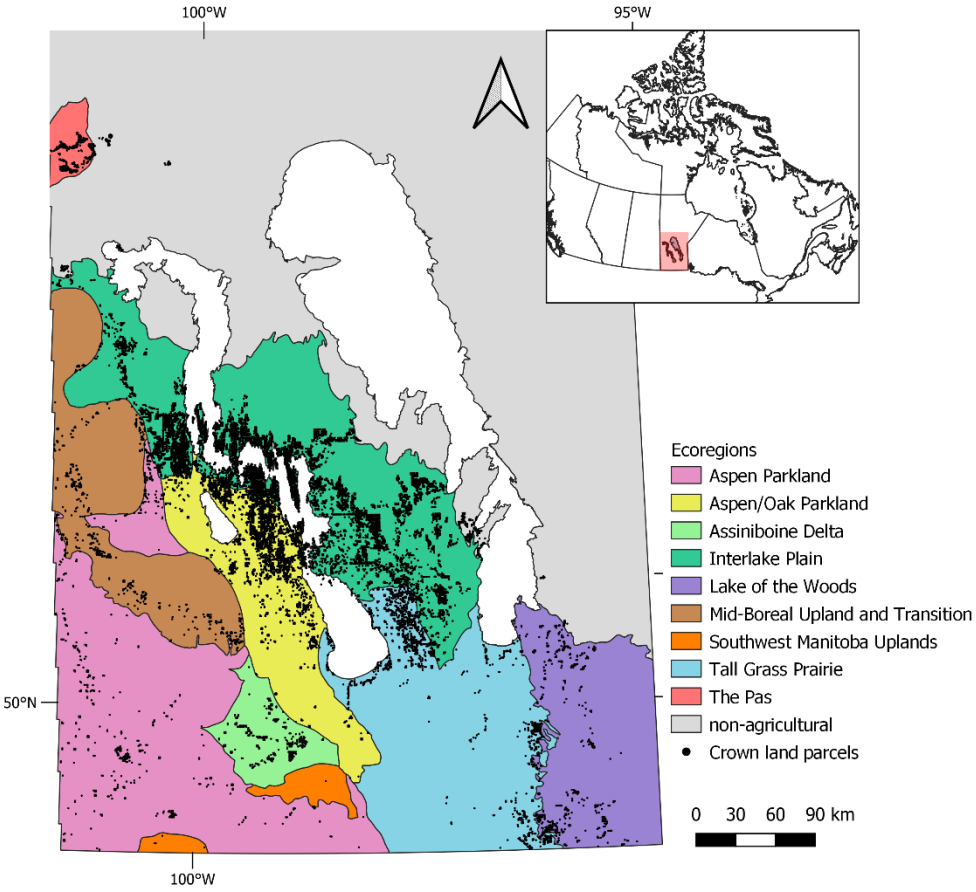

Figure 4: Locations of all agricultural crown lands in Manitoba within the nine ecoregions.

4.3.2. Grassland classification using remotely sensed inventories

Two remotely sensed inventories encompassing the whole extent of Agro-Manitoba were used to extract land cover types in each crown land parcel. The main remotely sensed inventory used to classify 75% of all parcels was the newly developed MGI with a 10-m resolution,

produced by Grassland Analytica and ARD using active SAR (synthetic aperture radar) and passive optical imagery captured in summer 2019 and 2020 from the Sentinel-1 and Sentinel-2 sensors, respectively (Grassland Analytica 2021). Its RF classification model was trained using various data sources, such as the Manitoba Agricultural Services Corporation (MASC) and the Native Pasture Improvement Project. The remaining 25% of the parcels located mostly in the northern areas of the Interlake region of Manitoba were classified using the 30-m resolution ACI (Agriculture and Agri-Food Canada 2021a). The 2020 ACI used passive optical images from Landsat-8 and Sentinel-2 sensors, which were trained and validated using data from MASC and classified using a less robust DT algorithm (Agriculture and Agri-Food Canada 2021b). To ensure that the class definitions in each dataset were equivalent, the classes in ACL, MGI and ACI inventories were aggregated into broad classes (Appendix C): native grasses, tame forages, shrubland, forest, cropland, water/wetlands and "others" (e.g., urban and barren areas). The water bodies and the wetlands were combined into a single class to avoid possible misclassification.

These remotely sensed inventories were further smoothed to remove isolated misclassified pixels or speckle using tools from ArcGIS. Majority filtering and boundary cleaning routines were first performed on a pixel-by-pixel basis. Majority filtering removed isolated pixels by reclassifying them based on the majority of the neighbouring pixels using a 3 x 3 moving window (ESRI 2020). Boundary cleaning reclassified isolated pixels within the boundaries between zones of the same value either through expansion or shrinkage of these zones, with larger zones being prioritized over smaller zones for this processing (ESRI 2020). The last set of raster smoothing tools was applied on regions or disconnected zones of the same value rather than individual pixels in which majority filtering and boundary cleaning were

previously performed. The Region Group tool identified regions of the same value and recorded the number of pixels for each one. Then, the Set Null tool assigned "NoData" values for small, isolated regions. In this case, those regions had an area of 2700 m^2 or less, which is equivalent to three 30 x 30 m pixels in ACI and 27 pixels 10 x 10 m pixels in MGI. Lastly, the Nibble tool reclassified these small "NoData" regions by the value of their nearest non-"NoData" neighbour (ESRI 2020). An example of the classification smoothing process is shown in Figure 5. The output rasters from the classification smoothing procedures were converted into vector datasets. These vectorized classified inventories were intersected with the crown land parcels to extract each land cover class within each parcel, which was achieved using the Identity tool on ArcGIS and the Collect Geometries tool on QGIS (QGIS.org 2020). The areas of land cover type in each parcel identified by the MGI and ACI were compared to the areas recorded in the ACL database and their differences were calculated on R. The classification results were summarized for the entire Agro-Manitoba and by ecoregion.

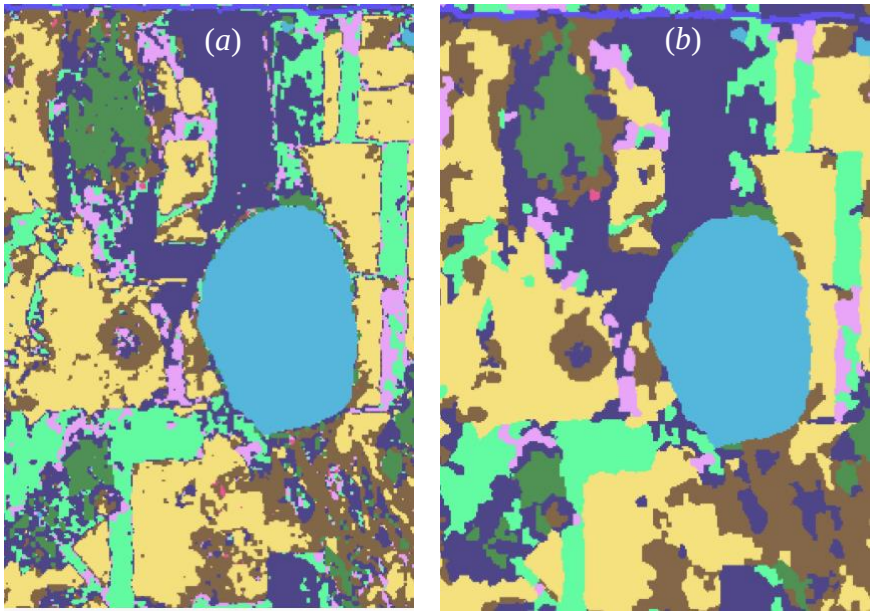

Figure 5: A portion of the original classified raster (*a*) is processed into a smoothed raster (*b*), removing isolated pixels or speckle.

4.4. Results

4.4.1. Overall classification results

We found that for the merged MGI/ACI inventories, most of the crown lands in Manitoba were classified as forest (30.43%) and shrublands (25.02%), both of which constitute woody vegetation (Table 4). These were followed by water/wetlands (22.30%), native (10.28%) and tame grasslands (9.04%). The inventories also detected cropland (2.37%) since some parcels were leased for annual cropping.

Table 4: Total areas by land cover type or class in the crown land parcels in Manitoba.

	Total area (ha)				
Class	ACL	%	MGI/ACI	%	% Diff.[1]
Native	103,815	14.21	75,144	10.28	-3.93
Tame	38,251	5.24	66,105	9.04	3.81
Grassy vegetation	*142,066*	*19.44*	*141,250*	*19.32*	*-0.12*
Shrubland	63,086	8.63	182,871	25.02	16.38
Forest	363,265	49.72	222,440	30.43	-19.29
Woody vegetation	*426,350*	*58.35*	*405,311*	*55.44*	*-2.91*
Cropland	2,081	0.28	17,315	2.37	2.08
Water/Wetlands	147,326	20.16	163,051	22.30	2.14
Others	12,832	1.76	4,102	0.56	-1.20
Total	730,655	100	731,028	100	

[1]The percentage differences or percentages of agreement between the two classifications were calculated by subtracting the percentages of each class according to their overall classification due to the minor discrepancy in the overall totals. The discrepancy of 373 ha between the overall totals was caused by including parcels with area differences between the two classifications of less than 2 ha in the analysis.

The remotely sensed classification showed large differences for the dominant cover classes when compared to the ACL dataset (Table 4). The differences varied between -19.29% for forests and 16.38% for shrublands. The percentage differences of native and tame grasslands between these datasets were -3.93% and 3.81%, respectively. When these vegetation classes were grouped into broader categories, the percentage differences decreased. When forest and shrubland were grouped into woody vegetation, the difference between the remotely sensed classification and the ACL database decreased to -2.91%. Similarly, the differences in

classification were -0.12% when native and tame grasslands were grouped into an overall grassy class. Classification of the other minor classes was at ±2% difference (Table 4; Figure 6).

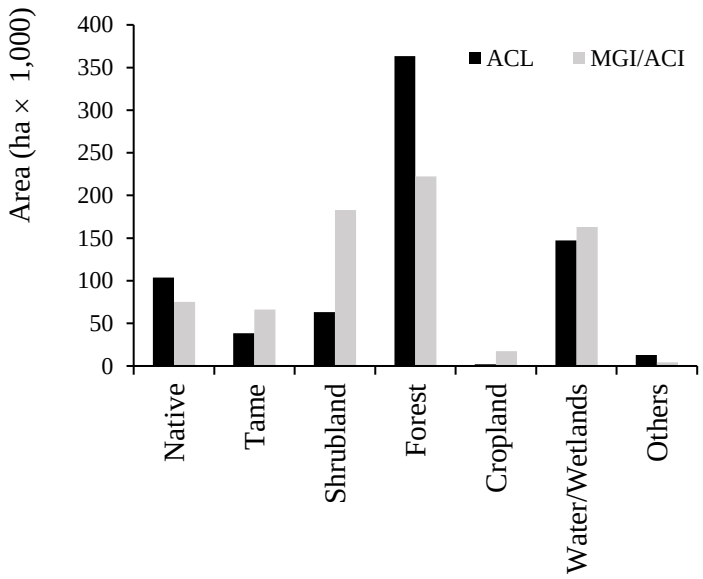

Figure 6: Total area (in ha) by land cover type between ARD agricultural crown lands (ACL) database and Manitoba Grassland Inventory/Annual Crop Inventory (MGI/ACI) classification.

4.4.2. Ecoregional classification results

Similar to the overall classification results, forest was the dominant land cover type in three ecoregions: Lake of the Woods, Mid-Boreal Upland and Transition, and Southwest Manitoba Uplands, ranging from 54% to 74% of the overall classification (Figure 7). In other ecoregions, such as Aspen Parkland, Aspen/Oak Parkland, Assiniboine Delta and Interlake Plain, woody vegetation, including shrubland, was the most common land cover type, despite that the individual forest and shrubland classes did not make up the majority of the classification. In general, woody vegetation represented between 18% and 81% of the overall crown land cover.

Native grasslands accounted for 4% to 23% of the overall crown land cover, with the highest percentage in Assiniboine Delta (Figure 7). Tame grasslands comprised between 1% and

18% across different ecoregions, with Aspen/Oak Parkland having the largest share. Overall, this grassy vegetation represented between 5% and 31% of the overall classification. On the other hand, water/wetlands was the largest class in Tall Grass Prairie and The Pas.

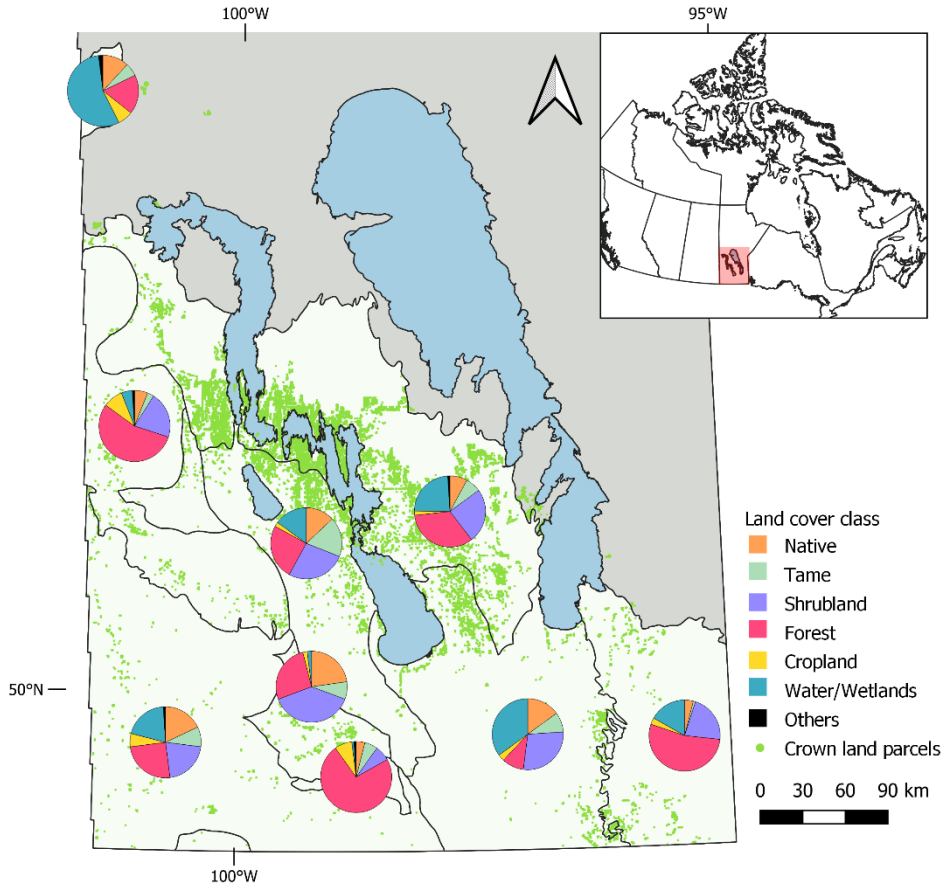

Figure 7: Class percentages by ecoregion based on Manitoba Grassland Inventory/Annual Crop Inventory (MGI/ACI) classification as shown in pie charts. Actual percentages can be found in Appendix D.

4.5. Discussion

The comparison of the ground-collected ACL and the remotely sensed MGI/ACI classification datasets in this study revealed class agreements and disagreements within the agricultural crown lands of Manitoba. The lack of class agreement between these datasets was prominent in woody vegetation, which occupies the majority of land cover of the crown lands.

The weak agreement of these woody classes stemmed from ACL having a larger coverage of forest in ACL (49.72%) compared to MGI/ACI (30.43%) and a considerably smaller coverage in shrublands (8.63%) than MGI/ACI (25.02%). Despite this, the user's and producer's accuracies of shrubland and forest in the overall MGI classification ranged between 70% and >90%, showing a strong agreement with reference ground data. Similar to MGI's data fusion approach, a study that combined Sentinel-1 active SAR and Sentinel-2 passive optical images, found that forests, shrubs and pastures have lower spectral separability, making them difficult to discriminate (Campos-Taberner et al. 2019). However, those authors found that the inclusion of Sentinel-1 SAR data improved the classification accuracies and the discrimination of these classes, in contrast to using only Sentinel-2 optical data.

The original MGI version, which was used to classify 75% of all crown land parcels, recorded an overall accuracy of 96.65%, which was comparable to the results of Saskatchewan's 2019 PLI results, which achieved an overall accuracy of 90.2% following a similar RF classification methodology (Badreldin et al. 2021). The accuracy assessment of the overall MGI classification employed a reliability map in its methodology, which showed where errors may exist in the classification. Very low to moderate reliabilities were identified in most northern regions of Agro-Manitoba, which had a significant effect on the disagreement of MGI with the ACL database because the majority of the crown lands were located in these areas (Manitoba Agriculture and Resource Development 2021).

Although active SAR data from spaceborne Sentinel-1 can provide structural and canopy height information, airborne active LiDAR (light detection and ranging) data could support the MGI/ACI classification in the discrimination between shrubs and trees. Many studies have reported an increase in classification accuracy with the inclusion of LiDAR data to passive

optical data, such as Landsat-8 and Sentinel-2, but one should note that LiDAR-only classification fared significantly worse than passive optical-only classification (Fassnacht et al. 2016). Li et al. (2017) noted that estimating biomass solely from LiDAR data can be a disadvantage when different species have similar structural arrangements but significantly different aboveground biomass (e.g., young trees can be misclassified as shrubs just based on similar height thresholds). Canopy height metrics derived from LiDAR are also not good predictors of tree species classes as they are mainly correlated to tree age, site conditions and competition (Ghosh et al. 2014; Fassnacht et al. 2016). Despite this, LiDAR data can adequately capture the height variability within sparse vegetation, such as in semi-arid shrublands (Li et al. 2017). Furthermore, LiDAR-derived height metrics can improve the classification of younger trees, when used synergistically with passive optical data (Fassnacht et al. 2016).

On the other hand, the ability of LiDAR to discriminate grasses has been found to be limited (Li et al. 2017). Grass biomass was poorly detected by LiDAR due to their short structural arrangements which caused a low number of return signals. Furthermore, it was found that grasses were often confused with the soil background (Li et al. 2017) or with shrubs (Fassnacht et al. 2021). The availability of LiDAR in the province can pose a problem due to its absence in other parts of Agro-Manitoba, particularly the Parkland, northern Interlake and The Pas regions (Manitoba Land Initiative 2021).

Studies have demonstrated that multispectral sensors, particularly Sentinel-2, can adequately capture and discriminate between different grass types without the use of LiDAR-derived canopy height metrics. Due to the presence of red-edge bands and improved spatial resolution, most of these studies highlighted the superior performance of Sentinel-2 over Landsat-8 (Chaves et al. 2020), with the former sensor being employed by MGI and the latter by

ACI. The red-edge bands are located in a region of transition from strong chlorophyll absorption to large near-infrared reflectance (Mutanga and Skidmore 2004). Shorter wavelengths of the red-edge portion, which are closer to the red bands, are sensitive to chlorophyll concentration, while the longer wavelengths, which are closer to the near-infrared bands, are sensitive to internal leaf scattering (Mutanga and Skidmore 2004; Chaves et al. 2020). With these properties, red-edge bands have been shown to improve the accuracy of biomass estimates and allow feature separability in heterogenous environments (Chaves et al. 2020). Using Sentinel-2, Filho et al. (2020) recorded higher accuracies for estimating natural grassland biomass when using red-edge vegetation indices than those without red-edge bands. Sentinel-2 and WorldView-2 also outperformed Landsat-8 in classifying and discriminating C_3 and C_4 grasses, which differs in photosynthetic pathways and phenologies, due to the red-edge bands in both sensors (Shoko and Mutanga 2017a, 2017b). Otunga et al. (2019) also found that the inclusion of red-edge bands improved the classification accuracies of both Sentinel-2 and RapidEye sensors in discriminating between C_3 and C_4 grasses. On the other hand, Radoux et al. (2016) noted that the Sentinel-2's red-edge bands did not significantly improve class separability in contrast to other bands.

The harmonized Landsat and Sentinel (HLS) data, as used by the ACI, can offer an alternative in land cover mapping, as multi-sensor data can bridge long data gaps with high cloud cover (Chaves et al. 2020; Misra et al. 2020). Wang et al. (2019) noted that the HLS data predicted the seasonal dynamics of the aboveground biomass of tallgrass prairie better than single-sensor data. It should be noted that in Manitoba, the 2020 ACI, which was used for 25% of all parcels in the northern outskirts of the Interlake region, only achieved 68.97% overall accuracy for non-crop classes, which includes the major classes of grasses, shrubs and forests (Agriculture and Agri-Food Canada 2021b). This is understandable given that this inventory is

focused on accurate crop classification, with overall provincial accuracies exceeding 85%, with 93.47% recorded in Manitoba, owing to consistent validation with crop insurance data. On the other hand, training and validation data for non-crop classes, such as grasslands and forests, are derived from past AAFC land cover and land use products (Agriculture and Agri-Food Canada 2021b).

The lack of class agreement between ACL and MGI/ACI datasets was also seen in the discrimination between native and tame grasslands. The MGI/ACI classification detected similar area percentages of native and tame grasslands of 10% and 9%, respectively, while the ACL database recorded 14% native and 5% tame grasslands. The trend of a significantly larger coverage of native grasslands compared to tame grasslands in the ACL database was also reported in other previous assessments from the literature. Kulshreshtha et al. (2015) identified a larger land cover for native grasslands (184,100 ha) than tame grasslands (41,379 ha) in Manitoba crown lands compiled from various government sources. Despite this, the user's and producer's accuracies of grasslands in the overall MGI classification ranged from >70% to >90%, with mixed grasslands having the lowest class accuracies of less than 70%.

It is always assumed that the ground truth or reference data are the accurate representation of reality but they may also contain errors (Foody 2002). The ACL database was compiled based on the traditional field sampling methods compared to the remotely sensed MGI/ACI database. The former includes visual estimation, which can be highly subjective and prone to operator bias because quantifications were done by different crown land specialists and range managers (Ali et al. 2016; Murphy et al. 2021), while the latter was satellite-generated imagery built upon machine learning approaches. Furthermore, the sampling units in ground data

collection are often different from the minimum mapping unit captured by a remote sensor (Foody 2002).

Another factor influencing the disagreement between MGI/ACI and ACL datasets may be the sampling frequency of the crown lands. The ARD only inspects their leased pastures when they are released and put up for allocation or auction, as opposed to annually (T. Gillis, personal communication, 2022). Prior to 2020, lease terms lasted until the lessee reached the age of 65 but after regulatory reforms, new lease terms are now capped at 15 years before being released for reallocation. This means that all crown lands will eventually cycle through an auction and inspection every 15 years (Manitoba Agriculture and Resource Development 2019; T. Gillis, personal communication, 2022). Currently, it is estimated that less than 5% of all crown lands are put up for allocation every year and thus, only these many parcels are assessed for land cover annually (T. Gillis, personal communication, 2022). The assessment intervals for the ACL data are therefore irregular and variable, which likely influenced the agreement with the satellite classifications. The latter have more frequent, complete and synchronous coverage over the entire region in the study. This could be an issue, especially when plant communities undergo an ecological succession, which involves changes in the species composition of an ecosystem by replacing the current plant species (Odum 1971). In a temperate forest biome, grasslands can serve as early developmental or seral communities before transitioning to a forest climax community. Ecological succession can take hundreds of years to establish a mature climax community or as little as a few decades if the process is secondary succession (Odum 1971). In the absence of disturbances, such as fires and grazing, woody encroachment in the crown lands would represent a secondary succession from grasses to shrubs (Schütz 2010). While secondary succession is a possibility, the class disagreements may be influenced more by the asynchrony of

assessment intervals between ACL and MGI/ACI, with the former being classified irregularly and the latter using 2019 and 2020 imagery. Agreement between these datasets may improve if the crown land parcels were classified contemporaneously.

Errors in the class agreement may also arise from different class definitions (Foody 2002) as they vary between the ACL and MGI/ACI datasets. The definitions of grassland classes are not uniform among these datasets. The ACL database divides native grasslands into three classes depending on elevation, which influences the grass species that grow in upland and lowlands. Furthermore, the MGI also includes a mixed grasslands class which is defined as containing less than 75% native or/and less than 75% tame grasses (Badreldin 2021). Studies have found that greater classification complexity or the number of specific classes used led to a decrease in classification accuracy, partly due to the increasing presence of mixed pixels (Castilla et al. 2014; Yu et al. 2014). The use of a fuzzy or soft classification approach is seen as an alternative for dealing with mixed pixels. This approach provides probabilities of class membership instead of the standard hard classification of discrete and mutually exclusive classes, which can be beneficial for mapping vegetation transition or continuum (Foody 2002; Xie et al. 2008). Alberta's GVI used percentages of land cover in each of its landscape polygons, instead of assigning only one class (Alberta Sustainable Resource Development 2010).

Despite these disagreements in the dominant classes, both datasets agreed well in minor classes, such as croplands and water/wetlands, with less than a 2% difference between them. Additionally, the combined woody and grassy vegetation classes also recorded less than a 2% difference, particularly with the grassy vegetation differing by -0.12%. This shows the capability for both ground-collected and remotely sensed datasets to agree on classification. In most cases, the performance of remotely sensed classification is assessed using a confusion matrix or

contingency table with ground truth data (Lillesand et al. 2015). Accuracy measures, such as user's and producer's accuracies, are then derived from this matrix to further analyze class accuracies. This kind of analysis was not feasible due to the non-spatially explicit classification of ACL; however, the small 2% difference between these datasets offers a glimpse into the good performance and capability of remotely sensed data in classifying vegetation and land cover.

The insights gained from this study are relevant to the current efforts to develop other grassland products in Canada, including a national grassland inventory. However, other challenges must be addressed to that end as well. First, a large-scale grassland inventory carried out in different geographic areas requires a standardized methodology for defining and classifying different vegetation types. Additionally, field surveys for ground-truthing need a consistent sampling protocol that can be applied in all areas (Canadian Forage & Grassland Association 2022). Error from reproducibility bias can be reduced by adhering to a robustly designed sampling protocol (Murphy et al. 2021). Developing a comprehensive grassland inventory would present new opportunities for evaluating the value of ecosystem services of grasslands, such as carbon sequestration and forage production. Kulshreshtha et al. (2015) found that 250.5 million tons of carbon were sequestered by Manitoba's grasslands annually based on the estimated total grassland area. Remote sensing technology can provide a greater opportunity for accurate land cover monitoring, especially on a regional level, which has the potential to improve the estimates of grassland ecosystem services.

4.6. Conclusions

In this study, we used two remotely sensed datasets in mapping the land cover or vegetation in the crown lands of Manitoba and compared them against ground-collected government records. To date, there have been no published attempts in validating the ACL

against a remotely sensed product. We found that there were class disagreements between the ACL and the remotely sensed MGI/ACI classification, particularly in woody and grassy vegetation. Potential reasons causing these disagreements were the non-uniform terminology defining grassland classes, sampling bias and frequency. These results suggest possible refinements on both sensor and ground data that could enhance the classification agreement between these datasets. Future research should focus on incorporating LiDAR data and recent ground-truthing data based on standardized protocols to improve the classification of these classes.

In recent years, there has been a renewed interest in creating a comprehensive inventory solely for grasslands to track its land cover changes and aid in the development of conservation and management policies. Remotely sensed products, such as the MGI, are an integral part of future efforts to develop these inventories, which can be used to estimate appropriate sustainable stocking rates and identify areas of potential undergrazing or overgrazing. However, these products have to be assessed in order to keep a continuous improvement in terms of quality and reliability. In the future, the MGI methodology can provide a framework for the development of a national grassland inventory in Canada, which will be crucial for monitoring different grassland ecosystem services, such as forage production, and guiding land management policies.

BRIDGE TO CHAPTER 5

As suggested earlier, vegetation classification derived from remotely sensed datasets can be used to estimate the carrying capacity and the stocking rates of grasslands. The following chapter used vegetation distribution maps in Chapter 4 obtained from MGI and ACI inventories to estimate the carrying capacity and the stocking rates of the agricultural crown lands in Manitoba. Furthermore, their grazing rates were assessed in comparison to the current lease contracts allowed by the provincial government.

CHAPTER 5: ESTIMATION OF CARRYING CAPACITIES AND STOCKING RATES IN CROWN LANDS OF MANITOBA, CANADA

5.1. Abstract

Agricultural crown lands in Manitoba, Canada have been largely used for grazing beef cattle, specifically the cow-calf herd. Stocking rates, expressed in animal unit months (AUM), were determined by the provincial government based on the sustainable carrying capacities for a given grazing period to avoid overgrazing and grassland degradation. The objective of this study was to assess the grazing status of agricultural crown lands in Manitoba by estimating current carrying capacities (AUM/ha) through available biomass yield data and remotely sensed grassland inventories. Aboveground biomass sampling was carried out in different years throughout the province and was used to determine grassland productivity. The remotely sensed Manitoba Grassland Inventory (MGI) and Annual Crop Inventory (ACI) were used to determine the vegetation or land cover types in each crown land parcel. The sampled average carrying capacities were interpolated across the agricultural region of the province or Agro-Manitoba and were used to estimate the stocking rates of each parcel based on land cover type, ecosite and climate variables. Several regression models, including linear regression models and generalized additive models (GAM), were used to assess the relationship between carrying capacities and climate variables, which revealed a nonlinear relationship. Average carrying capacities by ecoregion ranged from 0.71 AUM/ha in the Lake of the Woods to 1.99 AUM/ha in Aspen/Oak Parkland. Overall, the forage resources of the agricultural crown lands in Manitoba were being undergrazed by -44.64%. Only two of the nine ecoregions were overgrazed: Lake of the Woods and Mid-Boreal Upland and Transition.

5.2. Introduction

Since ancient times, meat has been a significant source of protein for omnivorous human diets, with beef being one of the major types (Geiker et al. 2021). Global rates of meat consumption have been declining, with 2.9% between 1961 and 2007 and 1.3% forecast from 2005-07 to 2050 (Alexandratos and Bruinsma 2012). Despite the slower growth, global meat consumption is still expected to increase due to the increased economic development and rising incomes in developing countries. Consequently, meat production is anticipated to rise from 258 Mt in 2005-07 to 455 Mt in 2050, with developing countries accounting for 70% of the total production.

Global beef production is projected to increase from 64 Mt in 2005-07 to 106 Mt in 2050 (Alexandratos and Bruinsma 2012). In Canada, beef production is an important livestock commodity and continued to be the most consumed red meat with 18.1 kg per person in 2019 (Patrice and Lamboni 2020). In 2021, the Prairie Provinces accounted for 83% of the total national beef production, with Manitoba being the third-largest beef-producing province. The beef industry in Canada is dominated by cow-calf enterprises that produce calves for future sale, which account for 64% of all operations in 2021 (Hoar and Angelos 2015; Statistics Canada 2022a). In the same year, Manitoba was home to 12% of the total herd for cow-calf operations in the country, generating $71 million in gross revenue from the sale of calves (Statistics Canada 2022a, 2022b).

Raised calves are heavily reliant on forage grazed from pastures as the main dietary requirements during the summer and shoulder seasons (Marx 2008), with crown lands in the Prairie Provinces being used for this purpose along with privately-owned lands. Crown lands in Manitoba are rented out through a provincial leasing program every summer and as of 2019,

about 1,750 leaseholders used these parcels for grazing (Manitoba Agriculture and Resource Development 2019a). The province's leasing program bases its rents on the average sale price of a 45-kg beef and the stocking rate of the parcel (Manitoba Agriculture and Resource Development 2020b). The stocking rate, or the number of animal unit months (AUM), that the parcel is capable of producing in an average year, depends heavily on a carrying capacity. Carrying capacity considers the ecological health of the land, taking into account the grassland productivity, site ecology and animal requirements (Qin et al. 2021). Assessment of carrying capacity is critical to regulate sustainable stocking rates and prevent overgrazing, which can lead to grassland degradation.

Currently, the agricultural crown lands in Manitoba used for grazing leases are only assessed by field inspection or forage clippings when they are released and put up for allocation or auction, rather than on an annual basis (T. Gillis, personal communication, 2022). The field assessments result in the identification of land cover types and the determination of their respective stocking rates. After the leasing program reforms in 2020, new leases will expire after 15 years before being released for reallocation, implying that a crown land parcel will go through a maximum 15-year cycle before being reassessed (Manitoba Agriculture and Resource Development 2019; T. Gillis, personal communication, 2022). Currently, less than 5% of all crown lands are reallocated and reassessed for land cover and stocking rates annually (T. Gillis, personal communication, 2022). In comparison to traditional field surveys conducted on crown lands by the provincial leasing program, remote sensing technology allows for biomass estimations with faster data acquisition over large areas (Ali et al. 2016; Murphy et al. 2021). Some studies have estimated forage yields from remote sensing products and used these data to

estimate carrying capacity and stocking rates of grasslands, such as Yu et al. (2010) and Qin et al. (2021).

Remotely sensed assessments of grazing capacities and stocking rates are even more critical for Manitoba as the Province has recently implemented a strategy, the Manitoba Protein Advantage, to expand the animal and plant protein industries through research and innovation, which will require increasing the productivity of agricultural lands. One of the goals of this strategy is to increase animal protein processing by 35% while reducing the carbon footprint per kilogram of animal protein by 15% and increasing the productivity of crown lands and privately-owned pastures also by 15% (Manitoba Agriculture and Resource Development 2019b).

Given the availability of newly developed remotely sensed products in Manitoba and the goal to sustainably increase meat production in the province, the main objectives of this study were to i) estimate the carrying capacities and stocking rates of each agricultural crown land parcel in Manitoba using recently developed remote sensing products, ii) evaluate the relationship between climate variables and carrying capacity through regression models and iii) compare the estimated stocking rates to the actual stocking rates of the crown land parcels currently used by the provincial leasing program.

5.3. Materials and Methods

5.3.1. Land cover classification

Land cover rasters were used to obtain information about vegetation types and other land cover classes for each crown land parcel. The first version of the Manitoba Grassland Inventory (MGI) with a 10-m resolution was used to classify the majority of the parcels using images from the Sentinel-1 and Sentinel-2 sensors (Grassland Analytica 2021). A second dataset, the 30-m Annual Crop Inventory (ACI), derived from Landsat-8 and Sentinel-2 images (Agriculture and

Agri-Food Canada 2021a), was applied in areas not covered by MGI, which are concentrated in the northern section of the Interlakes. The raster inventories were converted into vector data and intersected with the crown land parcel vector data to extract their land cover information and location. All raster operations were performed in ArcGIS (ESRI 2021).

5.3.2. Forage yield collection

Available forage dry matter (DM) yield data from three separate field surveys conducted in different time periods were used to assess the productivity of the crown lands. The first data source was the Manitoba Forage Benchmarking Project, which was a large-scale field campaign organized by the Manitoba Agriculture, Food and Rural Initiatives (now known as Manitoba Agriculture and Resource Development or ARD) and the Manitoba Forage Council (currently, the Manitoba Forage and Grassland Association or MFGA). The project was carried out from 2004 to 2009 to collect baseline forage yield data from native rangelands (Agriculture and Agri-Food Canada 2019). Forage clippings were obtained from 240 grazing enclosures in 12 sites distributed within 4 of the 9 ecoregions and 8 of the 21 ecosites in the province as illustrated in Figure 8. They were clipped once in June and August to simulate a twice-over grazing system annually (Manitoba Sustainable Agriculture Practices Program 2010). Each cage covered an area of 1 m^2 and was sampled according to vegetation type. In the present analysis, these vegetation types were reclassified to broad land cover types in accordance with the MGI and the ACI. The vegetation types of upland, lowland and transitional grasslands are equivalent to the broad native grassland class in the remote sensing products, while open woodland corresponds to the shrubland class and woodland corresponds to the forest class (Appendix C).

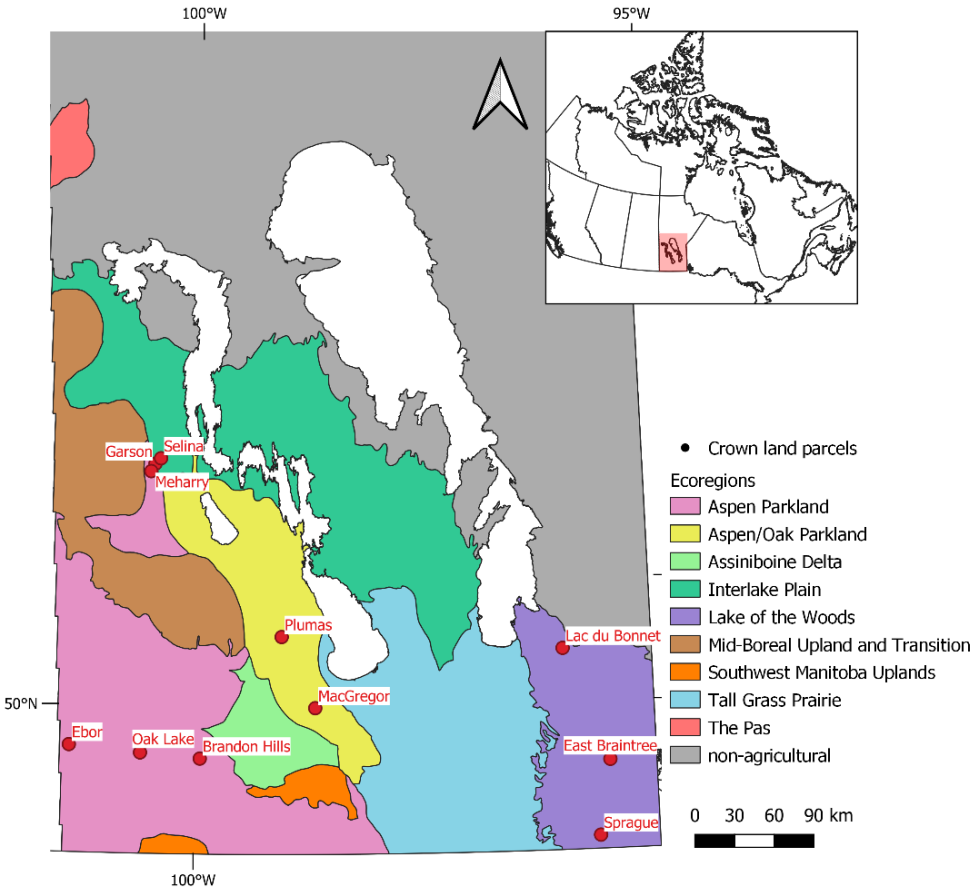

Figure 8: Field sites of the Manitoba Forage Benchmarking Project within the nine ecoregions.

The other two field surveys were carried out to determine the productivity of tame pastures. The Gopher Project was conducted by the Agriculture and Agri-Food Canada (AAFC)'s Brandon Research Centre in 2013 using 1.5 x 1.5 m grazing enclosures that followed a rotational grazing system (Agriculture and Agri-Food Canada 2020). Three samples were collected from 10 paddocks, six of which contained grass-legume mixtures of alfalfa (*Medicago sativa*), meadow bromegrass (*Bromus riparius*) and Kentucky bluegrass (*Poa pratensis*), and four of which had all-grass mixtures of meadow bromegrass and Kentucky bluegrass. The final field survey was also conducted by AAFC as part of their Living Labs initiative north of Darlingford, Manitoba in 2020 using 0.5 x 0.5 m quadrats that followed rotational and hay grazing systems (Agriculture and Agri-Food Canada 2020). Five samples were taken from each

of the four rotationally grazed pastures and one hay field at two different dates during the growing season, (i.e. once during their peak productivity and another at the end of the growing season, to measure biomass residue for fall regrowth analysis). The rotational pastures were dominated by smooth bromegrass (*Bromus inermis*), alfalfa and cicer milkvetch (*Astragalus cicer*), whereas meadow bromegrass, alfalfa and cicer milkvetch dominated the hayfield.

5.3.3. Carrying capacity assessment

Forage yield data collected from different field surveys were used for the carrying capacity assessment of the crown lands. The calculation of carrying capacities for rangelands was adjusted by applying proper use factors or utilization rates (Table 5). These adjustments, adopted from the benchmarking project (Agriculture and Agri-Food Canada 2019), account for annual carryover or amount of forage left after the grazing season, along with forage consumption based on vegetation type (either native grasses, shrubland or forest) and ecosite under moderate grazing management:

Table 5: Forage utilization rates used for adjusting rangeland carrying capacities.

	Vegetation type				
Ecosite	Lowland grassland	Upland grassland	Transitional grassland	Open woodland	Woodland
Clay	—	0.55	0.55	0.55	0.30
Loam	—	0.55	—	0.55	0.30
Moist Loam	—	0.40	0.55	0.40	0.30
Moist Sand	—	0.40	0.55	0.40	0.30
Sand	—	0.35	—	0.35	0.30
Sandy Loam	—	0.40	—	0.40	0.30
Shallow Marsh	—	—	—	—	—
Wet Meadow	0.30	—	0.30	—	—

The average measured biomass for both Gopher and Living Lab surveys was used as a constant for calculating the carrying capacity for all tame pastures across the province. A 50%

forage utilization rate was also applied for tame pastures, regardless of their underlying ecosites, which is considered an ecologically sustainable rate that would allow carryover of the remaining biomass for the maintenance of other ecological functions of the grasslands (e.g., nutrient cycling, hydrological function, etc.) (Alberta Sustainable Resource Development 2004; Legesse et al. 2018).

The carrying capacity (*CC*) of the grazed crown lands was calculated in terms of animal unit months per hectare (AUM/ha). An animal unit month (AUM) is defined as the amount of forage consumed in a month by a 454-kg mature cow with or without a calf which totals to 355 kg; therefore, one AUM equals 355 kg of forage (Society for Range Management 1998). The *CC* is calculated using the following equation:

$$CC = \frac{FY * UR}{DM} \quad (1)$$

where *FY* is the average forage dry matter yield (kg/ha), *UR* is the utilization rate (%) and *DM* is the monthly dry matter forage requirement for one AUM (355 kg). As the Manitoba Forage Benchmarking Project did not sample 13 ecosites, the recommended carrying capacities from the Manitoba Rangeland Classification were used for the missing ecosites (Thorpe 2014b). The recommended carrying capacities were derived from historical stocking rates of Prairie Farm Rehabilitation Administration (PFRA) community pastures in Manitoba as well as comparable sites in Saskatchewan and North Dakota. These are intended to provide baseline estimates of ecologically sustainable values for each ecosite, which must be adjusted to account for local factors, such as rangeland health and climate conditions. For parcels not covered by the ecosite vector layer (Thorpe 2017), predominantly in northern Agro-Manitoba, the average carrying capacities for the entire vegetation type of the assigned sampling site were used. The estimated

average carrying capacities by sampling site, ecosite and vegetation class are found in Appendix E.

5.3.4. Ecoregions and ecosite classification

In addition to the vegetation types identified by remote sensing products, distinctive local properties, such as soil types, categorized into ecosites were a major factor in determining the carrying capacities of the crown lands. The rangeland sites were sampled based on ecoregions and ecosites defined by the Manitoba Rangeland Classification (Thorpe 2014b). The National Ecological Framework for Canada defines an ecoregion as one that is characterized by distinctive ecological factors related to climate and physiography (Ecological Stratification Working Group et al. 1995). The ecoregions in the rangeland classification mirrored most of the ecoregions established in Agro-Manitoba under the national ecological framework. Modifications were made in the ecological framework's ecoregions of Aspen Parkland, Lake Manitoba Plain and Interlake Plain to align with the Natural Regions map developed by Manitoba's Protected Areas Initiative (Thorpe 2014b; Ecological Stratification Working Group and Manitoba's Protected Areas Initiative 2013; Manitoba's Protected Areas Initiative 2005). The Assiniboine Delta was separated from Aspen Parkland, and the Lake Manitoba Plain was divided into Aspen/Oak Parkland and Tall Grass Prairie. The eastern boundary of Tall Grass Prairie was extended to border the Lake of the Woods, reducing the area of Interlake Plain to the north of Tall Grass Prairie. The Pas ecoregion was also established out of the Mid-Boreal Lowland to encompass the agricultural lands in the northern Manitoba municipalities of Kelsey and The Pas.

The ecoregions were further subdivided into ecosites or ecological sites that have specific local soil and physical characteristics, which differ from one another in their ability i) to produce

a distinctive kind of vegetation and ii) to respond to management practices and natural disturbances (Caudle et al. 2013). Different ecosites exhibit local differences in soil properties, topography, moisture regime and salinity. The ecosites developed by the rangeland classification were viewed as a broad simplification of soil map units of the Manitoba Soil Survey, which has resulted in some ecosites being named after soil types (Thorpe 2014b). The rangeland classification estimated sustainable carrying capacities for each ecosite based on the productivity data from the benchmarking project, which sampled 8 of the 21 ecosites. Unknown productivity of the missing ecosites was estimated in relation to those measured in sampled ecosites (Thorpe 2014b).

5.3.5. Interpolation of carrying capacities using climate data

The estimated carrying capacities from sampled sites were interpolated for crown land parcels. Average carrying capacities were assigned to each parcel based on the similarities of their historical climate normals from 1991 to 2020 (Wang et al. 2016) with those estimated at each sampling site. The association between historical climate normals and carrying capacities of grasslands is analogous to the relationship between climate and vegetation productivity, as carrying capacities are derived from productivity (Schellenberg et al. 1999). Thorpe et al. (2008) evaluated the relationship between forage production and climate variables using regression analyses and modelled the impact of climate change on the carrying capacity of grasslands in the Canadian Prairies.

The climate variables for each crown land parcel and sampling site were estimated using reference climate grids that were interpolated using the Parameter Regression of Independent Slopes Model (PRISM), the same method used in the climate analysis of ecoregions of the rangeland classification (Thorpe 2014b). The PRISM assumes that for a local area, elevation is

the most important factor in the distribution of climate variables such as temperature and precipitation. For each pixel in the digital elevation model (DEM), PRISM calculates a linear climate-elevation regression using adjacent weather stations which can be interpolated in areas lacking historical climate data. This model has a station weighting function to account for climate variability across the landscape, such as proximity to water bodies, and cold air pools, as well as windward and leeward mountain slopes with leeward slopes suffering rain shadows (Daly et al. 2008).

The climate variables in the 4 x 4 km PRISM gridded data were further refined to scale-free point data and generated from the ClimateNA application developed by Wang et al. (2016). ClimateNA downscaled the PRISM data using a combination of bilinear interpolation and elevation adjustments. The bilinear interpolation converted the PRISM grid into a seamless surface, eliminating the step-like appearance caused by gridded data. The step-like appearance is more prominent along the boundaries of pixels, which acts as a transition between lower and higher data values like from colder to warmer temperatures. The generated seamless surface was adjusted based on elevation using empirical lapse rates that vary depending on location, elevation and climate variable of interest. This elevation adjustment enhanced the predictive accuracy at specific sites as it reflects climate gradients related to topography (Wang et al. 2012, 2016).

The climate variables used for analysis and generated from the ClimateNA application (Wang et al. 2016) for each sampling site and crown land parcel were:

i. mean annual temperature or MAT (°C)
ii. mean annual precipitation or MAP (mm)
iii. mean May-to-September precipitation or MSP (mm): selected to represent the annual total precipitation during the growing season

iv. growing degree-days (GDD) or degree-days above 5°C: the mean annual total heat accumulation determined by the number of degrees Celsius (°C) that each mean daily temperature is above the base temperature of 5°C during the growing season and calculated as $\frac{T_{max} - T_{min}}{2} - 5°C$. This variable is also a good weather indicator for predicting plant development stages (Edey 1977). As GDDs are based on daily weather data which are not always available in all weather stations, ClimateNA applied a piecewise function to estimate monthly GDD based on the relationship between GDD calculated from daily observations and GDD estimated from monthly data. The estimated monthly GDD was then summed on an annual basis (Wang et al. 2016).

v. Hogg's climate moisture index or CMI (mm): the mean difference between annual precipitation and potential evapotranspiration (PET) calculated from the simplified Penman-Monteith equation (Hogg 1997). This variable was selected because studies have shown that it is a strong drought indicator due to its ability to delineate moisture regimes within arid regions such as the Canadian Prairies. It was able to correlate positive CMI values, (indicating moist areas), to boreal forests and negative values, (indicating dry areas), to grasslands (Hogg 1994, 1997).

Aside from the climate variables, the object ID of the nearest sampling site was also added as a variable which was determined using the Near tool on ArcGIS (ESRI 2021). Each crown land parcel was assigned to a sampling site or a combination of sampling sites from where the average carrying capacities were obtained. The sampling sites were assigned based on the similarity index calculated from the climate variables and the nearest sampling site ID using ArcGIS's Similarity Search tool. This tool has three methods for calculating similarity indices, and the method that calculates the sum of squared standardized attribute value differences was used. This

method first standardized all six variables for both sampling sites and crown land parcels to common, unitless Z-scores. Then, the difference between the standardized variables of the sampling site and each parcel was calculated. All variable differences were squared and added together to produce the parcel's similarity index to the sampling site. The smallest similarity index indicates the most similar sampling site to the parcel in terms of climate variables and distance (ESRI 2019). The procedure was performed 27 times to account for every potential similar single site and site combinations and resulted in the assignment of sampling sites for each crown land parcel (Figure 9). Average carrying capacities from the most similar sampling site were used to calculate the stocking rates of each parcel.

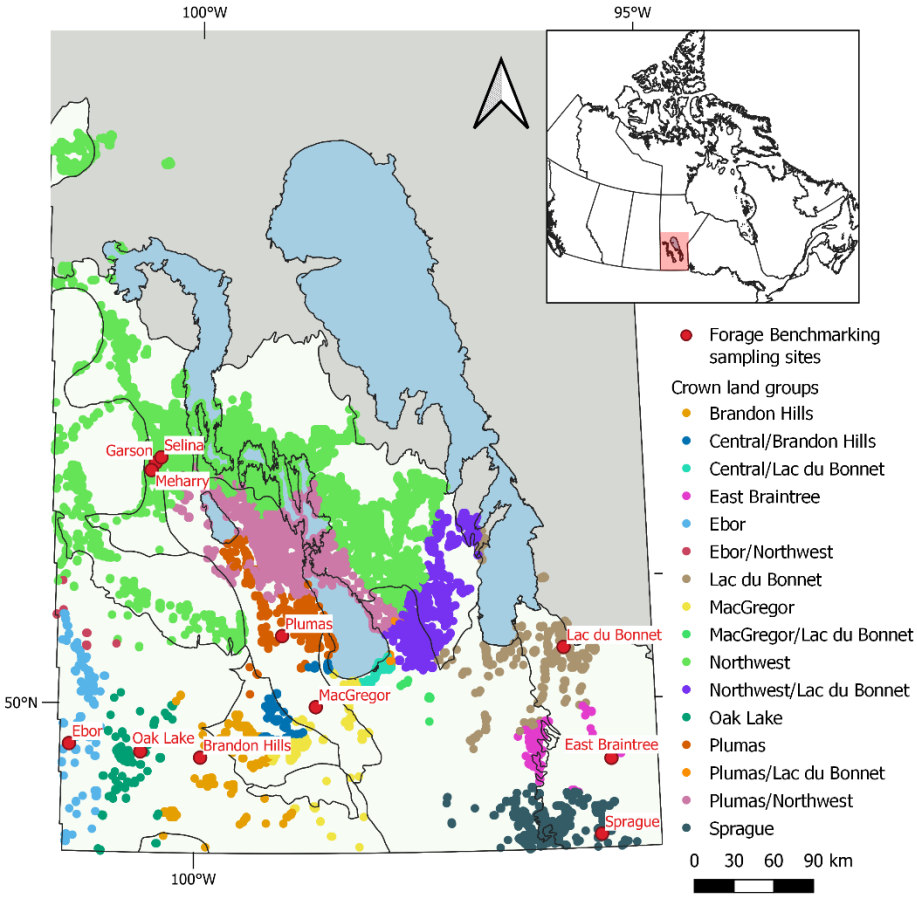

Figure 9: Crown land parcels assigned to different sampling sites and site combinations based on the similarity index calculated by the Similarity Search tool.

5.3.6. Assessment of the relationship between carrying capacities and climate variables

Different statistical models were used to evaluate the relationship between the mean carrying capacities of agricultural crown lands as the response variable and climate variables as the predictors, such as multiple linear regression (MLR), polynomial regression (PR), interaction models and generalized additive models (GAM).

In addition to PR models, GAMs can be used to handle nonlinear relationships between response and predictor variables. Nonlinearity is commonly observed in analyzing relationships of environmental variables, such as species abundances, animal density and soil salinity (Youcef et al. 2013; Alcaraz-Hernández et al. 2016; Song et al. 2016; Xue et al. 2018). This facilitated the use of GAMs in this study to address the nonlinearity of the relationship between carrying capacities and climate variables.

Instead of a linear function, GAMs use a sum of smooth functions of the predictors and follow the equation:

$$g(Y) = \beta_0 + \sum_{j=1}^{n} f_j(X_j) + \varepsilon \quad (2)$$

where g is the link function defining the relationship between the response variable Y and the predictors X_j, β_0 is the model intercept term and f_j is the smooth function of each predictor X_j (Pedersen et al. 2019). GAMs were performed using the mgcv package (Wood 2021) on RStudio (R Core Team 2020; RStudio Team 2020). These models were calibrated using some default parameters of the gam function in R, such as the thin plate regression spline smoothing function with maximum effective degrees of freedom (edf) of 10 and the Gaussian distribution with an

identity link function for model fitting. The smoothing parameter was estimated using restricted maximum likelihood (REML).

The adjusted coefficient of determination (R^2_{adj}) and the root-mean-square error (RMSE) were also calculated to evaluate the predictive performance of the models. The Akaike information criterion (AIC) was also calculated to assess the models' goodness of fit. The relative contribution of each predictor to the full models was determined by removing selected predictors and calculating the change in R^2_{adj} between the full and reduced models with the predictors dropped (Youcef et al. 2013; Song et al. 2016; Xue et al. 2018). While a stepwise approach could have been used to select a reduced predictor set, this approach was not used in the analysis because the effect of each predictor was assessed. A stepwise regression only keeps significant predictors (Gomez and Gomez 1984), which could result in the exclusion of some climate variables being studied.

5.3.7. Stocking rate assessment

With the average carrying capacities interpolated using climate data, the stocking rate (*SR*) in terms of AUM based on vegetation type is calculated using the following equation:

$$SR = A * CC \quad (3)$$

where *A* is the area of the specific vegetation type (ha), and *CC* is the carrying capacity based on that vegetation type (AUM/ha). The *SR* calculations for rangelands were carried out at the ecosite level in which *A* represents the total ecosite area within the parcel. Some map units in the ecosite layer did not have a dominant ecosite or an ecosite that covers more than half of the map unit area but are composed of multiple ecosites with varying proportions. In this case, area-weighted stocking rates were calculated using the following equation:

$$SR = \sum_{i=1}^{n} A * E_i * CC_i \quad (4)$$

where *i* is the ith ecosite, *A* is the total area of the map unit derived from the ecosite layer (ha), E_i is the extent covered by ith ecosite (%) and CC_i is the carrying capacity based on that i^{th} ecosite (AUM/ha). These stocking rates were summed to represent the overall *SR* of the parcels comprised of various vegetation types and ecosites. The total estimated *SR* of each parcel was compared to the total current *SR* derived from the ARD crown land (ACL) provincial database by calculating the grazing rate (*GR*, %) using the following equation (Yu et al. 2010; Qin et al. 2021):

$$GR = \frac{Current\ SR - Estimated\ SR}{Estimated\ SR} * 100 \quad (5)$$

A positive *GR* indicates that the grassland is overgrazed, and a negative *GR* indicates undergrazing.

There were instances where areas of parcels differed from those recorded in the ACL database and GIS software. Any area differences greater than 2 ha (i.e., approximately 3% of the total quarter section area) were regarded as mapping or delineation errors and were removed from the analysis. The crown land parcels with area differences of less than 2 ha accounted for 80% of the total number of crownland parcels, or 13,098 out of 16,363 parcels, hence only these were included in this study.

5.4. Results

5.4.1. Carrying capacity estimates

Estimated carrying capacities based on forage yields gathered from the field surveys ranged from 0 to 2.65 AUM/ha, with 0 AUM/ha associated with marshes and peats and 6.54

AUM/ha associated with tame pastures (Figure 10). When averaged by parcel, carrying capacities ranged from 0 to 5.52 AUM/ha with 5.52 AUM/ac being recorded in Tall Grass Prairie. The highest mean carrying capacities were recorded in Aspen/Oak Parkland (1.99 AUM/ha) while the lowest mean carrying capacity was recorded in Lake of the Woods (0.71 AUM/ha).

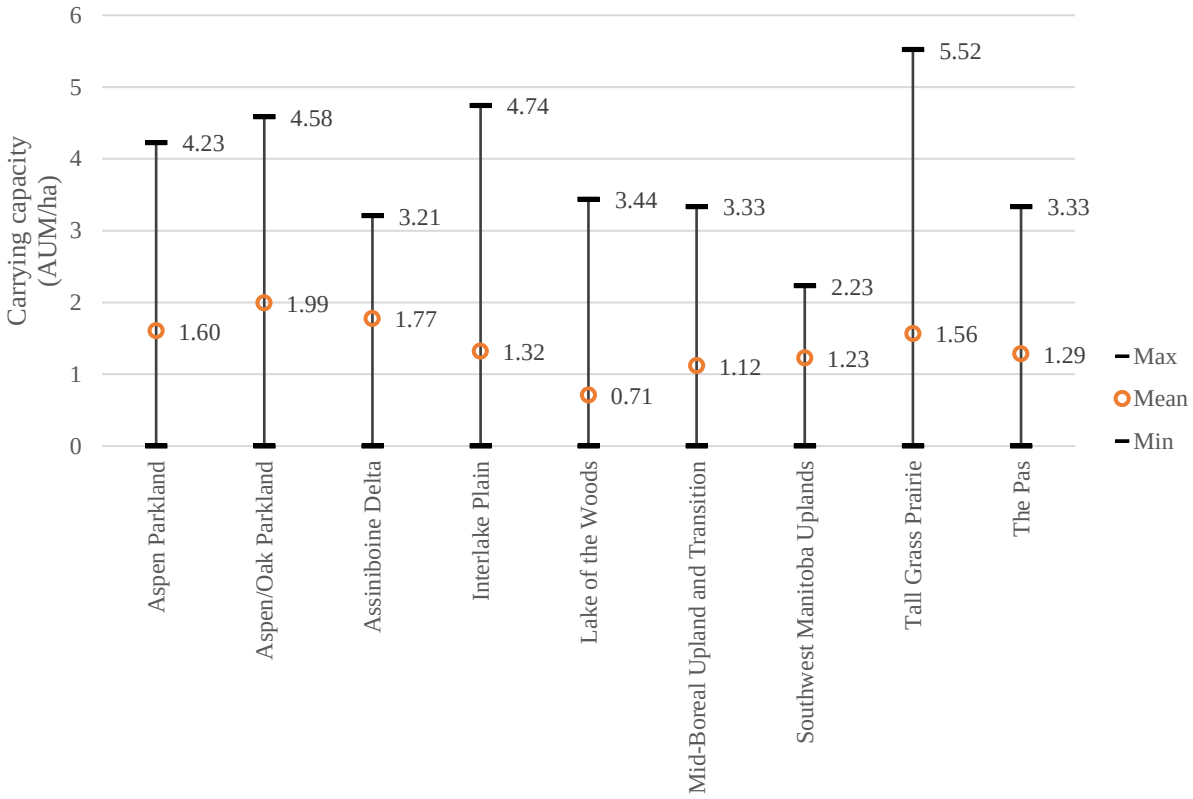

Figure 10: Summary statistics of carrying capacities by ecoregion in Manitoba.

5.4.2. Relationship between average carrying capacities and climate variables

Lower MAT, ranging between 0.78°C and 1.57˚C, were generally observed in northern ecoregions of Agro-Manitoba, such as The Pas, Mid-Boreal Upland and Transition and Interlake Plain (Table 6). Higher annual mean temperatures were observed in southwestern Manitoba, with the Southwest Manitoba Uplands reaching 3.06°C. Higher MAP was recorded in eastern ecoregions like Tall Grass Prairie and Lake of the Woods with 568 mm and 585 mm,

respectively, while western areas received lower amounts. The MSP generally followed similar trends as MAP with western and northern ecoregions receiving less precipitation than eastern ecoregions. Higher accumulations of GDD were observed in ecoregions that also experience higher MAT, such as Assiniboine Delta, Lake of the Woods and Southwest Manitoba Uplands, indicating a direct correlation between MAT and GDD. Only one ecoregion, Assiniboine Delta, had a negative CMI value, indicating its dry conditions, which is typical for grasslands. Positive CMI values near 0 were recorded in Aspen Parkland and Southwest Manitoba Uplands, suggesting that these ecoregions were relatively dry. Higher CMI values were recorded in Lake of the Woods and Mid-Boreal Upland and Transition, largely due to vast forest covers that are linked to moist or wet conditions.

Table 6: Average values of each climate variable by ecoregion in Manitoba.

Ecoregion	MAT[1] (°C)	MAP[2] (mm)	MSP[3] (mm)	GDD[4]	CMI[5] (mm)
Aspen Parkland	2.67	503	335	1686	1.07
Aspen/Oak Parkland	2.20	511	337	1651	4.76
Assiniboine Delta	2.95	511	350	1756	-0.80
Interlake Plain	1.57	514	334	1562	6.94
Lake of the Woods	2.88	585	394	1747	12.03
Mid-Boreal Upland and Transition	1.30	520	342	1446	9.44
Southwest Manitoba Uplands	3.06	541	371	1735	2.17
Tall Grass Prairie	2.24	568	374	1669	8.40
The Pas	0.78	462	309	1473	5.49

[1]Mean annual temperature
[2]Mean annual precipitation
[3]Mean May-to-September (growing-season) precipitation
[4]Growing degree-days
[5]Hogg's climate moisture index

Using these climate variables for similarity interpolation, similarity index values lower than 2 were determined in the majority of the crown land parcels, implying high similarity to sampling sites in terms of climate and distance variables (Figure 11). Higher values ranging from 9.6 to 26.5 were recorded primarily in Interlake Plain and Mid-Boreal Upland and Transition,

with some pockets in Tall Grass Prairie and Aspen Parkland, indicating a very low resemblance to the climate conditions of the sampling sites.

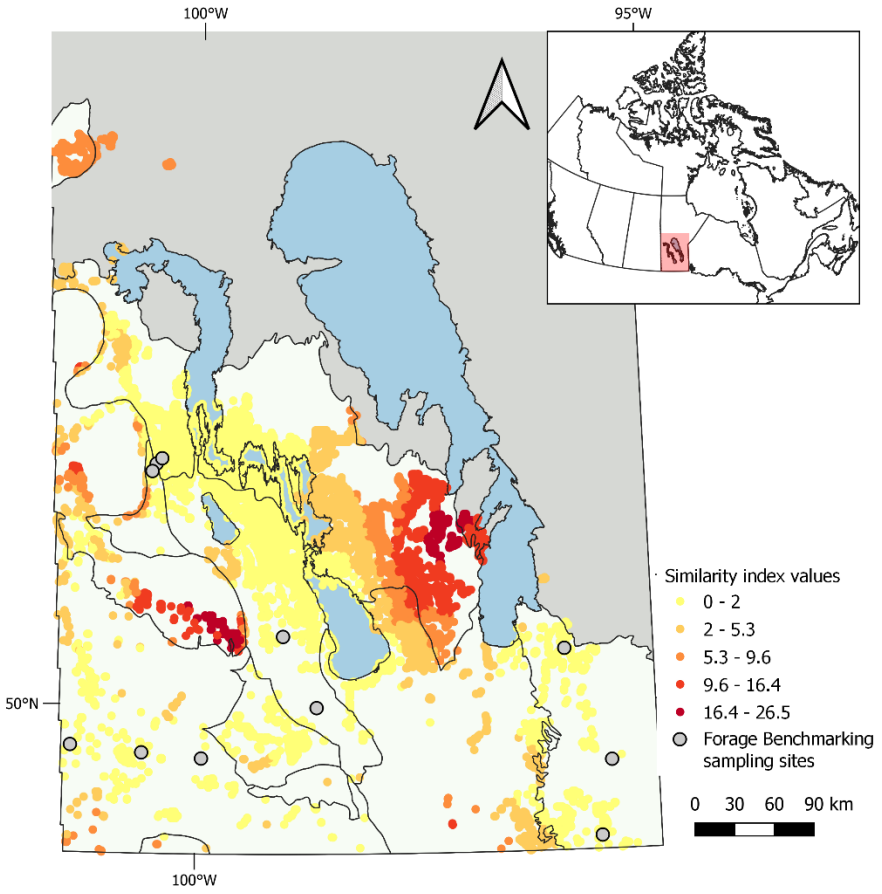

Figure 11: Similarity index values of crown land parcels based on different sampling sites and site combinations calculated by the Similarity Search tool according to climate variables and site proximity variable.

The correlations between climate variables derived from the ClimateNA application and average forage yields and average carrying capacities from the sampling sites of the benchmarking project were generally weak, with only 9 of the 24 variables having correlation coefficients of more than 0.3 (Appendix F). Only the number of frost-free days (NFFD) had a significant correlation with average forage yields and carrying capacities among all climate variables. The main five climate variables used for data interpolation, MAT, MAP, MSP, GDD and CMI, had absolute correlations ranging from 0.01 to 0.29, which indicated the lack of linear

relationships between these variables and grassland carrying capacity. Nevertheless, these five variables were still used for interpolating carrying capacity estimates to crown lands due to their impact on water balance and soil moisture which are important for vegetation growth (Hogg 1994; Li and Guo 2012; Thorpe 2014b; Liu and Menzel 2016). After the estimation of carrying capacities for each crown land parcel, the correlations were also determined for these five variables and further decreases in correlation were obtained (Appendix F), which demonstrates the absence of a linear relationship between carrying capacities and climate.

The shape of response curves of mean carrying capacities to the climate variables in scatterplots further revealed the absence of linear relationships (Figure 12). With the heavy concentration of observed data points around the x-axis, lines regressed using a nonparametric and local regression method (i.e., locally estimated scatterplot smoothing or LOESS) showed almost constant horizontal lines with no discernible trends in most explanatory climate variables. An apparent decrease in carrying capacities was attributed to the increase in MSP as seen from 375 to 425 mm (Figure 12c).

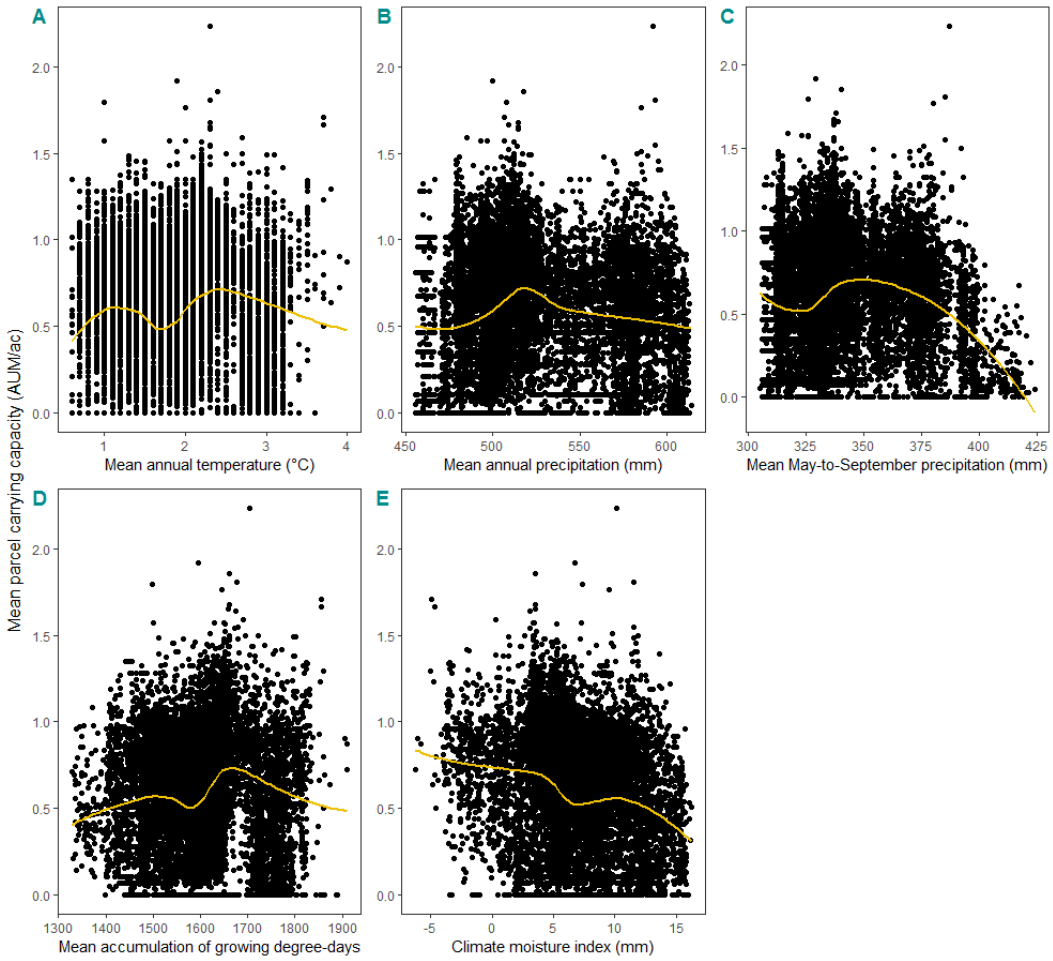

Figure 12: Relationships between mean carrying capacities (AUM/ac) and climate variables A) mean annual temperature (MAT), B) mean annual precipitation (MAP), C) mean May-to-September precipitation (MSP), D) mean accumulation of growing degree-days (GDD) and E) climate moisture index (CMI). Yellow lines represent locally estimated scatterplot smoothing (LOESS) regression.

Different regression models were used to evaluate the relationship between mean carrying capacities and climate variables. The variation in average carrying capacity explained by multiple linear regression (MLR) models ranged from 14% to 22% while the second-order (PR) models explained 17% to 23% (Table 7). The inclusion of interaction terms significantly enhanced the performance of MLR and PR models, nearly doubling the percent variation explained. Interaction models explained 32% to 43% of the variability of mean carrying capacities in MLR models and 33% to 43% in PR models. Significant interaction effects occur when an effect of one variable depends on the value of another variable. In both standard

interaction models, MSP, GDD and CMI each had significant interaction effects with the other three to four climate variables while MAT and MAP had significant interactions with two to three variables. GAMs explained 33% to 43% of the variability of mean carrying capacity, relatively similar to the interaction models.

Table 7: Summary of results of different regression models examining the relationship between mean carrying capacities and climate variables.

Regression model	R^2_{adj}	RMSE (AUM/ha)	AIC
Standard models			
MLR[1]	0.14***	0.73	6839
MLR with interactions[2]	0.32***	0.65	2964
2nd order PR[3]	0.17***	0.72	4791
2nd order PR with interactions[4]	0.33***	0.64	2656
GAM[5]	0.33	0.64	1952
Ecoregional models			
MLR[6]	0.22***	0.70	5261
MLR with interactions[7]	0.43***	0.59	551
2nd order PR[8]	0.23***	0.69	4985
2nd order PR with interactions[9]	0.43***	0.59	496
GAM[10]	0.43	0.59	89

***Significant at $\alpha = 0.001$. p-values for the overall GAM models cannot be calculated.

[1]Mean CC = MAT + MAP + MSP + GDD + CMI

[2]Mean CC = MAT + MAP + MSP + GDD + CMI + MAT*MAP*MSP*GDD*CMI

[3]Mean CC = MAT + MAP + MSP + GDD + CMI + MAT^2 + MAP^2 + MSP^2 + GDD^2 + CMI^2

[4]Mean CC = MAT + MAP + MSP + GDD + CMI + MAT^2 + MAP^2 + MSP^2 + GDD^2 + CMI^2 + MAT*MAP*MSP*GDD*CMI

[5]Mean CC = *s*(MAT) + *s*(MAP) + *s*(MSP) + *s*(GDD) + *s*(CMI)

[6]Mean CC = MAT + MAP + MSP + GDD + CMI + ER_{AP} + ER_{AOP} + ER_{AD} + ER_{IP} + ER_{LW} + ER_{MBUT} + ER_{SMU} + ER_{TGP} + ER_{PAS}

[7]Mean CC = MAT + MAP + MSP + GDD + CMI + ER_{AP} + ER_{AOP} + ER_{AD} + ER_{IP} + ER_{LW} + ER_{MBUT} + ER_{SMU} + ER_{TGP} + ER_{PAS} + MAT*MAP*MSP*GDD*CMI*ER_{AP}*ER_{AOP}*ER_{AD}*ER_{IP}*ER_{LW} *ER_{MBUT} *ER_{SMU}*ER_{TGP} *ER_{PAS}

[8]Mean CC = MAT + MAP + MSP + GDD + CMI + MAT^2 + MAP^2 + MSP^2 + GDD^2 + CMI^2 + ER_{AP} + ER_{AOP} + ER_{AD} + ER_{IP} + ER_{LW} + ER_{MBUT} + ER_{SMU} + ER_{TGP} + ER_{PAS}

[9]Mean CC = MAT + MAP + MSP + GDD + CMI + MAT^2 + MAP^2 + MSP^2 + GDD^2 + CMI^2 + MAT*MAP*MSP*GDD*CMI*ER_{AP}*ER_{AOP}*ER_{AD}*ER_{IP} *ER_{LW}*ER_{MBUT}*ER_{SMU}*ER_{TGP} *ER_{PAS}

[10]Mean CC = *s*(MAT, by = ER) + *s*(MAP, by = ER) + *s*(MSP, by = ER) + *s*(GDD, by = ER) + *s*(CMI, by = ER) + ER

MLR = multiple linear regression; PR = polynomial regression; GAM = generalized additive model; RMSE = root-mean-square error; AIC = Akaike information criterion

s = spline smoothing curve; CC = carrying capacity; MAT = mean annual temperature; MAP = mean annual precipitation; MSP = mean May-to-September (growing-season) precipitation; GDD = Growing degree-days; CMI = climate moisture index; AP = Aspen Parkland; AOP = Aspen/Oak Parkland; AD = Assiniboine Delta; IP = Interlake Plain; LW = Lake of the Woods; MBUT = Mid-Boreal Upland and Transition; SMU = Southwest Manitoba Uplands; TGP = Tall Grass Prairie; PAS = The Pas

Models regressed in this study were standard and ecoregional with the former models accounting for the overall trends of the estimated data while the latter models included a categorical variable that groups the data by ecoregion to the list of predictors. Ecoregional models generally performed better with higher R^2_{adj} than their counterparts in standard models (Table 7). When comparing the different regression methods, interaction models and GAMs outperformed those without interaction terms, with R^2_{adj} varying between 0.32 and 0.33 in standard models and 0.43 in ecoregional models. As the R^2_{adj} of interaction models and GAMs vary very little from each other, AIC values can be used to differentiate among models due to their considerable margin. Of all the models, ecoregional GAM showed the best fit of the data with an AIC of 89, despite having similar R^2_{adj} to ecoregional MLR and PR interaction models.

Analysis of reductions in the total R^2_{adj} between the full and reduced models with different variables dropped revealed that interaction terms had the highest relative contributions to the models with an overall average of 18.78% (Table 8). This was followed by ecoregional factors, contributing 8.75% to the ecoregional models. Among the climate variables, CMI explained the most variability in the mean carrying capacities with an overall average of 7.23%. The relative contribution of CMI was higher in standard models (8.84%) than in ecoregional models (4.54%), which can be attributed to the inclusion of ecoregional factors. The MAT and GDD were less important among the climate variables with overall averages of 1.43% and 1.92%, respectively. Quadratic terms were also among the least important to the models with 1.51%.

Table 8: Relative contributions of each predictor to the R^2_{adj} in the regression models.

	Predictors							
	MAT	MAP	MSP	GDD	CMI	Interaction terms	Quadratic terms	Ecoregion
Regression model	% Change in R^2_{adj} from full model							
Standard models								
MLR	0.32^{***}	6.44^{***}	2.25^{***}	0.37^{***}	6.65^{***}			
MLR with interactions	7.25^{NS}	8.06^{***}	6.41^{***}	3.82^{***}	13.58^{**}	18.27		
2nd order PR	0.94^{NS}	1.74^{***}	0.45^{NS}	0.62^{NS}	6.16^{***}		2.76	
2nd order PR with interactions	6.04^{NS}	5.68^{***}	5.02^{***}	3.89^{***}	10.78^{***}	16.77	1.26	
GAM	2.91^{***}	2.55^{***}	2.53^{***}	2.72^{***}	7.05^{***}			
Average	1.62	4.90	4.05	2.70	8.84	17.52	2.01	
Ecoregional models								
MLR	0.49^{***}	2.73^{***}	0.82^{***}	0.19^{***}	3.38^{***}			7.85
MLR with interactions	6.61^{NS}	4.09^{NS}	3.98^{NS}	4.82^{NS}	7.45^{NS}	20.76		10.33
2nd order PR	0.88^{NS}	1.18^{***}	0.15^{**}	0.54^{***}	4.12^{***}		1.72	6.80
2nd order PR with interactions	6.50^{NS}	2.57^{NS}	2.64^{NS}	5.10^{NS}	7.05^{NS}	19.34	0.31	9.38
GAM	1.98	1.04	0.78	1.90	6.14			9.40
Average	1.23	1.65	0.58	0.88	4.54	20.05	1.01	8.75
Overall average	**1.43**	**3.68**	**2.57**	**1.92**	**7.23**	**18.78**	**1.51**	**8.75**

**Significant at $\alpha = 0.01$; ***Significant at $\alpha = 0.001$; NS = not significant.

Statistical significance is only indicated on individual variables. The ecoregional GAM does not produce p-value significance for overall trends for each climate variable. Instead, statistical significance is determined specifically for each ecoregional trend of each climate variable. As a result, significance is not displayed in the ecoregional GAM. Additionally, relative contributions of non-significant (NS) variables were not included in the average values.

MLR = multiple linear regression; PR = polynomial regression; GAM = generalized additive model; MAT = mean annual temperature; MAP = mean annual precipitation; MSP = mean May-to-September (growing-season) precipitation; GDD = Growing degree-days; CMI = climate moisture index

The GAMs can illustrate the partial effects of the predictor on response variables. Figure 13 shows the response plots of climate variables from the standard GAM in their relationships to the average carrying capacity of the crown lands, with all climate variables having significant effects on the average carrying capacity. The annual temperature had a constant relationship with carrying capacities until 3.4^{o}C when carrying capacities increased substantially (Figure 13a). Annual precipitation also had an overall positive relationship with carrying capacities (Figure 13b). In contrast, carrying capacities generally decreased with growing season precipitation, particularly from 300 to 400 mm, but increased again to the constant amounts at 413 mm (Figure 13c). Accumulation of growing-degree days also had a constant effect on carrying capacities between 1300 and 1700 GDDs but this gradually decreased after 1700 GDDs, with a drastic decline at 1850 GDDs (Figure 13d). Carrying capacities declined greatly with climate moisture index values, especially at 4 mm (Figure 13e). These trends illustrated on GAM plots cannot be detected by simply applying a linear function or using a LOESS regression (Figure 12).

Concurvity was identified in all climate variables in the standard GAM model, with values ranging from 0.95 in CMI to 0.99 in MSP. High pairwise concurvities of over 0.9 were identified between MAT and GDD and MAP and MSP. Additionally, multicollinearity was identified in all climate variables in the MLR, except for CMI, with high variance inflation factors of over 10. The variance inflation factors ranged between 4.86 in CMI and 22.73 in MSP.

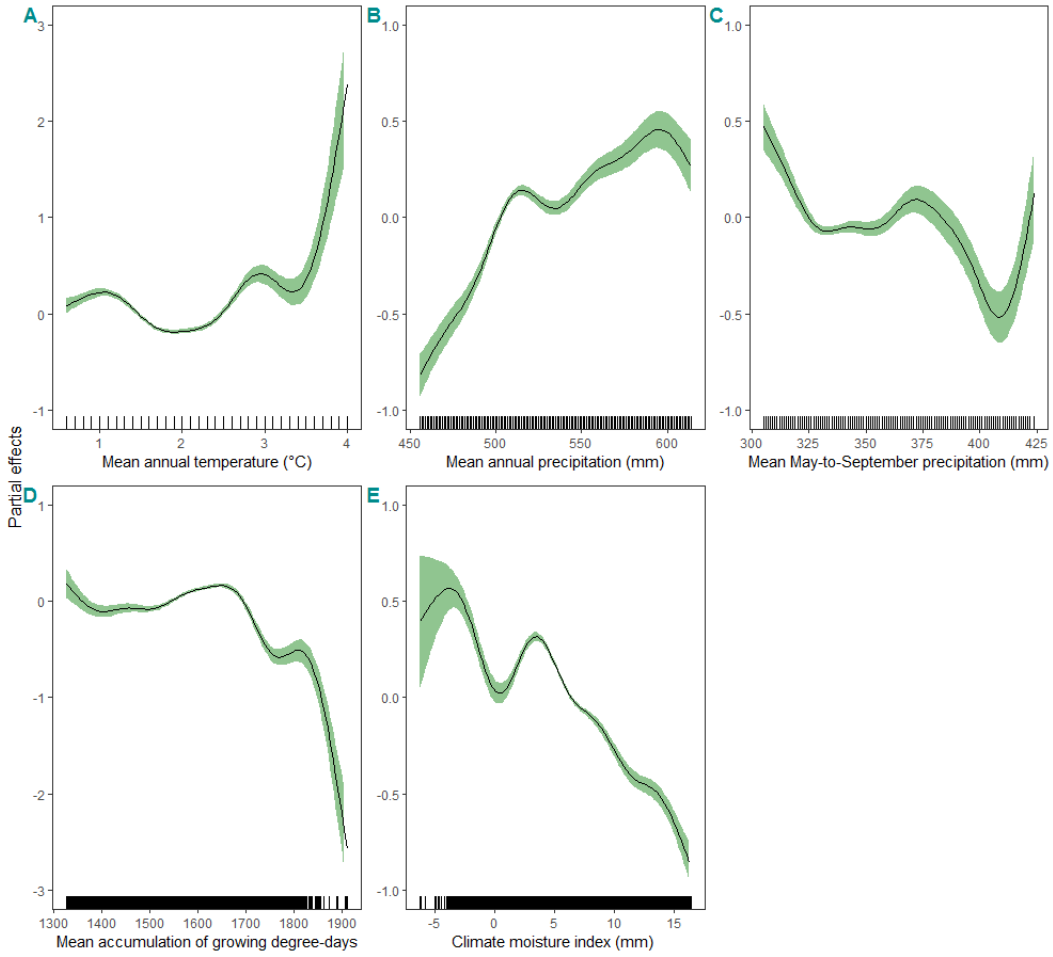

Figure 13: Generalized additive models (GAM) plots showing the partial effects of climate variables A) mean annual temperature (MAT), B) mean annual precipitation (MAP), C) mean May-to-September precipitation (MSP), D) mean accumulation of growing degree-days (GDD) and E) climate moisture index (CMI) on the mean carrying capacities of the crown lands. Solid line indicates the general trend of the considered variable effect on mean carrying capacities. The green shaded areas indicate the 95% confidence intervals. The tick marks on the x-axis are observed data points.

5.4.3. Stocking rate estimates

The total stocking rate estimated from the field surveys for all crown land parcels was about 900,000 AUMs, which was 1.8 times more than the existing stocking rates allowed by the provincial lease contracts. Higher stocking rates were anticipated in Interlake Plain and Aspen/Oak Parkland since these ecoregions contained 73% of the total number of parcels. Overall, the forage resources of the crown lands were being undergrazed, with a grazing rate of

-44.64%. Seven of the nine ecoregions exhibited underutilized grazing potential with grazing rates ranging from -13.49% in The Pas to -63.94% in Assiniboine Delta. Only two ecoregions, the Mid-Boreal Upland and Transition and the Lake of the Woods, were overgrazed by 4.74% and 42.54%, respectively. Overall, 72% of the total number of parcels were undergrazed compared to 24% which were overgrazed. Only 4% of the parcels had equal stocking rates between the lease contracts and those estimated. Eight of the nine ecoregions contained more undergrazed parcels than overgrazed parcels with percentages of undergrazed parcels varying between 52% and 86%, with the exception of the Lake of the Woods. In Assiniboine Delta and Aspen/Oak Parkland, more than 80% of their parcels were undergrazed, both in the southwestern portion of the province (Table 9).

Table 9: Total number of stocking rates and number of undergrazed and overgrazed parcels by ecoregion in Manitoba.

Ecoregion	Stocking rates (AUM)								
	Total stocking rates			Number of parcels					
	Current	Estimated	GR[1] (%)	Equal	%	UG[2]	%	OG[3]	%
Aspen Parkland	26,479	44,755	-40.84	39	*7*	361	*68*	131	*25*
Aspen/Oak Parkland	129,370	284,421	-54.51	37	*2*	2032	*84*	342	*14*
Assiniboine Delta	8,414	23,336	-63.94	5	*2*	270	*86*	38	*12*
Interlake Plain	244,112	431,468	-43.42	264	*4*	5257	*73*	1672	*23*
Lake of the Woods	14,164	9,937	+42.54	22	*5*	153	*32*	305	*64*
Mid-Boreal Upland and Transition	22,289	21,280	+4.74	19	*4*	280	*57*	189	*39*
Southwest Manitoba Uplands	177	284	-37.68	1	*14*	4	*57*	2	*29*
Tall Grass Prairie	49,138	84,206	-41.65	95	*7*	869	*66*	345	*26*
The Pas	10,964	12,674	-13.49	46	*13*	190	*52*	130	*36*
Overall	505,107	912,361	-44.64	528	*4*	9416	*72*	3154	*24*

[1]GR = grazing rate; positive (+) indicates overgrazed and negative (-) indicates undergrazed.
[2]UG = undergrazed parcels
[3]OG = overgrazed parcels

5.5. Discussion

5.5.1. Carrying capacity estimates

In terms of estimated carrying capacities, higher average values were observed in ecoregions with larger proportions of semi-arid grasslands, such as Aspen/Oak Parkland, Assiniboine Delta, Aspen Parkland and Tall Grass Prairie. This can be attributed to the high palatability of forage in grasslands compared to shrublands and forests. High electivity values related to cattle preference were recorded in grasslands than in aspen and mixedwood stands (Kaufmann 2011). In their study, similar crude protein (CP) concentrations of grasses and forbs were found in grasslands and forest cutblocks yet cattle preferred those in grasslands due to higher palatability and large amounts of unpalatable Canada thistle (*Cirsium arvense*). Notably, the present analysis indicated that these ecoregions were undergrazed according to the provincial leasing program, suggesting that the carrying capacity for those regions could be revised, noting that these were still baseline estimates.

The Lake of the Woods, Mid-Boreal Upland and Transition, and the Southwest Manitoba Uplands had lower mean carrying capacities compared to other ecoregions which had 1.29 AUM/ha or higher due to the dominance of forested cover in these ecoregions. Carrying capacities for forested areas are usually adjusted to lower forage utilization rates compared to grasslands due to access restrictions and forest regeneration. Where access is granted to cattle, they rely on understory vegetation within these forest stands, such as shrubs, forbs and unlignified tree seedlings. Access to understory vegetation becomes restricted with growing stands (Alberta Sustainable Resource Development 2004). Kaufmann (2011) observed low forage utilization of cutblocks in southwestern Alberta despite having significantly similar yields of forage biomass available as grasslands due to physical barriers. Furthermore, dense canopy

closure also reduces understory production due to increased shading, reducing sunlight and subsequently photosynthetic capacity (Alberta Sustainable Resource Development 2004). The benchmarking project used a forage utilization rate of 30% for forests compared to grasslands with rates, which can reach as high as 55%. In Alberta, only 25% is recommended for utilization levels of forested rangelands while this can increase to 50% for native grasslands and 70% for tame pastures (Alberta Sustainable Resource Development 2004).

Low forest utilization rates are also recommended to maintain plant health and vigour of the stands while maintaining their ecological functions, such as nutrient and water cycling, and timber regeneration (Beef Cattle Research Council 2022). Increasing utilization rates can introduce risks to agroforestry systems, such as reduction of canopy growth and soil compaction. In interior British Columbia, a study evaluating no grazing vs. a grazing treatment of 50% forage utilization rate on forest landings for four years found that ungrazed landings had 53% greater canopy cover than grazed landings due to damage on young lodgepole pine by trampling and browsing from cattle (Krzic et al. 2006). In contrast to grazing (i.e., feeding on low-growing vegetation like grasses), cattle browsing (i.e., feeding on high-growing vegetation like leaves, barks and shrubs) generally only occurs after most of the more palatable forage has been consumed. A study in British Columbia reported cattle browsing 46% of lodgepole pine only after less than 15% of forage was still available (Newman and Powell 1997). Krzic et al. (2006) also found lodgepole pines in grazed landings to be 21% shorter and had 27% smaller diameter than those in ungrazed landings, attributed to cattle trampling. Trampling damage is found to be highest during the first two to three years after stand planting when trees are not large enough to act as a natural barrier to cattle grazing (Newman and Powell 1997).

5.5.2. Influence of climate variables in carrying capacities and stocking rates

Nonlinear relationships were observed between average carrying capacities and climate variables of the crown lands in Manitoba, which allowed the use of nonparametric models such as GAMs. Although GAMs performed better than linear models, the variation they explained in the mean carrying capacities did not differ significantly from the interaction models. Despite this similarity, the AIC calculated for GAMs were lower than the AICs calculated for interaction models, which indicates that GAMs fit the data better, due to their ability to better capture the non-linear relationship between carrying capacity and climate variables. The superiority of GAMs has been proven in testing the nonlinearity of different environmental variables, such as species abundance (Youcef et al. 2013; Xue et al. 2018), animal density (Alcaraz-Hernández et al. 2016) and soil salinity (Song et al. 2016). Some studies had also used GAMs to analyze relationships between remote sensing spectral variables and environmental variables, such as biomass (Fassnacht et al. 2021) and vegetation distribution (Song et al. 2013). Similar to this study's analysis, Wu et al. (2016) and Wu et al. (2019) modelled the response of net primary productivity of alpine grasslands to climate factors using GAMs.

Generally, rising temperatures are associated with a decrease in forage yields and as a result, decreasing carrying capacities (Willms and Jefferson 1993). As this study incorporated MAT, this variable accounted for both winter and summer temperatures, with annual temperatures ranging from 0^{o}C to 4^{o}C. However, most studies in the literature used growing season temperature (i.e., temperature taken from May to September annually) to analyze the relationship between forage productivity and temperature. For example, Nuttall et al. (1991) analyzed the effect of temperature on cool-season alfalfa and bromegrass pastures in

Saskatchewan and found that their yields started decreasing when temperatures rose above 18°C during the summer. Another study found that yearlong vegetation growth in North America was significantly influenced by spring temperatures compared to summer temperatures (Chen et al. 2018). With climate change, the rise of spring temperatures may reduce the productivity of cool-season (C_3) forages, such as alfalfa and crested wheatgrass, which are usually preferred by beef producers. Warm-season (C_4) grasses, such as little bluestem, may be used to replace C_3 grasses as long as precipitation increases to offset the rising temperatures (Nuttall et al. 1991; Willms and Jefferson 1993). The timing of the grazing period would also be affected because the phenological stages of C_3 grasses differ from those of C_4 grasses. The peak productivity of C_3 grasses occurs in early summer while C_4 grasses produce more herbage in mid-summer (Willms and Jefferson 1993).

The increase in carrying capacities with annual precipitation observed in this study generally agrees with previous research since carrying capacities are dependent on biomass output, which is directly influenced by moisture availability and the rest period. Forage yield potential is subject to available soil moisture and therefore, modest increases in amounts of precipitation are expected to increase the carrying capacities of grasslands, especially those located within the semi-arid grasslands (Willms and Jefferson 1993; Li and Guo 2012). Furthermore, soil moisture availability is important during the critical stages of plant growth, such as seedling establishment (Willms and Jefferson 1993).

On the other hand, growing season precipitation had a negative influence on carrying capacities according to the standard GAM plot. These results are likely because, in the Canadian Prairies, antecedent soil moisture conditions in the previous fall and winter have a carryover

effect on grass productivity in the following spring. Willms and Jefferson (1993) noted that fall soil moisture is more important than growing season precipitation for grassland production, particularly for C_3 grasses that begin growth in early spring. In Saskatchewan, Schellenberg et al. (1999) found that the forage yields of native grasses and crested wheatgrass were significantly correlated with combined early April soil moisture and precipitation during the start of the growing season from April to June. In particular, available forage was correlated to the April-June precipitation of the previous year, which further proves that precipitation in the previous year would be more influential than in-season precipitation.

The accumulation of GDD is a good indicator of plant development. As the growing season progresses, higher rates of increase in GDD accumulation occur during June and July when temperatures are at their peak. This means that higher accumulations of GDDs are associated with increased forage maturity in the later months of the season (Edey 1977), which is linked to a decline in forage quality, palatability and feed intake (Aasen and Bjorge 2009). A decline of forage quality in warm-season grasses, big bluestem and switchgrass, with higher GDD accumulation was found in Nebraska and Kansas using CP and in vitro digestible DM as indicators of forage quality (Mitchell et al. 2001). This trend is consistent with the findings of this study in which the carrying capacities of the crown lands decreased when heat accumulated at 1700 GDDs and above. Carrying capacities account for forage utilization, which is related to forage quality, which declines with the stage of plant maturity. As forages mature, acid detergent fibre (ADF) and neutral detergent fibre (NDF) concentrations increase, indicating a decrease in DM digestibility and intake (Aasen and Bjorge 2009). Furthermore, CP concentration is expected to decrease with the stage of maturity, thus resulting in lower available feed quality. As a result, best management practices which target grazing at optimal stage of maturity to meet animal

needs, reduction of selective grazing (and commensurate proliferation of undesirable plants) and provision of an adequate rest period to maximize plant health and vigor are desirable to increase carrying capacity.

The decrease of carrying capacities with increasing CMI values on the GAM partial effects plot is associated with the differences in the moisture regimes of different vegetation types. Boreal forests are generally restricted to areas where there is a surplus of precipitation over potential evapotranspiration, resulting in positive CMI values. On the other hand, grasslands tend to have greater potential evapotranspiration than precipitation which would lead to drier soil conditions and negative CMI values (Hogg 1997). On the GAM plot, carrying capacities peaked at -4 mm with a slight increase at 0 mm and a further downward trend above 4 mm. He (2014) found that evapotranspiration-based indices, such as CMI, explained a higher variation in vegetation cover than precipitation because they take account for water availability that is crucial to plant growth. This author also reported that vegetation cover decreased with high temperatures (i.e., 15-20°C) and moderate precipitation (i.e., 100-150 mm), which may have been a result of the decline in water availability due to increased evapotranspiration.

The GAM plots of each variable showed specific peaks and troughs on their partial effects on the mean carrying capacities, instead of linear effects. The peaks and troughs have resulted in erratic trends in some variables, particularly in MAP, which saw an initial decline at 300 mm but increased at 413 mm, nearly equal the initial point where the decline started. Partial effects plots are intended to be interpreted naturally as you would with linear regression, assuming that all other variables in the GAM are at their average value. These peaks and troughs may be significant, but no specific reasons can be identified for the varying behavior of the

GAM models. These factors should be further assessed in future research along with the concurvity of these climate variables.

Overall, the current study found that the agricultural crown lands in Manitoba are undergrazed by -44.64%, with seven of the nine ecoregions indicating underutilized grazing potential. This infers that the production efficiency of these crown lands may be increased, in line with the goal of the Manitoba Protein Advantage to enhance their productivity by 15% (Manitoba Agriculture and Resource Development 2019b). Increasing stocking rates would result in higher liveweight gains produced per hectare, increasing the efficiency of the pastures (Aasen and Bjorge 2009). This strategy is consistent with future projections in 2050 that beef production will be more dependent on higher liveweight than on the expansion of cattle numbers, which is expected to slow down (Alexandratos and Bruinsma 2012). Furthermore, grasslands are particularly vulnerable to climate change due to the increased frequency of extreme events, such as droughts and floods (Li and Guo 2012), with the most recent drought in the Canadian Prairies occurring in 2021 (Statistics Canada 2021; Climenhaga 2022). Droughts have a significant negative impact on the viability of beef production systems in semi-arid grasslands that relies heavily on soil moisture for pasture growth and growth of annual grains for backgrounding and finishing sectors (Conant 2010). Rising temperatures coupled with reduced precipitation and increased evapotranspiration could lead to a dramatic reduction in grassland productivity, potentially leading to irreversible soil erosion rates (He 2014). In another climate scenario, rising temperatures with increased precipitation are likely to shift production towards warm-season or C_4 grasses (Thorpe et al. 2008) and potentially wipe out the distribution of widely preferred C_3 grasses if temperatures rise more than 4.5°C (Nuttall et al. 1991). The 2022 spring floods in Manitoba were a recent example of this scenario of high precipitation, which delayed the sowing

of crops and forages, constricting the window for their plant growth (Manitoba Agriculture and Resource Development 2022). Grassland management practices will need to consider these future extreme events in setting sustainable stocking rates.

5.5.3. Limitations of the study

This study concluded that 72% of the total number of crown lands have grazing potential using analyses based on available limited yield data and derived climate variables. However, the limitations of this study should still be considered when interpreting its findings. There were instances where areas of vegetation types within a parcel delineated by remotely sensed inventories did not match those reported in the ACL database. Furthermore, ACL uses a far more specific land cover classification than the remotely sensed inventories. For example, ACL divides the native grassland class into three different types: upland, lowland and transitional grasslands but ACI and MGI combine these into a single class. Both of these limitations affected the estimation of carrying capacities and stocking rates, which are heavily determined by vegetation differences.

There were also limitations on the forage yield data availability used in this study. Estimated carrying capacities were solely based on forage yields sampled in only four of the nine ecoregions and eight of the 21 ecosites, with the rest of the ecosites relying on constant carrying capacity values recommended by the Manitoba Rangeland Classification. Furthermore, average tame forage production from only two sampling sites was used to determine a constant carrying capacity value for the entire province. Due to the limitation of yield data, a similarity index was used to interpolate the field data to crown land parcels with similar climate variables. This method of interpolation may result in increased uncertainty of carrying capacities for areas far-

flung from the sampling sites, particularly in The Pas and Interlake Plain, based on the theory of spatial autocorrelation, in which neighbouring features are likely to have similar values, thus, longer distances increase heterogeneity between features (Longley et al. 2015). Large mean similarity index values of 7.16 and 7.61 were calculated for The Pas and Mid-Boreal Upland and Transition, respectively, suggesting that their crown lands are less similar to the sampling sites in terms of climate variables. The rest of the ecoregions have mean index values between 0.52 and 3.83. The Interlake Plain contained the most parcels with similarity index values greater than 9.6, indicating lower similarity, due to the absence of sampling sites within its boundaries. This suggests caution in analyzing its ecoregional trends, as well as the general trends for the province, given that the majority of all crown lands are located in this ecoregion. Carrying capacities for the parcels in Interlake Plain were estimated from five sites within Aspen/Oak Parkland and the Lake of the Woods, and along its boundaries with Mid-Boreal Upland and Transition, Aspen Parkland and Aspen/Oak Parkland. Aside from Interlake Plain, the least similar parcels were also found in Mid-Boreal Upland and Transition, mainly in the south of the Riding Mountain National Park, most likely due to higher elevations compared to the nearest sampling sites, implying cooler and moister conditions (Stadel 2015).

Despite these limitations, this study represents the first effort to estimate stocking rates in Manitoba's agricultural crown lands using remotely sensed datasets. Given that the estimation was done at the parcel level, a subset of all parcels can be assessed through field visits to further validate the findings of this study. Furthermore, future research should focus on addressing the aforementioned limitations in order to constrain the uncertainties in the carrying capacity estimates provided here. Possible approaches include undertaking large-scale sampling

campaigns to acquire productivity data across the province to better represent the physiographic conditions in different ecoregions and ecosites.

5.6. Conclusions

The relationship between carrying capacities and climate variables was found to be nonlinear which facilitated the use of GAM. Such a model has been used in many biological and ecological studies due to the ubiquity of nonlinear relationships in environmental variables such as species abundance. The non-linear relationship between productivity and any single climate variable suggests an interplay among several variables, both biotic (e.g., stand species composition) and abiotic (e.g., climate, as evidenced in the GAM analysis). Of all climate variables studied, CMI was shown to have the highest relative contribution to the regression models in explaining the variability in mean carrying capacities, signifying its relevance to detecting moisture regimes in semi-arid landscapes such as the Canadian Prairies.

Analyses using remote sensing and geographic information system (GIS) technologies suggested that the forage resources of the crown lands in Manitoba are currently undergrazed. This study provided preliminary large-scale estimates of carrying capacities and stocking rates of the agricultural crown lands in Manitoba which offers an overall picture of the current state of the crown lands and may support future decision-making in terms of grassland management in the province. Additionally, crown land parcels with potential underutilization or overutilization of forage resources were also identified. Nevertheless, future research efforts should focus on further improvements in the accuracy of estimation of carrying capacities and stocking rates by conducting an updated and larger benchmarking survey that encompasses every ecoregion and

ecosite in Manitoba. Furthermore, local soil properties and plant communities should be accounted for in future estimations.

CHAPTER 6: GENERAL DISCUSSION AND CONCLUSIONS

6.1. General discussion

This study explored the application of remote sensing in land cover inventory and monitoring of the agricultural crown lands in Manitoba. As early as 1976, the Manitoba Department of Agriculture explored using remote sensing to monitor grazing leases based on vegetation types, range condition and forage utilization in order to derive their carrying capacities over 5 years (Thompson 1977). Despite the success of this pilot project, a comprehensive inventory of provincial grasslands was not completed until the creation of MGI in 2020. The development of remote sensing products to track continuous changes in grassland cover has a definite impact on ongoing restoration and conservation initiatives since they can be a beneficial tool for the effective and sustainable allocation of forage resources (Qin et al. 2021; Canadian Forage & Grassland Association 2022). The present research builds on the effort of the province of Manitoba by assessing the agreement of the MGI with the provincial records of ACL distribution. The results indicated that possible refinements on both MGI and ACL data are needed to enhance the classification of the agricultural crownlands. While potential measures to improve the agreement between the MGI and ACL are provided, it was found that MGI and ACL agree on the broad grassland vegetation classes.

Remote sensing can be a beneficial tool in tracking ecosystem goods and services (Canadian Forage & Grassland Association 2022). Ecosystem goods and services from healthy and sustainable grassland systems directly and indirectly contribute to human welfare, such as food production through grazing activities, increased soil fertility through soil carbon sequestration, soil and water quality regulation through nutrient cycling, sediment filtration and soil erosion prevention (Bailey et al. 2010; Pogue et al. 2018). With the concerning trends of

climate change, studies have evaluated and estimated the ecosystem goods and services of grasslands. The quantitative valuation of these ecosystem goods and services can serve as the basis for grassland damage assessment and compensation systems (Kulshreshtha et al. 2015). Furthermore, it raises awareness of the importance of grasslands, which can contribute to improved sustainable management and conservation. For example, Kulshreshtha et al. (2015) conducted the valuation of different ecosystem goods and services of Manitoba grasslands. These authors estimated that the total value of Manitoba's annual forage production was approximately $524 million annually, with the native and tame pastures valued at $34.37 ha^{-1} yr^{-1} and $101.33 ha^{-1} yr^{-1}, respectively. The findings of this research allow for an accurate valuation of grassland across the crown lands in Manitoba. While the estimates should be seen with caution due to the uncertainties associated with datasets and methods used in the analysis, it still provides a starting point to define a valuation process in the province.

Grasslands serve as an important carbon sink in our ecosystems, with the majority of carbon stocks stored in their belowground biomass, which is comprised of root tissues, exudates and other root-derived organic material from root turnover (Bolinder et al. 2007; Kulshreshtha et al. 2015). A meta-analysis of carbon inputs in Canadian grasslands estimated that belowground carbon allocations in perennial legumes and grasses were 42.9% and 55.9%, compared to 24.9% in annual crops (Bolinder et al. 2007). This is mainly because perennial forages invest more energy in the growth of their roots than annual crops, evident in their shoot-to-root ratio of 1.6 compared to 5 in annual crops. A Saskatchewan study also observed that native grasses had higher carbon concentration in their soils than tame grasses and annual crops, particularly organic carbon which primarily determines the amount of carbon that can be sequestered (Cade-Menun et al. 2017).

Valuation of carbon sequestration based on the estimate of 105 t ha^{-1} yr^{-1} for Canadian grasslands found that grasslands in Manitoba sequestered 250.5 million tons of carbon annually, with an average value of \$280.35 ha^{-1} yr^{-1} for all types of grasses (Kulshreshtha et al. 2015). Alemu et al. (2017) found that increases in soil organic carbon (SOC) stocks can partially offset the greenhouse gas (GHG) emissions from beef production, particularly with light to moderate grazing intensities. They reported net farm GHG emissions per unit beef and unit area decreased by 12-25% and 13-32%, respectively. The remotely sensed approach used in this analysis allows for an update of carbon estimates in the province. Moreover, due to the spatial nature of the results, this quantification could be done in different areas of the ACL, with the identification of 'hot spots' for carbon sequestration in Manitoba and the development of targeted management practices for those areas.

Perennial forages can enhance soil productivity and fertility due to their biological nitrogen fixation, particularly legumes such as alfalfa (Bailey et al. 2010; Kulshreshtha et al. 2015; Pogue et al. 2018). Additionally, they also reduce the need for synthetic nitrogen fertilizers, minimizing nitrate leaching and nitrous oxide losses (Pogue et al. 2018). Based on nitrogen soil accumulation, the total value of nutrient cycling of Manitoba grasslands was estimated at \$127.04 million annually, with no accumulation in native grasslands and 0.056 t ha^{-1} accumulation in tame grasslands (Kulshreshtha et al. 2015). As for the carbon sequestration example describe above, spatially-explicit nutrient cycling estimates could also be obtained from the dataset generated in the present analysis.

Kulshreshtha et al. (2015) employed the benefit transfer approach to non-market goods and services in Manitoba grasslands, which uses valuation conducted in a different location from

the area being studied. The use of benefit transfer requires similar characteristics in terms of population and commodities for both locations. These authors applied benefit transfer in ecosystem services, such as water regulation, soil quality regulation, waste treatment and recreational services. They estimated that waste treatment in Manitoba grasslands was valued at approximately $153.92 million per year. Erosion control and water regulation were valued at $32 million and $12.26 million annually, respectively. Overall, they estimated that the total economic value of Manitoba grasslands was roughly $1,436 million or $630 ha^{-1} annually, with 42% of the total value attributed to carbon sequestration and 33% to forage production. These estimates relied on grassland area estimates compiled from different government sources, which were obtained through traditional field sampling. Remote sensors can easily provide these estimates through analysis of current and historical imagery of grassland landscapes. The MGI used in this analysis can provide these updated grassland cover estimates in the province to derive a valuation of other ecosystem services, aside from carbon sequestration and nutrient cycling.

The economic valuation of ecosystem services of grasslands through remote sensing would aid the development of sustainable management and conservation practices by serving as a measure to assess whether particular management strategies are effective in preserving the health of the ecosystem. With the rapidly changing climate, there has been increased adoption of beneficial management practices (BMPs) and nature-based solutions in reducing emissions and increasing soil carbon sequestration in agricultural lands, particularly grasslands (Drever et al. 2021; Environment and Climate Change Canada 2022). These management practices include cover crops, rotational grazing system, perennial cover for marginal lands, intercropping with annual crops and forage legumes, etc. (Manitoba Agriculture and Resource Development 2018; Drever et al. 2021).

Cover crops are crops that are not intended to be harvested but are instead planted to replace bare fallow and are ploughed under as green manure (Poeplau and Don 2015). By replacing a bare fallow period with cover crops, it improves the net carbon balance of agricultural soils because bare fallow is a carbon source (Poeplau and Don 2015; Drever et al. 2021). A meta-analysis found that the soil organic carbon (SOC) stocks through cover crops can increase at a mean annual carbon sequestration rate of 0.32 ± 0.08 Mg ha^{-1} yr^{-1} to an average maximum increase of 16.7 Mg ha^{-1} (Poeplau and Don 2015). Grazing cover crops had been explored to lengthen grazing season in the late fall when perennial forages mature and lose nutritive quality; however, they were found that they reduced SOC stocks (Tobin et al. 2020). Annual legume cover crops have been planted to increase soil nitrogen concentration, such as berseem clover (Asgedom and Kebreab 2011).

Controlling where cattle graze through fencing can promote uniform and even livestock distribution, such as in rotational grazing systems, which allows pastures to be rested and regenerated (Alberta Agriculture, Food and Rural Development and Alberta Beef Producers 2004; Bailey et al. 2010). Fencing also reduces selective grazing, particularly on ranges near the water source, and can also improve manure distribution (Aasen and Bjorge 2009). Rotational grazing systems were found to increase SOC stocks and reduce bulk density compared to continuous grazing systems based on a meta-analysis (Byrnes et al. 2018).

Restoration of marginal lands to permanent grasslands has the potential to improve carbon sequestration and soil quality while reducing GHG emissions from these areas (Asgedom and Kebreab 2011). In Canada, it was estimated that converting cultivated land to permanent grassland would reduce overall net GHG emissions by an average of 2.55 Mg CO_2 equivalent

ha^{-1} yr^{-1} (Grant et al. 2004). This change in management resulted in significantly more carbon being stored just in the first 10 years.

These BMPs and nature-based solutions generate net on-farm benefits that may partially or entirely offset the expenses of putting these strategies into operation in the short and long term (Pogue et al. 2020). Despite this, producers often cite time and financial constraints as the main drivers of the non-adoption of BMPs and nature-based solutions. As a result, some governments have provided incentives that will help producers to adopt these practices. One such government initiative is the federal Canadian Agricultural Partnership, which funds provincial BMP programs, such as Ag Action Manitoba and British Columbia Environmental Farm Plan (Manitoba Agriculture and Resource Development 2018; Environment and Climate Change Canada 2022; Investment Agriculture Foundation of British Columbia 2022). Furthermore, the assessment of the benefits of ecosystem services has formed as a basis of public policy in the implementation of these BMPs (Pannell 2008).

In addition to BMPs and nature-based solutions, the implementation of sustainable grazing management is vulnerable to drastic changes as a result of extreme climate events, such as droughts and spring flooding as evidenced in Manitoba over the last few years (Manitoba Agriculture and Resource Development 2022). More recently, frequent and long drought cycles had occurred in the Canadian Prairies (Statistics Canada 2021; Climenhaga 2022). It has been suggested to implement complementary rotational grazing during droughts, in which tame pastures are grazed first in spring and native grasslands are deferred until late summer and fall (Bailey et al. 2010). In general, tame pastures decline rapidly and are less resistant to droughts than native forages. Furthermore, this grazing system can also be complemented by forested and

shrub-covered rangelands from late spring through summer, which may retain more soil moisture than grasslands. Moderate stocking rates and longer pasture rest periods are also recommended during drought cycles.

The capability of remote sensing to detect grassland BMPs has not yet been adequately studied, nor is it possible. Despite this, remote sensing technology has been used in studies detecting grassland mowing/grazing events and grazing intensities (Reinermann et al. 2020). Different management strategies influence the biodiversity and species composition of grasslands, and the ability to detect grazing frequencies and intensities at a broader regional scale borne from these strategies may aid with research into the formulation of BMPs. In particular, remote sensing can be used to track the response of biomass yields and species composition to different grazing systems, such as rotational grazing systems. Furthermore, the development of comprehensive inventories of grasslands would have benefits beyond simply monitoring changes in plant cover and landscape fragmentation. This will trickle down to the assessment and valuation of carrying capacities and stocking rates, as well as ecosystem goods and services. Through increased awareness of the depressing and negative trends of our rapidly changing climate, further research can establish metrics for evaluating outcomes from various BMPs, which can influence farmers to understand the benefits of adopting these practices (Pogue et al. 2020).

6.2. General conclusions

Carrying capacity and stocking rate estimates are critical for developing sustainable grazing management practices, particularly in the context of climate change adaptation. Appropriate stocking rates must guarantee the long-term health of forage resources while also

maintaining and optimizing animal performance. Advances in remote sensing technology have enabled its application in the assessment of biomass, land cover and carrying capacities for use in grazing management plans. Furthermore, remote sensing products could identify areas of potential underutilization or overutilization of forage resources. The prediction of carrying capacities using remote sensing could allow range managers and cattle producers to adjust their stocking rates to be ecologically sustainable, avoiding grassland degradation and allowing its preservation for future use.

This study concluded that significant variations were found between the remotely sensed MGI/ACI inventories and the ACL database in discriminating between forests and shrublands and between native and tame forages. Reconciling the overall areas of forests and shrublands together, as well as native and tame forages, decreased the percentage differences between the two datasets. Another point to consider in light of the discrepancies between both datasets is that the current ACL data is updated irregularly because parcels are only inspected when they are up for allocation or auction, with less than 5% of all parcels being allocated every year. In terms of vegetation distribution, it was found that agricultural crown lands in Manitoba are heavily dominated by forests and shrublands, as opposed to native and tame forages, which are more preferred by grazers due to higher forage quality, palatability and yields.

The relationship between average carrying capacities and climate variables was found to be nonlinear, which is very common in environmental variables, and this facilitated the use of the GAM. The ecoregional GAM performed the best in fitting the data compared to MLR and PR. Of all climate variables tested, CMI had the highest relative contribution to the regression

models in explaining the variability in mean carrying capacities, indicating its usefulness in identifying moisture regimes in semi-arid landscapes such as the Canadian Prairies.

Finally, stocking rates were calculated based on the interpolated carrying capacities and land surface areas. The crown lands in two out of nine ecoregions in Agro-Manitoba were found to be overgrazed. Overall, the forage resources of the crown lands in Agro-Manitoba were being undergrazed by -44.64%, supporting the recommendation to increase stocking rates on these lands. Caution must be practiced in interpreting these findings as further validations and methodological improvements are needed to address the limitations of this study. Furthermore, the management of sustainable stocking rates should take into account the increased frequency of extreme weather events in the future caused by climate change, such as droughts.

6.3. Recommendations for future research

1. Boundary refinements should be made on the 20% of the crown land parcels not included in this study to correct delineation errors and to match the overall surface areas mapped in the GIS software to those recorded in the ACL database. This requires validation by ARD as errors cannot be corrected using publicly available online resources, such as the property assessment database.
2. Improvement of the land cover classification of MGI by incorporating recent ground-truthing data to improve the model training of its RF algorithm. The possible incorporation of LiDAR data can also help improve the land cover classification.
3. Additional sampling sites that cover all ecoregions and all ecosites should be used to estimate productivity. Currently, the forage benchmarking data used in this study only accounted for four of the nine ecoregions and eight of the 21 ecosites. The absence of

productivity data collected in Interlake Plain is concerning, given that the majority of the crown land parcels are located in that ecoregion. Obtaining data from all ecosites is also crucial as local soil properties play a significant role in vegetation productivity, in addition to climate factors. More sampling sites would allow more accurate interpolation using the similarity index of climate variables.

4. If there are additional sampling sites throughout Agro-Manitoba, well-known spatial interpolation methods, such as kriging, can offer an alternative for interpolating climate variables and carrying capacities instead of using the climate similarity index.
5. Aside from climate variables and soil properties, plant communities should be accounted for in future carrying capacity estimations. This would mean using satellite sensors with very fine spatial resolutions or field hyperspectral spectroradiometers to build a library of unique reflectances or spectral signatures that identifies specific plant communities. At the same time, the acquisition of images from these sensors would be more expensive than medium-resolution sensors used in this study like the 10-m Sentinel-2 and the 30-m Landsat-8. Therefore, the financial implications of increasing spatial resolution should be considered.

REFERENCES

Aasen, A., and Bjorge, M. 2009. Alberta forage manual. 2nd edition. Alberta Agriculture and Rural Development, Edmonton, AB. [Online] Available: https://open.alberta.ca/dataset/077326082x.

Agriculture and Agri-Food Canada 2019. Manitoba Forage Benchmarking Project [Microsoft Excel spreadsheet].

Agriculture and Agri-Food Canada 2020. AAFC forage productivity projects [Microsoft Excel spreadsheet].

Agriculture and Agri-Food Canada 2021a. Annual Crop Inventory, 2020 [GIS dataset]. Government of Canada. [Online] Available: https://open.canada.ca/data/en/dataset/ba2645d5-4458-414d-b196-6303ac06c1c9.

Agriculture and Agri-Food Canada 2021b. ISO 19131 Annual Crop Inventory – data product specifications. [Online] Available: https://agriculture.canada.ca/atlas/supportdocument_documentdesupport/annualCropInventory/en/ISO%2019131_AAFC_Annual_Crop_Inventory_Data_Product_Specifications.pdf.

Alberta Agriculture, Food and Rural Development, and Alberta Beef Producers 2004. Beneficial management practices: environmental manual for Alberta cow/calf producers - Open Government. Edmonton, AB. [Online] Available: https://open.alberta.ca/publications/2909821.

Alberta Sustainable Resource Development 2004. Methodology for calculating carrying and grazing capacity on public rangelands. Alberta Public Lands & Forests, Edmonton, AB. [Online] Available: https://open.alberta.ca/publications/0778536459.

Alberta Sustainable Resource Development 2010. Grassland Vegetation Inventory (GVI) specifications. Government of Alberta.

Alcaraz-Hernández, J.D., Muñoz-Mas, R., Martínez-Capel, F., Garófano-Gómez, V., and Vezza, P. 2016. Generalized additive models to predict adult and young brown trout (Salmo trutta Linnaeus, 1758) densities in Mediterranean rivers. J. Appl. Ichthyol. **32**: 217–228. doi:10.1111/jai.13025.

Alemu, A.W., Janzen, H., Little, S., Hao, X., Thompson, D.J., Baron, V., Iwaasa, A., Beauchemin, K.A., and Kröbel, R. 2017. Assessment of grazing management on farm greenhouse gas intensity of beef production systems in the Canadian Prairies using life cycle assessment. Agricultural Systems **158**: 1–13. doi:10.1016/j.agsy.2017.08.003.

Alexandratos, N., and Bruinsma, J. 2012. World agriculture towards 2030/2050: the 2012 revision. FAO, Rome. [Online] Available: https://www.fao.org/3/ap106e/ap106e.pdf.

Ali, I., Cawkwell, F., Dwyer, E., Barrett, B., and Green, S. 2016. Satellite remote sensing of grasslands: from observation to management. J. Plant Ecol. **9**: 649–671. doi:10.1093/jpe/rtw005.

Asgedom, H., and Kebreab, E. 2011. Beneficial management practices and mitigation of greenhouse gas emissions in the agriculture of the Canadian Prairie: a review. Agronomy Sust. Developm. **31**: 433–451. doi:10.1007/s13593-011-0016-2.

Badreldin, N. 2021. MGI grassland sampling protocol. Grassland Analytica. [Online] Available: https://www.gov.mb.ca/agriculture/land-management/pubs/mgi-sampling-protocol.pdf. Archived at:

[https://web.archive.org/web/20221113000243/https://www.gov.mb.ca/agriculture/land-management/pubs/mgi-sampling-protocol.pdf].
Badreldin, N., Prieto, B., and Fisher, R. 2021. Mapping grasslands in Mixed Grassland ecoregion of Saskatchewan using big remote sensing data and machine learning. Remote Sensing **13**: 4972. Multidisciplinary Digital Publishing Institute. doi:10.3390/rs13244972.
Bailey, A., McCartney, D., and Schellenberg, M. 2010. Management of Canadian prairie rangeland. Agriculture and Agri-Food Canada. [Online] Available: https://publications.gc.ca/site/eng/433214/publication.html.
Bédard, F., Crump, S., and Gaudreau, J. 2006. A comparison between Terra MODIS and NOAA AVHRR NDVI satellite image composites for the monitoring of natural grassland conditions in Alberta, Canada. Can. J. Remote. Sens. **32**: 44–50. doi:10.5589/m06-001.
Beef Cattle Research Council 2022. Forested rangeland grazing. [Online] Available: https://www.beefresearch.ca/topics/forested-rangeland-grazing/. Archived at: [https://web.archive.org/web/20221113001009/https://www.beefresearch.ca/topics/forested-rangeland-grazing/].
Bolinder, M.A., Janzen, H.H., Gregorich, E.G., Angers, D.A., and VandenBygaart, A.J. 2007. An approach for estimating net primary productivity and annual carbon inputs to soil for common agricultural crops in Canada. Agric. Ecosyst. Environ. **118**: 29–42. doi:10.1016/j.agee.2006.05.013.
Boswell, A., Petersen, S., Roundy, B., Jensen, R., Summers, D., Hulet, A., Boswell, A., Petersen, S., Roundy, B., Jensen, R., Summers, D., and Hulet, A. 2017. Rangeland monitoring using remote sensing: comparison of cover estimates from field measurements and image analysis. AIMSES **4**: 1–16. doi:10.3934/environsci.2017.1.1.
Byrnes, R.C., Eastburn, D.J., Tate, K.W., and Roche, L.M. 2018. A global meta-analysis of grazing impacts on soil health indicators. J. Environ. Qual. **47**: 758–765. doi:10.2134/jeq2017.08.0313.
Cade-Menun, B., Bainard, L., LaForge, K., Schellenberg, M., Houston, B., and Hamel, C. 2017. Long-term agricultural land use affects chemical and physical properties of soils from Southwest Saskatchewan. Can. J. Soil. Sci. **97**: 650–666. doi:10.1139/CJSS-2016-0153.
Campos-Taberner, M., García-Haro, F.J., Martínez, B., Sánchez-Ruíz, S., and Gilabert, M.A. 2019. A Copernicus Sentinel-1 and Sentinel-2 classification framework for the 2020+ European Common Agricultural Policy: a case study in València (Spain). Agronomy **9**: 556. Multidisciplinary Digital Publishing Institute. doi:10.3390/agronomy9090556.
Canadian Forage & Grassland Association 2022. Canada Grassland Inventory. [Online] Available: https://www.canadianfga.ca/projects-projets/grassland-inventory/. Archived at: [https://web.archive.org/web/20221113001559/https://www.canadianfga.ca/projects-projets/grassland-inventory/].
Castilla, G., Hird, J., Hall, R.J., Schieck, J., and McDermid, G. 2014. Completion and updating of a Landsat-based land cover polygon layer for Alberta, Canada. Can. J. Remote. Sens. **40**: 92–109. doi:10.1080/07038992.2014.933073.
Caudle, D., DiBenedetto, J., Karl, M., Sanchez, H., and Talbot, C. 2013. Interagency ecological site handbook for rangelands. Natural Resources Conservation Service, Bureau of Land Management and Forest Service. [Online] Available: https://jornada.nmsu.edu/files/InteragencyEcolSiteHandbook.pdf. Archived at:

[https://web.archive.org/web/20220909011429/https://jornada.nmsu.edu/files/InteragencyEcolSiteHandbook.pdf].
Chaves, M.E.D., Picoli, M.C.A., and Sanches, I.D. 2020. Recent applications of Landsat 8/OLI and Sentinel-2/MSI for land use and land cover mapping: a systematic review. Remote Sensing **12**: 3062. Multidisciplinary Digital Publishing Institute. doi:10.3390/rs12183062.
Chen, C., He, B., Guo, L., Zhang, Y., Xie, X., and Chen, Z. 2018. Identifying critical climate periods for vegetation growth in the Northern Hemisphere. J. Geophys. Res. Biogeosci. **123**: 2541–2552. doi:10.1029/2018JG004443.
Climenhaga, C. 2022.March 28. Severity and sweep of Prairie droughts to spiral as climate changes. CBC News. Edmonton, AB. [Online] Available: https://www.cbc.ca/news/canada/edmonton/severity-and-sweep-of-prairie-droughts-could-spiral-as-climate-changes-1.6391982. Archived at: [https://web.archive.org/web/20220701083525/https://www.cbc.ca/news/canada/edmonton/severity-and-sweep-of-prairie-droughts-could-spiral-as-climate-changes-1.6391982].
Conant, R.T. 2010. Challenges and opportunities for carbon sequestration in grassland systems: a technical report on grassland management and climate mitigation. FAO, Rome. [Online] Available: https://www.fao.org/3/i1399e/i1399e.pdf.
Coupland, R.T. 1961. A reconsideration of grassland classification in the northern Great Plains of North America. J. Ecol. **49**: 135–167. [Wiley, British Ecological Society]. doi:10.2307/2257431.
Daly, C., Halbleib, M., Smith, J.I., Gibson, W.P., Doggett, M.K., Taylor, G.H., Curtis, J., and Pasteris, P.P. 2008. Physiographically sensitive mapping of climatological temperature and precipitation across the conterminous United States. Int. J. Climatol. **28**: 2031–2064. doi:10.1002/joc.1688.
Davidson, A., Fisette, T., McNairn, H., and Daneshfar, B. 2017. Detailed crop mapping using remote sensing data (crop data layers). Pages 91–129 *in* J. Delincé, ed. Handbook on remote sensing for agricultural statistics. FAO, Rome. [Online] Available: https://www.fao.org/3/ca6394en/ca6394en.pdf.
Dechka, J.A., Franklin, S.E., Watmough, M.D., Bennett, R.P., and Ingstrup, D.W. 2002. Classification of wetland habitat and vegetation communities using multi-temporal IKONOS imagery in southern Saskatchewan. Can. J. Remote. Sens. **28**: 679–685. doi:10.5589/m02-064.
Doherty, K., Howerter, D., Devries, J., and Walker, J. 2018. Prairie Pothole Region of North America. Pages 679–688 *in* C.M. Finlayson, G.R. Milton, R.C. Prentice, and N. Davidson, eds. The wetland book, 1st edition. Springer Science+Business Media B.V, Dordrecht, NL. doi:10.1007/978-94-007-4001-3_15.
Downing, D.J., and Pettapiece, W.W. 2006. Natural regions and subregions of Alberta. Natural Regions Committee (Government of Alberta), Edmonton, AB. [Online] Available: https://open.alberta.ca/publications/0778545725.
Doytsher, Y., and Gelbman, E. 1995. Rubber-sheeting algorithm for cadastral maps. J. Surv. Eng. **121**: 155–162. American Society of Civil Engineers. doi:10.1061/(ASCE)0733-9453(1995)121:4(155).
Drever, C.R., Cook-Patton, S.C., Akhter, F., Badiou, P.H., Chmura, G.L., Davidson, S.J., Desjardins, R.L., Dyk, A., Fargione, J.E., Fellows, M., Filewod, B., Hessing-Lewis, M.,

Jayasundara, S., Keeton, W.S., Kroeger, T., Lark, T.J., Le, E., Leavitt, S.M., LeClerc, M.-E., Lemprière, T.C., Metsaranta, J., McConkey, B., Neilson, E., St-Laurent, G.P., Puric-Mladenovic, D., Rodrigue, S., Soolanayakanahally, R.Y., Spawn, S.A., Strack, M., Smyth, C., Thevathasan, N., Voicu, M., Williams, C.A., Woodbury, P.B., Worth, D.E., Xu, Z., Yeo, S., and Kurz, W.A. 2021. Natural climate solutions for Canada. Sci. Adv. **7**. doi:10.1126/sciadv.abd6034.

Dusseux, P., Hubert-Moy, L., Corpetti, T., and Vertès, F. 2015. Evaluation of SPOT imagery for the estimation of grassland biomass. Int. J. Appl. Earth Obs. Geoinf. **38**: 72–77. doi:10.1016/j.jag.2014.12.003.

Ecological Stratification Working Group, Agriculture and Agri-Food Canada, Centre for Land and Biological Resources Research, and Environment Canada, State of the Environment Directorate 1995. A national ecological framework for Canada. Centre for Land and Biological Resources Research, Research Branch, Agriculture and Agri-Food Canada, Ottawa. [Online] Available: https://sis.agr.gc.ca/cansis/publications/manuals/1996/A42-65-1996-national-ecological-framework.pdf.

Ecological Stratification Working Group, and Manitoba's Protected Areas Initiative 2013. Map of ecoregions of Manitoba. [Online] Available: https://www.gov.mb.ca/sd/pubs/protected_areas/ecoregion_map.pdf. Archived at: [https://web.archive.org/web/20220125021612/https://www.gov.mb.ca/sd/pubs/protected_areas/ecoregion_map.pdf].

Edey, S.N. 1977. Growing degree-days and crop production in Canada. Agriculture Canada, Ottawa. [Online] Available: https://archive.org/details/growingdegreeday00cana.

Eisfelder, C., Kuenzer, C., and Dech, S. 2012. Derivation of biomass information for semi-arid areas using remote-sensing data. Int. J. Remote Sens. **33**: 2937–2984. doi:10.1080/01431161.2011.620034.

Environment and Climate Change Canada 2022. 2030 Emissions reduction plan: Canada's next steps to clean air and a strong economy. ECCC, Gatineau, QC. [Online] Available: https://publications.gc.ca/site/eng/9.909338/publication.html.

Environment and Parks Alberta 2012. Native Prairie Vegetation Inventory (NPVI) polygons metadata. [Online] Available: https://geodiscover.alberta.ca/geoportal/rest/metadata/item/048a4cbf5df74ac8940166061a442c0/html.

Environment and Parks Alberta 2019. Grassland Vegetation Inventory (GVI) metadata. [Online] Available: https://geodiscover.alberta.ca/geoportal/rest/metadata/item/9dea946a24314ca399b89723fcd857fc/html.

ESRI 2019. How Similarity Search works. [Online] Available: https://desktop.arcgis.com/en/arcmap/latest/tools/spatial-statistics-toolbox/how-similarity-search-works.htm. Archived at: [https://web.archive.org/web/20190617195151/https://desktop.arcgis.com/en/arcmap/latest/tools/spatial-statistics-toolbox/how-similarity-search-works.htm].

ESRI 2020. ArcGIS Desktop 10.8/Pro 2.8. Environmental Systems Research Institute, Redlands, CA. [Online] Available: https://www.esri.com/.

ESRI 2021. ArcGIS Desktop 10.8/Pro 2.8. Environmental Systems Research Institute, Redlands, CA. [Online] Available: https://www.esri.com/.

Fassnacht, F.E., Latifi, H., Stereńczak, K., Modzelewska, A., Lefsky, M., Waser, L.T., Straub, C., and Ghosh, A. 2016. Review of studies on tree species classification from remotely sensed data. Remote Sens. Environ. **186**: 64–87. doi:10.1016/j.rse.2016.08.013.

Fassnacht, F.E., Poblete-Olivares, J., Rivero, L., Lopatin, J., Ceballos-Comisso, A., and Galleguillos, M. 2021. Using Sentinel-2 and canopy height models to derive a landscape-level biomass map covering multiple vegetation types. Int. J. Appl. Earth Obs. Geoinf. **94**: 102236. doi:10.1016/j.jag.2020.102236.

Fern, R.R., Foxley, E.A., Bruno, A., and Morrison, M.L. 2018. Suitability of NDVI and OSAVI as estimators of green biomass and coverage in a semi-arid rangeland. Ecological Indicators **94**: 16–21. doi:10.1016/j.ecolind.2018.06.029.

Filho, M.G., Kuplich, T.M., and De Quadros, F.L.F. 2020. Estimating natural grassland biomass by vegetation indices using Sentinel 2 remote sensing data. Int. J. Remote Sens. **41**: 2861–2876. Taylor & Francis. doi:10.1080/01431161.2019.1697004.

Foody, G.M. 2002. Status of land cover classification accuracy assessment. Remote Sens. Environ. **80**: 185–201. doi:10.1016/S0034-4257(01)00295-4.

Gage, A.M., Olimb, S.K., and Nelson, J. 2016. Plowprint: tracking cumulative cropland expansion to target grassland conservation. Great Plains Res. **26**: 107–116. University of Nebraska Press. [Online] Available: http://www.jstor.org/stable/44685737.

Gauthier, D.A., and Wiken, E.B. 2003. Monitoring the conservation of grassland habitats, Prairie Ecozone, Canada. Environ. Monit. Assess. **88**: 343–364. doi:10.1023/A:1025585527169.

Geiker, N.R.W., Bertram, H.C., Mejborn, H., Dragsted, L.O., Kristensen, L., Carrascal, J.R., Bügel, S., and Astrup, A. 2021. Meat and human health—current knowledge and research gaps. Foods **10**: 1556. doi:10.3390/foods10071556.

Ghosh, A., Fassnacht, F.E., Joshi, P.K., and Koch, B. 2014. A framework for mapping tree species combining hyperspectral and LiDAR data: role of selected classifiers and sensor across three spatial scales. Int. J. Appl. Earth Obs. Geoinf. **26**: 49–63. doi:10.1016/j.jag.2013.05.017.

Gomez, K., and Gomez, A. 1984. Statistical procedures for agricultural research. 2nd edition. International Rice Research Institute and Wiley, Los Baños, PH. [Online] Available: https://pdf.usaid.gov/pdf_docs/PNAAR208.pdf. Archived at: [https://web.archive.org/web/20220311095240/https://pdf.usaid.gov/pdf_docs/PNAAR208.pdf].

Grant, B., Smith, W.N., Desjardins, R., Lemke, R., and Li, C. 2004. Estimated N2O and CO2 emissions as influenced by agricultural practices in Canada. Climatic Change **65**: 315–332. doi:10.1023/B:CLIM.0000038226.60317.35.

Grant, K.M., Johnson, D.L., Hildebrand, D.V., and Peddle, D.R. 2013. Quantifying biomass production on rangeland in southern Alberta using SPOT imagery. Can. J. Remote. Sens. **38**: 695–708. Taylor & Francis. doi:10.5589/m12-056.

Grassland Analytica 2021. Manitoba Grassland Inventory [GIS dataset]. Manitoba Agriculture and Resource Development.

Grekousis, G., Mountrakis, G., and Kavouras, M. 2015. An overview of 21 global and 43 regional land-cover mapping products. Int. J. Remote Sens. **36**: 5309–5335. doi:10.1080/01431161.2015.1093195.

He, Y. 2014. The effect of precipitation on vegetation cover over three landscape units in a protected semi-arid grassland: Temporal dynamics and suitable climatic index. J. Arid. Environ. **109**: 74–82. doi:10.1016/j.jaridenv.2014.05.022.

Hoar, B., and Angelos, J. 2015. Beef cattle production. Pages 22–34 *in* A. Arens and J. Humphrey, eds. Food animal production manual. UC Davis Western Institute for Food Safety & Security, Davis, CA. [Online] Available: http://www.wifss.ucdavis.edu/wp-content/uploads/2016/05/Food_Animal_Production_Complete_Manual.pdf. Archived at: [https://web.archive.org/web/20190711013922/http://www.wifss.ucdavis.edu/wp-content/uploads/2016/05/Food_Animal_Production_Complete_Manual.pdf].

Hogg, E.H. 1994. Climate and the southern limit of the western Canadian boreal forest. Can. J. For. Res. **24**: 1835–1845. NRC Research Press. doi:10.1139/x94-237.

Hogg, E.H. 1997. Temporal scaling of moisture and the forest-grassland boundary in western Canada. Agric. For. Meteorol. **84**: 115–122. doi:10.1016/S0168-1923(96)02380-5.

Investment Agriculture Foundation of British Columbia 2022. Environmental Farm Plan: Beneficial Management Practices Policy and Descriptions (2022-2023) Program. [Online] Available: https://iafbc.ca/wp-content/uploads/2022/10/2022-10-03-BMP-List-Climate-Mitigation-and-Adpatation.pdf. Archived at: [https://web.archive.org/web/20221126221744/https://iafbc.ca/wp-content/uploads/2022/10/2022-10-03-BMP-List-Climate-Mitigation-and-Adpatation.pdf].

Jin, Y., Liu, X., Chen, Y., and Liang, X. 2018. Land-cover mapping using random forest classification and incorporating NDVI time-series and texture: a case study of central Shandong. Int. J. Remote Sens. **39**: 8703–8723. doi:10.1080/01431161.2018.1490976.

Jin, Y., Yang, X., Qiu, J., Li, J., Gao, T., Wu, Q., Zhao, F., Ma, H., Yu, H., and Xu, B. 2014. Remote sensing-based biomass estimation and its spatio-temporal variations in temperate grassland, northern China. Remote Sensing **6**: 1496–1513. Multidisciplinary Digital Publishing Institute. doi:10.3390/rs6021496.

Kaufmann, J. 2011. Interactions between cattle grazing and forestry on Alberta's public lands. University of Alberta, Edmonton, AB. [Online] Available: https://library-archives.canada.ca/eng/services/services-libraries/theses/Pages/item.aspx?idNumber=1019492915.

Krzic, M., Newman, R., Trethewey, C., Bulmer, C., and Chapman, B. 2006. Cattle grazing effects on plant species composition and soil compaction on rehabilitated forest landings in central interior British Columbia. J. Soil Water Conserv. **61**: 137–144.

Kulshreshtha, S., Undi, M., Zhang, J., Ghorbani, M., Wittenberg, K., Stewart, A., Salvano, E., Kebreab, E., and Ominski, K. 2015. Challenges and opportunities in estimating the value of goods and services in temperate grasslands — a case study of prairie grasslands in Manitoba, Canada. Pages 147–169 *in* V. Pilipavičius, ed. Agroecology. IntechOpen, London. doi:10.5772/59899.

Latifovic, R. 2010. 2010 Land Cover of Canada [GIS dataset]. Canada Centre for Remote Sensing, Natural Resources Canada. [Online] Available: https://open.canada.ca/data/en/dataset/c688b87f-e85f-4842-b0e1-a8f79ebf1133.

Latifovic, R. 2015. 2015 Land Cover of Canada [GIS dataset]. Canada Centre for Remote Sensing, Natural Resources Canada. [Online] Available: https://open.canada.ca/data/en/dataset/4e615eae-b90c-420b-adee-2ca35896caf6.

Latifovic, R. 2020. 2020 Land Cover of Canada [GIS dataset]. Canada Centre for Remote Sensing, Natural Resources Canada. [Online] Available: https://open.canada.ca/data/en/dataset/ee1580ab-a23d-4f86-a09b-79763677eb47.

de Leeuw, J., Rizayeva, A., Namazov, E., Bayramov, E., Marshall, M.T., Etzold, J., and Neudert, R. 2019. Application of the MODIS MOD 17 Net Primary Production product in grassland carrying capacity assessment. Int. J. Appl. Earth Obs. Geoinf. **78**: 66–76. doi:10.1016/j.jag.2018.09.014.

Legesse, G., Cordeiro, M.R.C., Ominski, K.H., Beauchemin, K.A., Kroebel, R., McGeough, E.J., Pogue, S., and McAllister, T.A. 2018. Water use intensity of Canadian beef production in 1981 as compared to 2011. Sci. Total Environ. **619–620**: 1030–1039. doi:10.1016/j.scitotenv.2017.11.194.

Li, A., Dhakal, S., Glenn, N.F., Spaete, L.P., Shinneman, D.J., Pilliod, D.S., Arkle, R.S., and McIlroy, S.K. 2017. LiDAR aboveground vegetation biomass estimates in shrublands: prediction, uncertainties and application to coarser scales. Remote Sensing **9**: 903. Multidisciplinary Digital Publishing Institute. doi:10.3390/rs9090903.

Li, Z., and Guo, X. 2012. Detecting climate effects on vegetation in northern mixed prairie using NOAA AVHRR 1-km time-series NDVI data. Remote Sensing **4**: 120–134. Molecular Diversity Preservation International. doi:10.3390/rs4010120.

Lillesand, T., Kiefer, R., and Chipman, J. 2015. Remote sensing and image interpretation. 7th edition. Wiley, Hoboken, NJ.

Liu, Z., and Menzel, L. 2016. Identifying long-term variations in vegetation and climatic variables and their scale-dependent relationships: A case study in Southwest Germany. Global Planet. Change **147**: 54–66. doi:10.1016/j.gloplacha.2016.10.019.

Longley, P., Goodchild, M., Maguire, D., and Rhind, D. 2015. Geographic information science and systems. 4th edition. Wiley, Hoboken, NJ.

Lu, D. 2006. The potential and challenge of remote sensing-based biomass estimation. Int. J. Remote Sens. **27**: 1297–1328. doi:10.1080/01431160500486732.

Lu, D., and Weng, Q. 2007. A survey of image classification methods and techniques for improving classification performance. Int. J. Remote Sens. **28**: 823–870. doi:10.1080/01431160600746456.

Manitoba Agriculture and Resource Development 2018. Ag Action Manitoba Program for farmers: a program guide to the terms and conditions. [Online] Available: https://www.gov.mb.ca/agriculture/canadian-agricultural-partnership/pubs/guidebook/ag-action-mb-program-guide-for-farmers.pdf. Archived at: [https://web.archive.org/web/20210727150846/https://www.gov.mb.ca/agriculture/canadian-agricultural-partnership/pubs/guidebook/ag-action-mb-program-guide-for-farmers.pdf].

Manitoba Agriculture and Resource Development 2019a. Modernizing the Agricultural Crown Lands Leasing Program in Manitoba. [Online] Available: https://www.gov.mb.ca/agriculture/land-management/crown-land/pubs/modernizing-acl-leasing-program.pdf. Archived at: [https://web.archive.org/web/20210725053838/https://www.gov.mb.ca/agriculture/land-management/crown-land/pubs/modernizing-acl-leasing-program.pdf].

Manitoba Agriculture and Resource Development 2019b. The Manitoba Protein Advantage. [Online] Available: https://www.gov.mb.ca/agriculture/protein/pubs/manitoba-protein-

strategy.pdf. Archived at: [https://web.archive.org/web/20220709085255/https://www.gov.mb.ca/agriculture/protein/pubs/manitoba-protein-strategy.pdf].
Manitoba Agriculture and Resource Development 2020a. ARD Crown Land Database [Microsoft Excel spreadsheet].
Manitoba Agriculture and Resource Development 2020b. Policy ACL 01-03: Allocation and rent of agricultural leases or permits. [Online] Available: https://www.gov.mb.ca/agriculture/land-management/crown-land/pubs/acl-01-03-allocation-and-rent-policy.pdf. Archived at: [https://web.archive.org/web/20220319212627/http://www.gov.mb.ca/agriculture/land-management/crown-land/pubs/acl-01-03-allocation-and-rent-policy.pdf].
Manitoba Agriculture and Resource Development 2021. Manitoba Grassland Inventory (MGI): land identification project. [Online] Available: https://www.gov.mb.ca/agriculture/land-management/land-id-tool.html. Archived at: [https://web.archive.org/web/20221113003505/https://www.gov.mb.ca/agriculture/land-management/land-id-tool.html].
Manitoba Agriculture and Resource Development 2022. Crop report: issue 2 (week 20). [Online] Available: https://www.gov.mb.ca/agriculture/crops/seasonal-reports/crop-report-archive/pubs/crop-report-2022-05-17.pdf. Archived at: [https://web.archive.org/web/20220621020815/https://www.gov.mb.ca/agriculture/crops/seasonal-reports/crop-report-archive/pubs/crop-report-2022-05-17.pdf].
Manitoba Land Initiative 2018. Manitoba Cadastral Mapping [GIS dataset]. [Online] Available: https://mli2.gov.mb.ca/cadastral/index.html.
Manitoba Land Initiative 2021. Manitoba LiDAR tracker. [Online] Available: https://geoportal.gov.mb.ca/maps/manitoba-lidar-tracker.
Manitoba Municipal Relations 2020. Manitoba Property Assessment online map [GIS dataset]. ESRI. [Online] Available: https://www.arcgis.com/home/item.html?id=2c09ffc330684c7a9a7ff1065ee6859b.
Manitoba Museum 2014. Prairie types. [Online] Available: https://www.prairiepollination.ca/bienvenue_dans_les_prairies-welcome_to_the_prairies/types_de_prairie-prairie_types/. Archived at: [https://web.archive.org/web/20220906220647/https://www.prairiepollination.ca/bienvenue_dans_les_prairies-welcome_to_the_prairies/types_de_prairie-prairie_types/].
Manitoba Sustainable Agriculture Practices Program 2010. Development of models to quantify and monitor the spatiotemporal distribution of vegetation biomass in Manitoba grasslands/pastures using satellite imagery. Manitoba Agriculture and Resource Development. [Online] Available: https://umanitoba.ca/faculties/afs/ncle/pdf/2010_Satellite_Imagery_of_Vegetation_Distribution.pdf. Archived at: [https://web.archive.org/web/20210325101533/https://umanitoba.ca/faculties/afs/ncle/pdf/2010_Satellite_Imagery_of_Vegetation_Distribution.pdf].
Manitoba's Protected Areas Initiative 2005. Map of natural regions of Manitoba. [Online] Available: https://www.gov.mb.ca/sd/pai/images/maps/nat-regions.pdf. Archived at: [https://web.archive.org/web/20221113003830/https://www.gov.mb.ca/sd/pai/images/maps/nat-regions.pdf].

Marx, T. (ed.) 2008. The beef cow-calf manual. 4th edition. Alberta Agriculture and Food, Edmonton, AB. [Online] Available: https://open.alberta.ca/publications/0773260757.
McInnes, W.S., Smith, B., and McDermid, G.J. 2015. Discriminating native and nonnative grasses in the Dry Mixedgrass Prairie with MODIS NDVI time series. IEEE J. Sel. Top. Appl. Earth Observ. Remote Sens. **8**: 1395–1403. doi:10.1109/JSTARS.2015.2416713.
McKercher, R., and Wolfe, B. 1986. Understanding Western Canada's Dominion Land Survey. University of Saskatchewan, Division of Extension and Community Relations, Saskatoon, SK. [Online] Available: https://static1.squarespace.com/static/6148b130f68d7f1bb745938c/t/6185ab073b28f4218e2ed168/1636150031489/Understanding+_DL_Survey_System.pdf. Archived at: [https://web.archive.org/web/20221113004201/https://static1.squarespace.com/static/6148b130f68d7f1bb745938c/t/6185ab073b28f4218e2ed168/1636150031489/Understanding%2B_DL_Survey_System.pdf].
Meshesha, D.T., Ahmed, M.M., Abdi, D.Y., and Haregeweyn, N. 2020. Prediction of grass biomass from satellite imagery in Somali regional state, eastern Ethiopia. Heliyon **6**: e05272. doi:10.1016/j.heliyon.2020.e05272.
Meshesha, D.T., Moahmmed, M., and Yosuf, D. 2019. Estimating carrying capacity and stocking rates of rangelands in Harshin District, Eastern Somali Region, Ethiopia. Ecol. Evol. **9**: 13309–13319. doi:10.1002/ece3.5786.
Misra, G., Cawkwell, F., and Wingler, A. 2020. Status of phenological research using Sentinel-2 data: a review. Remote Sensing **12**: 2760. Multidisciplinary Digital Publishing Institute. doi:10.3390/rs12172760.
Mitchell, R., Fritz, J., Moore, K., Moser, L., Vogel, K., Redfearn, D., and Wester, D. 2001. Predicting forage quality in switchgrass and big bluestem. Agron. J. **93**: 118–124. doi:10.2134/agronj2001.931118x.
Munyati, C. 2022. Detecting the distribution of grass aboveground biomass on a rangeland using Sentinel-2 MSI vegetation indices. Adv. Space Res. **69**: 1130–1145. doi:10.1016/j.asr.2021.10.048.
Murphy, D.J., Murphy, M.D., O'Brien, B., and O'Donovan, M. 2021. A review of precision technologies for optimising pasture measurement on Irish grassland. Agriculture **11**: 600. Multidisciplinary Digital Publishing Institute. doi:10.3390/agriculture11070600.
Mutanga, O., and Skidmore, A.K. 2004. Narrow band vegetation indices overcome the saturation problem in biomass estimation. Int. J. Remote Sens. **25**: 3999–4014. doi:10.1080/01431160310001654923.
Newman, R., and Powell, G. 1997. Forest grazing: effects of cattle trampling and browsing on lodgepole pine plantations. British Columbia Ministry of Forests, Kamloops, BC. [Online] Available: https://www.for.gov.bc.ca/hre/pubs/pubs/0639.htm. Archived at: [https://web.archive.org/web/20040710020303/http://www.for.gov.bc.ca/hfd/pubs/Docs/En/En13.pdf].
Nuttall, W.F., McCartney, D.H., Horton, P.R., Bittman, S., and Waddington, J. 1991. The effect of N, P, S fertilizer, temperature and precipitation on the yield of bromegrass and alfalfa pasture established on a Luvisolic soil. Can. J. Plant Sci. **71**: 1047–1055. doi:10.4141/cjps91-147.
Odum, E. 1971. Fundamentals of ecology. 3rd edition. W. B. Saunders, Philadelphia, PA. [Online] Available: http://archive.org/details/fundamentalsofec0000odum.

Otunga, C., Odindi, J., Mutanga, O., and Adjorlolo, C. 2019. Evaluating the potential of the red edge channel for C3 (Festuca spp.) grass discrimination using Sentinel-2 and Rapid Eye satellite image data. Geocarto Int. **34**: 1123–1143. Taylor & Francis. doi:10.1080/10106049.2018.1474274.

Pannell, D.J. 2008. Public benefits, private benefits, and policy mechanism choice for land-use change for environmental benefits. Land Economics **84**: 225–240. University of Wisconsin Press. doi:10.3368/le.84.2.225.

Patrice, T., and Lamboni, D. 2020. COVID-19 and the beef supply chain: an overview. [Online] Available: https://www150.statcan.gc.ca/n1/pub/45-28-0001/2020001/article/00086-eng.htm. Archived at: [https://web.archive.org/web/20220917133640/https://www150.statcan.gc.ca/n1/pub/45-28-0001/2020001/article/00086-eng.htm].

Pebesma, E., Bivand, R., Racine, E., Sumner, M., Cook, I., Keitt, T., Lovelace, R., Wickham, H., Ooms, J., Müller, K., Pedersen, T.L., Baston, D., and Dunnington, D. 2021. sf: Simple features for R (standardized support for spatial vector data). [Online] Available: https://cran.r-project.org/package=sf.

Pedersen, E.J., Miller, D.L., Simpson, G.L., and Ross, N. 2019. Hierarchical generalized additive models in ecology: an introduction with mgcv. PeerJ **7**: e6876. PeerJ Inc. doi:10.7717/peerj.6876.

Poeplau, C., and Don, A. 2015. Carbon sequestration in agricultural soils via cultivation of cover crops – A meta-analysis. Agric. Ecosyst. Environ. **200**: 33–41. doi:10.1016/j.agee.2014.10.024.

Pogue, S.J., Kröbel, R., Janzen, H.H., Alemu, A.W., Beauchemin, K.A., Little, S., Iravani, M., de Souza, D.M., and McAllister, T.A. 2020. A social-ecological systems approach for the assessment of ecosystem services from beef production in the Canadian Prairie. Ecosystem Services **45**: 101172. doi:10.1016/j.ecoser.2020.101172.

Pogue, S.J., Kröbel, R., Janzen, H.H., Beauchemin, K.A., Legesse, G., de Souza, D.M., Iravani, M., Selin, C., Byrne, J., and McAllister, T.A. 2018. Beef production and ecosystem services in Canada's Prairie Provinces: a review. Agricultural Systems **166**: 152–172. doi:10.1016/j.agsy.2018.06.011.

QGIS.org 2020. QGIS 3.16. QGIS Association. [Online] Available: https://qgis.org/.

Qin, P., Sun, B., Li, Z., Gao, Z., Li, Y., Yan, Z., and Gao, T. 2021. Estimation of grassland carrying capacity by applying high spatiotemporal remote sensing techniques in Zhenglan Banner, Inner Mongolia, China. Sustainability **13**: 3123. Multidisciplinary Digital Publishing Institute. doi:10.3390/su13063123.

R Core Team 2020. R: a language and environment for statistical computing. R Foundation for Statistical Computing, Vienna, Austria. [Online] Available: https://www.R-project.org/.

Radoux, J., Chomé, G., Jacques, D.C., Waldner, F., Bellemans, N., Matton, N., Lamarche, C., D'Andrimont, R., and Defourny, P. 2016. Sentinel-2's potential for sub-pixel landscape feature detection. Remote Sensing **8**: 488. Multidisciplinary Digital Publishing Institute. doi:10.3390/rs8060488.

Ramoelo, A., Cho, M.A., Mathieu, R., Madonsela, S., van de Kerchove, R., Kaszta, Z., and Wolff, E. 2015. Monitoring grass nutrients and biomass as indicators of rangeland quality and quantity using random forest modelling and WorldView-2 data. Int. J. Appl. Earth Obs. Geoinf. **43**: 43–54. doi:10.1016/j.jag.2014.12.010.

Rees, W.E. 1996. Revisiting carrying capacity: area-based indicators of sustainability. Popul. Environ. **17**: 195–215. doi:10.1007/BF02208489.

Reinermann, S., Asam, S., and Kuenzer, C. 2020. Remote sensing of grassland production and management—a review. Remote Sensing **12**: 1949. Multidisciplinary Digital Publishing Institute. doi:10.3390/rs12121949.

Ren, H., and Feng, G. 2015. Are soil-adjusted vegetation indices better than soil-unadjusted vegetation indices for above-ground green biomass estimation in arid and semi-arid grasslands? Grass Forage Sci. **70**: 611–619. doi:10.1111/gfs.12152.

Rigge, M., Smart, A., Wylie, B., Gilmanov, T., and Johnson, P. 2013. Linking phenology and biomass productivity in South Dakota mixed-grass prairie. Rangeland Ecol. Manage. **66**: 579–587. doi:10.2111/REM-D-12-00083.1.

RStudio Team 2020. RStudio: integrated development environment for R. RStudio, PBC, Boston, MA. [Online] Available: http://www.rstudio.com/.

Samson, F., and Knopf, F. 1994. Prairie conservation in North America. BioScience **44**: 418–421. doi:10.2307/1312365.

Saskatchewan GeoHub 2021. Prairie Landscape Inventory (PLI) classification [GIS dataset]. [Online] Available: https://geohub.saskatchewan.ca/maps/prairie-landscape-inventory-pli-classification/.

Schellenberg, M.P., Holt, N.W., and Waddington, J. 1999. Effects of grazing dates on forage and beef production of mixed prairie rangeland. Can. J. Anim. Sci. **79**: 335–341. NRC Research Press. doi:10.4141/A98-066.

Schütz, M. 2010. Woody encroachment on pastures in western Canada. University of Manitoba, Winnipeg. [Online] Available: https://mspace.lib.umanitoba.ca/handle/1993/4073.

Shimizu, E., and Fuse, T. 2003. Rubber-sheeting of historical maps in GIS and its application to landscape visualization of old-time cities: focusing on Tokyo of the past. Proceedings of the 8th international conference on computers in urban planning and urban management **11**: 3–8. [Online] Available: http://planner.t.u-tokyo.ac.jp/archive/member/fuse/rubber_sheeting.pdf. Archived at: [https://web.archive.org/web/20190712144926/http://planner.t.u-tokyo.ac.jp/archive/member/fuse/rubber_sheeting.pdf].

Shoko, C., and Mutanga, O. 2017a. Examining the strength of the newly-launched Sentinel 2 MSI sensor in detecting and discriminating subtle differences between C3 and C4 grass species. ISPRS J. Photogramm. Remote Sens. **129**: 32–40. doi:10.1016/j.isprsjprs.2017.04.016.

Shoko, C., and Mutanga, O. 2017b. Seasonal discrimination of C3 and C4 grasses functional types: An evaluation of the prospects of varying spectral configurations of new generation sensors. Int. J. Appl. Earth Obs. Geoinf. **62**: 47–55. doi:10.1016/j.jag.2017.05.015.

Shoko, C., Mutanga, O., and Dube, T. 2016. Progress in the remote sensing of C3 and C4 grass species aboveground biomass over time and space. ISPRS J. Photogramm. Remote Sens. **120**: 13–24. doi:10.1016/j.isprsjprs.2016.08.001.

Shoko, C., Mutanga, O., Dube, T., and Slotow, R. 2018. Characterizing the spatio-temporal variations of C3 and C4 dominated grasslands aboveground biomass in the Drakensberg, South Africa. Int. J. Appl. Earth Obs. Geoinf. **68**: 51–60. doi:10.1016/j.jag.2018.02.006.

Silleos, N.G., Alexandridis, T.K., Gitas, I.Z., and Perakis, K. 2006. Vegetation indices: advances made in biomass estimation and vegetation monitoring in the last 30 years. Geocarto Int. **21**: 21–28. doi:10.1080/10106040608542399.

Smith, A.M., and Buckley, J.R. 2011. Investigating RADARSAT-2 as a tool for monitoring grassland in western Canada. Can. J. Remote. Sens. **37**: 93–102. doi:10.5589/m11-027.

Society for Range Management 1998. Glossary of terms used in range management. 4th edition. Denver, CO.

Song, C., Huang, C., and Liu, H. 2013. Predictive vegetation mapping approach based on spectral data, DEM and generalized additive models. Chin. Geogr. Sci. **23**: 331–343. doi:10.1007/s11769-013-0590-0.

Song, C., Ren, H., and Huang, C. 2016. Estimating soil salinity in the Yellow River Delta, Eastern China—an integrated approach using spectral and terrain indices with the generalized additive model. Pedosphere **26**: 626–635. doi:10.1016/S1002-0160(15)60071-6.

Stadel, C. 2015. A mountain in the prairies – the Riding Mountain Biosphere Reserve, Manitoba, Canada. ecomont **7**: 83–88. doi:10.1553/eco.mont-7-2s83.

Statistics Canada 2017. Table 32-10-0406-01: Land use, Census of Agriculture, 2011 and 2016. [Online] Available: https://doi.org/10.25318/3210040601-eng.

Statistics Canada 2021.July 29. Impacts of the drought on crop quality indicators. The Daily. [Online] Available: https://www150.statcan.gc.ca/n1/daily-quotidien/210729/dq210729d-eng.htm. Archived at: [https://web.archive.org/web/20220324111524/https://www150.statcan.gc.ca/n1/daily-quotidien/210729/dq210729d-eng.htm].

Statistics Canada 2022a. Table 32-10-0130-01: Number of cattle, by class and farm type (x 1,000). [Online] Available: https://doi.org/10.25318/3210013001-eng.

Statistics Canada 2022b. Table 32-10-0045-01: Farm cash receipts, annual (x 1,000). [Online] Available: https://doi.org/10.25318/3210004501-eng.

Statistics Canada 2022c. Table 32-10-0249-01: Land use, Census of Agriculture, 2021. [Online] Available: https://doi.org/10.25318/3210024901-eng.

Sveinson, J.M.A. 2003. Restoring tallgrass prairie in southern Manitoba, Canada. University of Manitoba. [Online] Available: https://mspace.lib.umanitoba.ca/xmlui/handle/1993/3808.

Thompson, M.D. 1977. Remote sensing in operational range management programs in Western Canada. Page *in* ERIM Proc. of the 11th Intern. Symp. on Remote Sensing of Environment. [Online] Available: https://ntrs.nasa.gov/citations/19780006613.

Thorpe, J. 2014a. Saskatchewan rangeland ecosystems: ecoregions and ecosites. Saskatchewan Research Council. [Online] Available: https://www.pcap-sk.org/rsu_docs/documents/1_ecoregions_and_ecosites6784.pdf. Archived at: [https://web.archive.org/web/20220305135446/https://www.pcap-sk.org/rsu_docs/documents/1_ecoregions_and_ecosites6784.pdf].

Thorpe, J. 2014b. Rangeland classification for Agri-Manitoba. Saskatchewan Research Council, Manitoba Forage and Grassland Association. [Online] Available: https://static1.squarespace.com/static/5c6d9be4797f740e645a4310/t/5c8464fdfa0d603600a6acff/1552180486687/Manitoba-Rangeland-Classification-v3.pdf. Archived at: [https://web.archive.org/web/20221006190659/https://static1.squarespace.com/static/5c6

d9be4797f740e645a4310/t/5c8464fdfa0d603600a6acff/1552180486687/Manitoba-Rangeland-Classification-v3.pdf].
Thorpe, J. 2017. Ecosites of Agri-Manitoba [GIS dataset]. Manitoba Forage and Grassland Association.
Thorpe, J., Wolfe, S.A., and Houston, B. 2008. Potential impacts of climate change on grazing capacity of native grasslands in the Canadian prairies. Can. J. Soil. Sci. **88**: 595–609. doi:10.4141/CJSS07094.
Tieszen, L.L., Reed, B.C., Bliss, N.B., Wylie, B.K., and DeJong, D.D. 1997. NDVI, C3 and C4 production, and distributions in Great Plains grassland land cover classes. Ecol. Appl. **7**: 59–78. doi:10.1890/1051-0761(1997)007[0059:NCACPA]2.0.CO;2.
Tobin, C., Singh, S., Kumar, S., Wang, T., and Sexton, P. 2020. Demonstrating short-term impacts of grazing and cover crops on soil health and economic benefits in an integrated crop-livestock system in South Dakota. Open J. Soil Sci. **10**: 109. Scientific Research Publishing. doi:10.4236/ojss.2020.103006.
Tucker, C.J., and Sellers, P.J. 1986. Satellite remote sensing of primary production. Int. J. Remote Sens. **7**: 1395–1416. Taylor & Francis. doi:10.1080/01431168608948944.
Virk, R., and Mitchell, S.W. 2014. Effect of different grazing intensities on the spatial-temporal variability in above-ground live plant biomass in North American mixed grasslands. Can. J. Remote. Sens. **40**: 423–439. Taylor & Francis. doi:10.1080/07038992.2014.1009882.
Wang, G., Liu, S., Liu, T., Fu, Z., Yu, J., and Xue, B. 2019a. Modelling above-ground biomass based on vegetation indexes: a modified approach for biomass estimation in semi-arid grasslands. Int. J. Remote Sens. **40**: 3835–3854. Taylor & Francis. doi:10.1080/01431161.2018.1553319.
Wang, J., Xiao, X., Bajgain, R., Starks, P., Steiner, J., Doughty, R.B., and Chang, Q. 2019b. Estimating leaf area index and aboveground biomass of grazing pastures using Sentinel-1, Sentinel-2 and Landsat images. ISPRS J. Photogramm. Remote Sens. **154**: 189–201. doi:10.1016/j.isprsjprs.2019.06.007.
Wang, T., Hamann, A., Spittlehouse, D., and Carroll, C. 2016. Locally downscaled and spatially customizable climate data for historical and future periods for North America. PLoS ONE **11**: e0156720. doi:10.1371/journal.pone.0156720.
Wang, T., Hamann, A., Spittlehouse, D.L., and Murdock, T.Q. 2012. ClimateWNA—high-resolution spatial climate data for Western North America. J. Appl. Meteorol. Climatol. **51**: 16–29. American Meteorological Society. doi:10.1175/JAMC-D-11-043.1.
Wickham, H., François, R., Henry, L., Müller, K., and RStudio 2021. dplyr: A grammar of data manipulation. [Online] Available: https://cran.r-project.org/package=dplyr.
Willms, W.D., and Jefferson, P.G. 1993. Production characteristics of the mixed prairie: constraints and potential. Can. J. Anim. Sci. **73**: 765–778. NRC Research Press. doi:10.4141/cjas93-080.
Wood, S. 2021. mgcv: Mixed GAM computation vehicle with automatic smoothness estimation. [Online] Available: https://cran.r-project.org/web/packages/mgcv/.
World Wildlife Fund 2016. Plowprint reports. [Online] Available: https://www.worldwildlife.org/projects/plowprint-report. Archived at: [https://web.archive.org/web/20161210153413/https://www.worldwildlife.org/projects/plowprint-report].

Wu, J., Li, M., Fiedler, S., Ma, W., Wang, X., Zhang, X., and Tietjen, B. 2019. Impacts of grazing exclusion on productivity partitioning along regional plant diversity and climatic gradients in Tibetan alpine grasslands. J. Environ. Manage. **231**: 635–645. doi:10.1016/j.jenvman.2018.10.097.

Wu, J., Wurst, S., and Zhang, X. 2016. Plant functional trait diversity regulates the nonlinear response of productivity to regional climate change in Tibetan alpine grasslands. Scientific Reports **6**: 35649. Nature Publishing Group. doi:10.1038/srep35649.

Xie, Y., Sha, Z., and Yu, M. 2008. Remote sensing imagery in vegetation mapping: a review. J. Plant Ecol. **1**: 9–23. doi:10.1093/jpe/rtm005.

Xue, Y., Tanaka, K., Yu, H., Chen, Y., Guan, L., Li, Z., Yu, H., Xu, B., Ren, Y., and Wan, R. 2018. Using a new framework of two-phase generalized additive models to incorporate prey abundance in spatial distribution models of juvenile slender lizardfish in Haizhou Bay, China. Mar. Biol. Res. **14**: 508–523. Taylor & Francis. doi:10.1080/17451000.2018.1447673.

Yang, X., Smith, A.M., and Hill, M.J. 2017. Updating the Grassland Vegetation Inventory using change vector analysis and functionally-based vegetation indices. Can. J. Remote Sens. **43**: 62–78. doi:10.1080/07038992.2017.1263151.

Youcef, W.A., Lambert, Y., and Audet, C. 2013. Spatial distribution of Greenland halibut Reinhardtius hippoglossoides in relation to abundance and hypoxia in the estuary and Gulf of St. Lawrence. Fish. Oceanogr. **22**: 41–60. doi:10.1111/fog.12004.

Yu, L., Liang, L., Wang, J., Zhao, Y., Cheng, Q., Hu, L., Liu, S., Yu, L., Wang, X., Zhu, P., Li, X., Xu, Y., Li, C., Fu, W., Li, X., Li, W., Liu, C., Cong, N., Zhang, H., Sun, F., Bi, X., Xin, Q., Li, D., Yan, D., Zhu, Z., Goodchild, M.F., and Gong, P. 2014. Meta-discoveries from a synthesis of satellite-based land-cover mapping research. Int. J. Remote Sens. **35**: 4573–4588. doi:10.1080/01431161.2014.930206.

Yu, L., Zhou, L., Liu, W., and Zhou, H.-K. 2010. Using remote sensing and GIS technologies to estimate grass yield and livestock carrying capacity of alpine grasslands in Golog Prefecture, China. Pedosphere **20**: 342–351. doi:10.1016/S1002-0160(10)60023-9.

Zhang, C., and Guo, X. 2008. Monitoring northern mixed prairie health using broadband satellite imagery. Int. J. Remote Sens. **29**: 2257–2271. doi:10.1080/01431160701408378.

Zhang, J., Zhang, L., Liu, W., Qi, Y., and Wo, X. 2014. Livestock-carrying capacity and overgrazing status of alpine grassland in the Three-River Headwaters region, China. J. Geogr. Sci. **24**: 303–312. doi:10.1007/s11442-014-1089-z.

APPENDICES

Appendix A: R code for web scraping the property assessment database

```r
library(tidyverse)
library(rvest) #scraping package
library(progress) #package that tracks how many links have been scraped
#change below to your working directory
setwd("C:/Users/Owner/OneDrive - University of Manitoba/Documents/ANSC MSc Grassland Productivity")
```

```r
MPA <- read_csv("AreaDiffsOver20.csv") #put the exported csv from ArcMap
pages <- MPA$Asmt_Rpt_U #links of each parcel

#creates progress bar
pb <- progress_bar$new(format = "  scraping [:bar] :current/:total :percent eta: :eta", total = 2661, clear = FALSE, width= 60) #change total=2661 to the number of features in the exported csv

##create a function to scrape info from a vector of urls
#lapply applies a function to a list/vector as read_html can only execute to one url at at time
scrape_links <- lapply(pages, function(x){
  #progress bar
  pb$tick()
  #pauses the scraping for 0.01 secs. to avoid overloading the server
  Sys.sleep(1 / 100)

  #tibble for each feature/obs. with 4 variables (roll no., acres, legal desc., municipality)
  tibble(roll_no= read_html(x) %>%
           html_node("tr:nth-child(2) tr:nth-child(1) td:nth-child(4)") %>% #CSS selector derived from SelectorGadget
           html_text(),
         acres= read_html(x) %>%
           html_node("tr:nth-child(2) tr:nth-child(2) td:nth-child(4)") %>%
           html_text(),
         legal_desc= read_html(x) %>%
           html_node(".nested-table .nested-table td") %>%
           html_text(),
         municipality= read_html(x) %>%
           html_node("tr:nth-child(2) tr:nth-child(1) td:nth-child(2)") %>%
           html_text())
})

#merge separate tibbles
combined_scraped_data <- bind_rows(scrape_links)

#creates csv with scraped information
write.csv(combined_scraped_data, "AreaDiffsOver20_MPAscraped.csv", row.names = F)
```

Appendix B: R code for parcel geometry transfer to the crown land geodatabase

```{r include=TRUE}
library(sf) #simple features package for encoding spatial vector data
library(rgdal)
library(dplyr)
setwd("Z:/Docs/MB Crownlands/Part 2")
```

```{r}
#lists all layers within gdb
main_gdb <- st_layers("Z:/Docs/MB Crownlands/Part 2/QT7_spatial_adj.gdb")
#where geometry would be transferred
target_layer <- st_read(dsn="Z:/Docs/MB Crownlands/Part 2/QT7_spatial_adj.gdb",
layer="QT7_Dissolve2_SJ")
#where geometry comes from
source_layer <- st_read(dsn="Z:/Docs/MB Crownlands/Part 2/QT7_spatial_adj.gdb",
layer="QT7_matched_parcels")
```

```{r}
target_layer <-
  #left join adds needed variables from source to target based on having the same
legal desc.
  #also uses select function to only add specific variables, not all of them
  left_join(target_layer, source_layer %>% as.data.frame() %>%
select(QT7_MPA_scrapeddata_linesTopoly_legal_desc, scraped_municipality,
QT7_MPA_scrapeddata_linesTopoly_DLS, QT7_MPA_scrapeddata_linesTopoly_Source,
QT7_MPA_scrapeddata_linesTopoly_AREA_acres, MPA_acres, Shape), by= c("ARD_LegalD" =
"QT7_MPA_scrapeddata_linesTopoly_DLS")) %>%

  #modifies some variables in target, incl. the needed geometry from source
  mutate(Notes = QT7_MPA_scrapeddata_linesTopoly_legal_desc,
         Source = QT7_MPA_scrapeddata_linesTopoly_Source,
         Shape.x = ifelse(is.na(st_dimension(Shape.y)), Shape.x, Shape.y)) %>%

  #deletes the initially joined geom. from source (layer must only have one geom.);
also deletes unnecessary copied variables from source
  select(-Shape.y, -QT7_MPA_scrapeddata_linesTopoly_Source, -
QT7_MPA_scrapeddata_linesTopoly_legal_desc) %>%

  #renames longer variable names
  rename(scraped_RM=QT7_MPA_scrapeddata_linesTopoly_municipa_1,
         AREA_acre=QT7_MPA_scrapeddata_linesTopoly_AREA_acres,
         MPA_acres=QT7_MPA_scrapeddata_linesTopoly_MPA_acres)
```

```{r}
#assigns the correct coordinate reference system
st_crs(target_layer) = 26914

#creates the new modified feature class within gpkg (to avoid shp field length
limitations)
st_write(target_layer, dsn= "Z:/Docs/MB Crownlands/Part 2/GeomTrans.gpkg",
layer="QT7_Dissolve2_SJ_RTrans", delete_layer = TRUE)

#creates the new modified shapefile
st_write(target_layer, dsn= "Z:/Docs/MB Crownlands/Part
2/QT7_Dissolve2_SJ_RTrans.shp", delete_layer = TRUE)
```

Appendix C: Equivalent land cover classes from each reference inventory

Broad class	ACL class	MGI class	ACI class
Native	Upland grassland	Native	Grassland
	Lowland meadow	Mixed	
	Transitional grassland		
Tame	Multiple improved forage classes	Tame	Pasture/Forages
Shrubland	Open woodland	Shrub	Shrubland
Forest	Woodland	Forest	Forest (undifferentiated)
	Harvested woodland		Coniferous
			Broadleaf
			Mixedwood
Cropland	Cropped	Cropland	Agriculture (undifferentiated)
			Too Wet to be Seeded
			Fallow
			Cereals
			Barley
			Other Grains
			Millet
			Oats
			Rye
			Spelt
			Triticale
			Wheat
			Switchgrass
			Sorghum
			Quinoa
			Winter Wheat
			Spring Wheat
			Corn
			Tobacco
			Ginseng
			Oilseeds
			Borage
			Camelina
			Canola/Rapeseed
			Flaxseed
			Mustard
			Safflower
			Sunflower

			Soybeans
			Pulses
			Other Pulses
			Peas
			Chickpeas
			Beans
			Fababeans
			Lentils
			Vegetables
			Tomatoes
			Potatoes
			Sugarbeets
			Other Vegetables
			Fruits
			Berries
			Blueberry
			Cranberry
			Other Berry
			Orchards
			Other Fruits
			Vineyards
			Hops
			Sod
			Herbs
			Nursery
			Buckwheat
			Canaryseed
			Hemp
			Vetch
			Other Crops
Water/Wetlands	Open water	Water	Water
	Marsh	Wetland	Wetland
			Peatland
Others	Miscellaneous classes	Urban	Urban/Developed
			Exposed Land/Barren
			Greenhouses
			Cloud

Appendix D: Class percentages by ecoregion based on MGI/ACI classification in bar chart

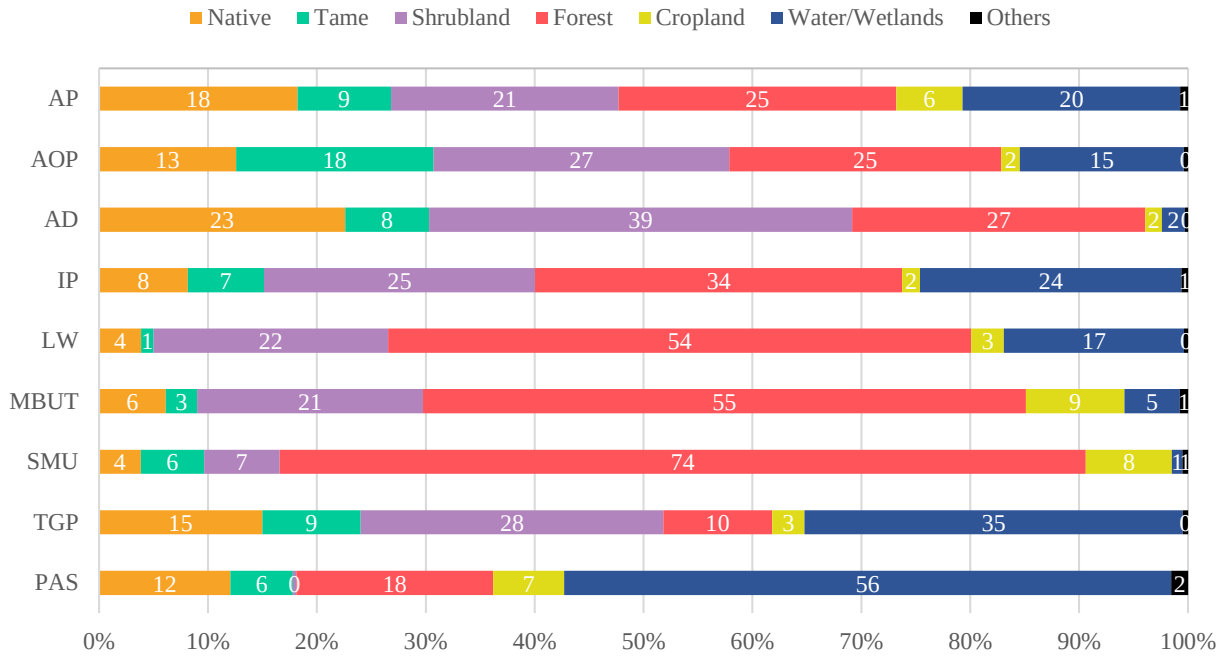

Percentages are superimposed on each class bar.
AP = Aspen Parkland; AOP = Aspen/Oak Parkland; AD = Assiniboine Delta; IP = Interlake Plain; LW = Lake of the Woods; MBUT = Mid-Boreal Upland and Transition; SMU = Southwest Manitoba Uplands; TGP = Tall Grass Prairie; PAS = The Pas

Appendix E: List of all possible carrying capacities calculated from field surveys and used to estimate stocking rates

Cage Location	Ecosite	Class	Broad Class	CC (AUM/ha)
Ebor	Loam	Upland	Native	4.5110
Ebor	Moist Loam	Transitional	Native	4.4271
Ebor	Moist Loam	Open Wood	Shrubland	1.8030
Ebor	Moist Loam	Woodland	Forest	1.0921
Ebor	Wet Meadow	Lowland	Native	3.1813
Oak Lake	Moist Sand	Upland	Native	2.2084
Oak Lake	Moist Sand	Transitional	Native	3.1258
Oak Lake	Moist Sand	Open Wood	Shrubland	1.1023
Oak Lake	Moist Sand	Woodland	Forest	0.5621
Oak Lake	Wet Meadow	Lowland	Native	2.2651
Brandon Hills	Moist Loam	Upland	Native	5.2301
Brandon Hills	Sand	Upland	Native	0.9396
Brandon Hills	Sand	Open Wood	Shrubland	1.3392
Brandon Hills	Sand	Woodland	Forest	0.5546
Brandon Hills	Sandy Loam	Upland	Native	2.4890
Brandon Hills	Sandy Loam	Open Wood	Shrubland	2.6670
Brandon Hills	Sandy Loam	Woodland	Forest	0.4777
MacGregor West	Moist Sand	Upland	Native	2.0273
MacGregor West	Moist Sand	Transitional	Native	3.5793
MacGregor West	Moist Sand	Open Wood	Shrubland	0.8250
MacGregor West	Moist Sand	Woodland	Forest	0.1221
MacGregor West	Sand	Upland	Native	1.0900
MacGregor West	Wet Meadow	Lowland	Native	2.7271
MacGregor West	Wet Meadow	Transitional	Native	0.7855
MacGregor East	Moist Sand	Upland	Native	1.9691
MacGregor East	Moist Sand	Transitional	Native	3.6714
MacGregor East	Moist Sand	Open Wood	Shrubland	1.1872
MacGregor East	Moist Sand	Woodland	Forest	0.5001
MacGregor East	Wet Meadow	Lowland	Native	2.9121
Plumas	Moist Loam	Upland	Native	2.4380
Plumas	Moist Loam	Transitional	Native	3.4813
Plumas	Moist Loam	Open Wood	Shrubland	1.1802
Plumas	Moist Loam	Woodland	Forest	0.3148
Plumas	Wet Meadow	Lowland	Native	3.9997
Plumas	Wet Meadow	Transitional	Native	2.9978
Meharry	Moist Loam	Upland	Native	1.6661
Meharry	Moist Loam	Transitional	Native	2.9910
Meharry	Moist Loam	Open Wood	Shrubland	1.3000
Meharry	Moist Loam	Woodland	Forest	0.5072
Meharry	Wet Meadow	Lowland	Native	2.7195
Garson	Clay	Upland	Native	3.3779
Garson	Clay	Transitional	Native	3.9023
Garson	Clay	Open Wood	Shrubland	1.6833
Garson	Clay	Woodland	Forest	0.5040
Garson	Wet Meadow	Lowland	Native	2.9586

Garson	Wet Meadow	Transitional	Native	1.6177
Selina	Moist Sand	Upland	Native	1.3015
Selina	Moist Sand	Open Wood	Shrubland	1.4552
Selina	Moist Sand	Woodland	Forest	0.5857
Selina	Wet Meadow	Lowland	Native	2.0904
Lac du Bonnet	Clay	Upland	Native	4.1214
Lac du Bonnet	Clay	Transitional	Native	5.1809
Lac du Bonnet	Clay	Open Wood	Shrubland	2.1983
Lac du Bonnet	Clay	Woodland	Forest	0.3889
Lac du Bonnet	Wet Meadow	Lowland	Native	4.4960
East Braintree	Moist Sand	Upland	Native	1.7977
East Braintree	Moist Sand	Transitional	Native	2.3911
East Braintree	Moist Sand	Open Wood	Shrubland	1.1589
East Braintree	Moist Sand	Woodland	Forest	0.3307
East Braintree	Wet Meadow	Lowland	Native	2.5806
East Braintree	Wet Meadow	Transitional	Native	2.4137
Sprague	Moist Sand	Upland	Native	2.1671
Sprague	Moist Sand	Transitional	Native	3.0588
Sprague	Moist Sand	Open Wood	Shrubland	0.7508
Sprague	Moist Sand	Woodland	Forest	0.2442
Sprague	Wet Meadow	Lowland	Native	1.7980
Sprague	Wet Meadow	Transitional	Native	1.7442
Central	Moist Loam	Upland	Native	2.4380
Central	Moist Loam	Transitional	Native	3.4813
Central	Moist Loam	Open Wood	Shrubland	1.1802
Central	Moist Loam	Woodland	Forest	0.3148
Central	Moist Sand	Upland	Native	1.9982
Central	Moist Sand	Transitional	Native	3.6254
Central	Moist Sand	Open Wood	Shrubland	1.0061
Central	Moist Sand	Woodland	Forest	0.3111
Central	Sand	Upland	Native	1.0900
Central	Wet Meadow	Lowland	Native	3.2130
Central	Wet Meadow	Transitional	Native	1.8917
Central/Brandon Hills	Moist Loam	Upland	Native	3.8341
Central/Brandon Hills	Moist Loam	Transitional	Native	3.4813
Central/Brandon Hills	Moist Loam	Open Wood	Shrubland	1.1802
Central/Brandon Hills	Moist Loam	Woodland	Forest	0.3148
Central/Brandon Hills	Moist Sand	Upland	Native	1.9982
Central/Brandon Hills	Moist Sand	Transitional	Native	3.6254
Central/Brandon Hills	Moist Sand	Open Wood	Shrubland	1.0061
Central/Brandon Hills	Moist Sand	Woodland	Forest	0.3111
Central/Brandon Hills	Sand	Upland	Native	1.0148
Central/Brandon Hills	Sand	Open Wood	Shrubland	1.3392
Central/Brandon Hills	Sand	Woodland	Forest	0.5546
Central/Brandon Hills	Sandy Loam	Upland	Native	2.4890
Central/Brandon Hills	Sandy Loam	Open Wood	Shrubland	2.6670
Central/Brandon Hills	Sandy Loam	Woodland	Forest	0.4777
Central/Brandon Hills	Wet Meadow	Lowland	Native	3.2130

Central/Brandon Hills	Wet Meadow	Transitional	Native	1.8917
Plumas/Northwest	Clay	Upland	Native	3.3779
Plumas/Northwest	Clay	Transitional	Native	3.9023
Plumas/Northwest	Clay	Open Wood	Shrubland	1.6833
Plumas/Northwest	Clay	Woodland	Forest	0.5040
Plumas/Northwest	Moist Loam	Upland	Native	2.0520
Plumas/Northwest	Moist Loam	Transitional	Native	3.2362
Plumas/Northwest	Moist Loam	Open Wood	Shrubland	1.2401
Plumas/Northwest	Moist Loam	Woodland	Forest	0.4110
Plumas/Northwest	Moist Sand	Upland	Native	1.3015
Plumas/Northwest	Moist Sand	Open Wood	Shrubland	1.4552
Plumas/Northwest	Moist Sand	Woodland	Forest	0.5857
Plumas/Northwest	Wet Meadow	Lowland	Native	3.2946
Plumas/Northwest	Wet Meadow	Transitional	Native	2.3077
Ebor/Northwest	Clay	Upland	Native	3.3779
Ebor/Northwest	Clay	Transitional	Native	3.9023
Ebor/Northwest	Clay	Open Wood	Shrubland	1.6833
Ebor/Northwest	Clay	Woodland	Forest	0.5040
Ebor/Northwest	Loam	Upland	Native	4.5110
Ebor/Northwest	Moist Loam	Upland	Native	1.6661
Ebor/Northwest	Moist Loam	Transitional	Native	3.7091
Ebor/Northwest	Moist Loam	Open Wood	Shrubland	1.5515
Ebor/Northwest	Moist Loam	Woodland	Forest	0.7996
Ebor/Northwest	Moist Sand	Upland	Native	1.3015
Ebor/Northwest	Moist Sand	Open Wood	Shrubland	1.4552
Ebor/Northwest	Moist Sand	Woodland	Forest	0.5857
Ebor/Northwest	Wet Meadow	Lowland	Native	2.8854
Ebor/Northwest	Wet Meadow	Transitional	Native	1.6177
Northwest	Clay	Upland	Native	3.3779
Northwest	Clay	Transitional	Native	3.9023
Northwest	Clay	Open Wood	Shrubland	1.6833
Northwest	Clay	Woodland	Forest	0.5040
Northwest	Moist Loam	Upland	Native	1.6661
Northwest	Moist Loam	Transitional	Native	2.9910
Northwest	Moist Loam	Open Wood	Shrubland	1.3000
Northwest	Moist Loam	Woodland	Forest	0.5072
Northwest	Moist Sand	Upland	Native	1.3015
Northwest	Moist Sand	Open Wood	Shrubland	1.4552
Northwest	Moist Sand	Woodland	Forest	0.5857
Northwest	Wet Meadow	Lowland	Native	2.5895
Northwest	Wet Meadow	Transitional	Native	1.6177
Northwest/Lac du Bonnet	Clay	Upland	Native	3.7496
Northwest/Lac du Bonnet	Clay	Transitional	Native	4.5416
Northwest/Lac du Bonnet	Clay	Open Wood	Shrubland	1.9408
Northwest/Lac du Bonnet	Clay	Woodland	Forest	0.4464
Northwest/Lac du Bonnet	Moist Loam	Upland	Native	1.6661
Northwest/Lac du Bonnet	Moist Loam	Transitional	Native	2.9910
Northwest/Lac du Bonnet	Moist Loam	Open Wood	Shrubland	1.3000

Northwest/Lac du Bonnet	Moist Loam	Woodland	Forest	0.5072
Northwest/Lac du Bonnet	Moist Sand	Upland	Native	1.3015
Northwest/Lac du Bonnet	Moist Sand	Open Wood	Shrubland	1.4552
Northwest/Lac du Bonnet	Moist Sand	Woodland	Forest	0.5857
Northwest/Lac du Bonnet	Wet Meadow	Lowland	Native	3.5428
Northwest/Lac du Bonnet	Wet Meadow	Transitional	Native	1.6177
Plumas/Lac du Bonnet	Clay	Upland	Native	4.1214
Plumas/Lac du Bonnet	Clay	Transitional	Native	5.1809
Plumas/Lac du Bonnet	Clay	Open Wood	Shrubland	2.1983
Plumas/Lac du Bonnet	Clay	Woodland	Forest	0.3889
Plumas/Lac du Bonnet	Moist Loam	Upland	Native	2.4380
Plumas/Lac du Bonnet	Moist Loam	Transitional	Native	3.4813
Plumas/Lac du Bonnet	Moist Loam	Open Wood	Shrubland	1.1802
Plumas/Lac du Bonnet	Moist Loam	Woodland	Forest	0.3148
Plumas/Lac du Bonnet	Wet Meadow	Lowland	Native	4.2479
Plumas/Lac du Bonnet	Wet Meadow	Transitional	Native	2.9978
Central/Lac du Bonnet	Clay	Upland	Native	4.1214
Central/Lac du Bonnet	Clay	Transitional	Native	5.1809
Central/Lac du Bonnet	Clay	Open Wood	Shrubland	2.1983
Central/Lac du Bonnet	Clay	Woodland	Forest	0.3889
Central/Lac du Bonnet	Moist Loam	Upland	Native	2.4380
Central/Lac du Bonnet	Moist Loam	Transitional	Native	3.4813
Central/Lac du Bonnet	Moist Loam	Open Wood	Shrubland	1.1802
Central/Lac du Bonnet	Moist Loam	Woodland	Forest	0.3148
Central/Lac du Bonnet	Moist Sand	Upland	Native	1.9982
Central/Lac du Bonnet	Moist Sand	Transitional	Native	3.6254
Central/Lac du Bonnet	Moist Sand	Open Wood	Shrubland	1.0061
Central/Lac du Bonnet	Moist Sand	Woodland	Forest	0.3111
Central/Lac du Bonnet	Sand	Upland	Native	1.0900
Central/Lac du Bonnet	Wet Meadow	Lowland	Native	3.8545
Central/Lac du Bonnet	Wet Meadow	Transitional	Native	1.8917
MacGregor/Lac du Bonnet	Clay	Upland	Native	4.1214
MacGregor/Lac du Bonnet	Clay	Transitional	Native	5.1809
MacGregor/Lac du Bonnet	Clay	Open Wood	Shrubland	2.1983
MacGregor/Lac du Bonnet	Clay	Woodland	Forest	0.3889
MacGregor/Lac du Bonnet	Moist Sand	Upland	Native	1.9982
MacGregor/Lac du Bonnet	Moist Sand	Transitional	Native	3.6254
MacGregor/Lac du Bonnet	Moist Sand	Open Wood	Shrubland	1.0061
MacGregor/Lac du Bonnet	Moist Sand	Woodland	Forest	0.3111
MacGregor/Lac du Bonnet	Sand	Upland	Native	1.0900
MacGregor/Lac du Bonnet	Wet Meadow	Lowland	Native	3.6578
MacGregor/Lac du Bonnet	Wet Meadow	Transitional	Native	0.7855
MacGregor	Moist Sand	Upland	Native	1.9982
MacGregor	Moist Sand	Transitional	Native	3.6254
MacGregor	Moist Sand	Open Wood	Shrubland	1.0061
MacGregor	Moist Sand	Woodland	Forest	0.3111
MacGregor	Sand	Upland	Native	1.0900
MacGregor	Wet Meadow	Lowland	Native	2.8196

MacGregor	Wet Meadow	Transitional	Native	0.7855
Manitoba	Precambrian Bedrock			0.7410
Manitoba	Shallow to Limestone			0.7410
Manitoba	Eroded Slopes			0.0000
Manitoba	Dunes			0.9880
Manitoba	Sand			1.2350
Manitoba	Sandy Loam			1.4820
Manitoba	Moist Sand			1.7290
Manitoba	Loam			1.9760
Manitoba	Calcareous Loam			1.7290
Manitoba	Moist Loam			2.2230
Manitoba	Clay			2.4700
Manitoba	Alluvium			2.2230
Manitoba	Moist Saline			1.7290
Manitoba	Wet Meadow			2.7170
Manitoba	Saline Wet Meadow			2.2230
Manitoba	Shallow Marsh			0.0000
Manitoba	Saline Shallow Marsh			0.0000
Manitoba	Deep Marsh			0.0000
Manitoba	Saline Deep Marsh			0.0000
Manitoba	Fen Peat			0.0000
Manitoba	Forest Peat			0.0000
Manitoba	Bare Soil			0.0000
Manitoba	Urban			0.0000
Manitoba	Water			0.0000
Manitoba			Water/Wetlands	0.0000
Manitoba			Others	0.0000
Manitoba			Cropland	0.0000
Manitoba			No Data	0.0000
Manitoba			Tame	6.5427
Ebor			Native	4.0398
Oak Lake			Native	2.5331
Brandon Hills			Native	2.8862
MacGregor			Native	2.1897
Plumas			Native	3.2257
Meharry			Native	2.4589
Garson			Native	3.0321
Selina			Native	1.6959
Lac du Bonnet			Native	4.5994
East Braintree			Native	2.2603
Sprague			Native	2.1222
Central			Native	2.6848
Central/Brandon Hills			Native	2.8488
Plumas/Northwest			Native	2.8957
Ebor/Northwest			Native	2.8920
Northwest			Native	2.9440
Northwest/Lac du Bonnet			Native	3.8047
Plumas/Lac du Bonnet			Native	3.2704

Central/Lac du Bonnet			Native	3.0861
MacGregor/Lac du Bonnet			Native	2.1897
Ebor			Shrubland	1.8030
Oak Lake			Shrubland	1.1023
Brandon Hills			Shrubland	2.0031
MacGregor			Shrubland	1.0061
Plumas			Shrubland	1.1802
Meharry			Shrubland	1.3000
Garson			Shrubland	1.6833
Selina			Shrubland	1.4552
Lac du Bonnet			Shrubland	2.1983
East Braintree			Shrubland	1.1589
Sprague			Shrubland	0.7508
Central			Shrubland	1.0931
Central/Brandon Hills			Shrubland	1.5481
Plumas/Northwest			Shrubland	1.4595
Ebor/Northwest			Shrubland	1.5633
Northwest			Shrubland	1.5653
Northwest/Lac du Bonnet			Shrubland	1.6893
Plumas/Lac du Bonnet			Shrubland	1.4615
Central/Lac du Bonnet			Shrubland	1.6022
MacGregor/Lac du Bonnet			Shrubland	1.0061
Ebor			Forest	1.0921
Oak Lake			Forest	0.5621
Brandon Hills			Forest	0.5161
MacGregor			Forest	0.3111
Plumas			Forest	0.3148
Meharry			Forest	0.5072
Garson			Forest	0.5040
Selina			Forest	0.5857
Lac du Bonnet			Forest	0.3889
East Braintree			Forest	0.3307
Sprague			Forest	0.2442
Central			Forest	0.3130
Central/Brandon Hills			Forest	0.4145
Plumas/Northwest			Forest	0.5002
Ebor/Northwest			Forest	0.6298
Northwest			Forest	0.5131
Northwest/Lac du Bonnet			Forest	0.3518
Plumas/Lac du Bonnet			Forest	0.3383
Central/Lac du Bonnet			Forest	0.3500
MacGregor/Lac du Bonnet			Forest	0.3111
Ebor	Wet Meadow		Native	3.1813
Oak Lake	Wet Meadow		Native	2.2651
MacGregor West	Wet Meadow		Native	1.7563
MacGregor East	Wet Meadow		Native	2.9121
Plumas	Wet Meadow		Native	3.4988
Meharry	Wet Meadow		Native	2.7195

Garson	Wet Meadow		Native	2.2881
Selina	Wet Meadow		Native	2.0904
Lac du Bonnet	Wet Meadow		Native	4.4960
East Braintree	Wet Meadow		Native	2.4972
Sprague	Wet Meadow		Native	1.7711
Central	Wet Meadow		Native	2.5523
Central/Brandon Hills	Wet Meadow		Native	2.5523
Plumas/Northwest	Wet Meadow		Native	2.8012
Ebor/Northwest	Wet Meadow		Native	2.2515
Northwest	Wet Meadow		Native	2.1036
Northwest/Lac du Bonnet	Wet Meadow		Native	2.5802
Plumas/Lac du Bonnet	Wet Meadow		Native	3.6228
Central/Lac du Bonnet	Wet Meadow		Native	2.8731
MacGregor/Lac du Bonnet	Wet Meadow		Native	2.2217
MacGregor	Wet Meadow		Native	1.8025
Ebor	Loam		Native	4.5110
Ebor	Moist Loam		Native	4.4271
Oak Lake	Moist Sand		Native	2.6671
Brandon Hills	Moist Loam		Native	5.2301
Brandon Hills	Sand		Native	0.9396
Brandon Hills	Sandy Loam		Native	2.4890
MacGregor West	Moist Sand		Native	2.8033
MacGregor West	Sand		Native	1.0900
MacGregor East	Moist Sand		Native	2.8203
Plumas	Moist Loam		Native	2.9596
Meharry	Moist Loam		Native	2.3286
Garson	Clay		Native	3.6401
Selina	Moist Sand		Native	1.3015
Lac du Bonnet	Clay		Native	4.6512
East Braintree	Moist Sand		Native	2.0944
Sprague	Moist Sand		Native	2.6130
Central	Moist Loam		Native	2.9596
Central	Moist Sand		Native	2.8118
Central	Sand		Native	1.0900
Central/Brandon Hills	Moist Loam		Native	3.6577
Central/Brandon Hills	Moist Sand		Native	2.8118
Central/Brandon Hills	Sand		Native	1.0148
Central/Brandon Hills	Sandy Loam		Native	2.4890
Plumas/Northwest	Clay		Native	3.6401
Plumas/Northwest	Moist Loam		Native	2.6441
Plumas/Northwest	Moist Sand		Native	1.3015
Ebor/Northwest	Clay		Native	3.6401
Ebor/Northwest	Loam		Native	4.5110
Ebor/Northwest	Moist Loam		Native	2.6876
Ebor/Northwest	Moist Sand		Native	1.3015
Northwest	Clay		Native	3.6401
Northwest	Moist Loam		Native	2.3286
Northwest	Moist Sand		Native	1.3015

Northwest/Lac du Bonnet	Clay		Native	4.1456
Northwest/Lac du Bonnet	Moist Loam		Native	2.3286
Northwest/Lac du Bonnet	Moist Sand		Native	1.3015
Plumas/Lac du Bonnet	Clay		Native	4.6512
Plumas/Lac du Bonnet	Moist Loam		Native	2.9596
Central/Lac du Bonnet	Clay		Native	4.6512
Central/Lac du Bonnet	Moist Loam		Native	2.9596
Central/Lac du Bonnet	Moist Sand		Native	2.8118
Central/Lac du Bonnet	Sand		Native	1.0900
MacGregor/Lac du Bonnet	Clay		Native	4.6512
MacGregor/Lac du Bonnet	Moist Sand		Native	2.8118
MacGregor/Lac du Bonnet	Sand		Native	1.0900
MacGregor	Moist Sand		Native	2.8118
MacGregor	Sand		Native	1.0900

Appendix F: Correlation coefficients between response forage yields and carrying capacities, and explanatory climate variables

Climate variables	Field sampling data				Estimated crown lands data			
	Mean yields		Mean CC		Mean CC		Max CC	
	Pearson's r	Spearman's ρ	Pearson's r	Spearman's ρ	Pearson's r	Spearman's ρ	Pearson's r	Spearman's ρ
MAT	0.20	-0.01	0.20	0.11	0.05**	0.10**	0.08**	0.12**
MAP	-0.15	-0.18	-0.24	-0.18	-0.01	0.08**	0.12**	0.18**
MSP	-0.25	-0.18	-0.29	-0.17	-0.05**	0.07**	0.10**	0.18**
GDD	0.17	0.06	0.15	0.15	0.09**	0.15**	0.07**	0.11**
CMI	-0.03	-0.23	-0.24	-0.25	-0.19**	-0.21**	-0.08**	-0.12**
MWMT[1]	0.26	0.13	0.21	0.20				
MCMT[2]	0.27	0.12	0.37	0.29				
TD[3]	-0.05	-0.02	-0.18	-0.02				
AHM[4]	0.24	0.27	0.35	0.31				
SHM[5]	0.30	0.26	0.36	0.38				
DD<0[6]	-0.19	0.04	-0.23	-0.14				
DD<18[7]	-0.18	0.07	-0.19	-0.08				
DD>18[8]	0.20	0.05	0.16	0.13				
NFFD[9]	0.66*	0.57	0.58	0.69*				
bFFP[10]	-0.46	-0.02	-0.26	-0.18				
eFFP[11]	0.38	-0.14	0.14	0.02				
FFP[12]	0.43	-0.14	0.16	0.01				
SP[13]	0.20	0.01	0.03	-0.10				
EMT[14]	0.33	-0.11	0.15	-0.02				
EXT[15]	0.02	0.09	0.19	0.17				
Eref[16]	-0.16	-0.11	0.10	0.02				
CMD[17]	0.08	0.31	0.29	0.36				
RH[18]	0.35	-0.09	0.01	-0.09				
DD1040[19]	0.18	0.06	0.16	0.15				

*Significant at $\alpha = 0.05$; **Significant at $\alpha = 0.01$

[1]Mean warmest month temperature (°C)

[2]Mean coldest month temperature (°C)

[3]Temperature difference between MWMT and MCMT or continentality (°C)

[4]Annual heat-moisture index calculated as a ratio of (MAT+10)/(MAP/1000)
[5]Summer heat-moisture index calculated as a ratio of MWMT/(MSP/1000)
[6]Degree-days below 0°C or chilling degree-days
[7]Degree-days below 18°C or heating degree-days
[8]Degree-days above 18°C or cooling degree-days
[9]Number of frost-free days
[10]Day of the year on which frost-free period begins
[11]Day of the year on which frost-free period ends
[12]Frost-free period
[13]Snow precipitation (mm)
[14]Extreme minimum temperature over 30 years (°C)
[15]Extreme maximum temperature over 30 years (°C)
[16]Hargreaves' reference evaporation (mm)
[17]Hargreaves' climatic moisture deficit (mm)
[18]Mean annual relative humidity (%)
[19]Degree-days above 10°C and below 40°C